Dansgaard–Oeschger (D/O) & Heinrich events

EPS 231 Climate dynamics
Eli Tziperman

The Glacial world/ ice cores

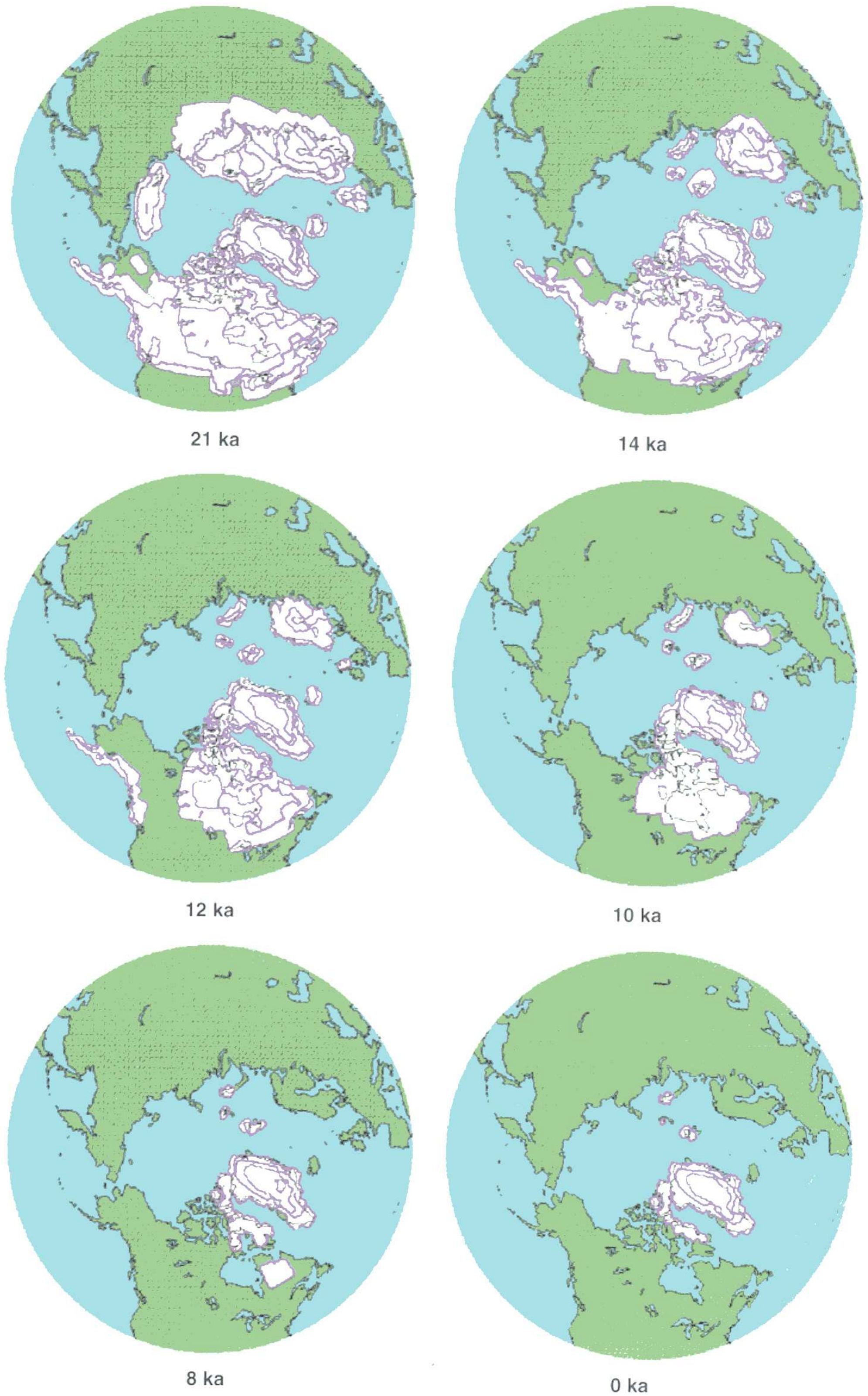

Fig. 4. Thickness isopachs for the ICE-4G model for a sequence of times beginning at Last Glacial Maximum at 21 ka and ending at the present. The contour interval is 1 km.

SCIENCE • VOL. 265 • 8 JULY 1994

Peltier 1994, Science

← Ice sheet elevation: 2-3 km,

sea level drop: 120 meter

Ice core taken out of drill, Byrd, Antarctica (L. Thompson)

https://en.wikipedia.org/wiki/File:Icecore_4.jpg

Dansgaard-Oeschger events

D/O events

Dansgaard-Oeschger events: abrupt warming events seen in Greenland ice cores; occur every ~1500 years, last a few hundred years;

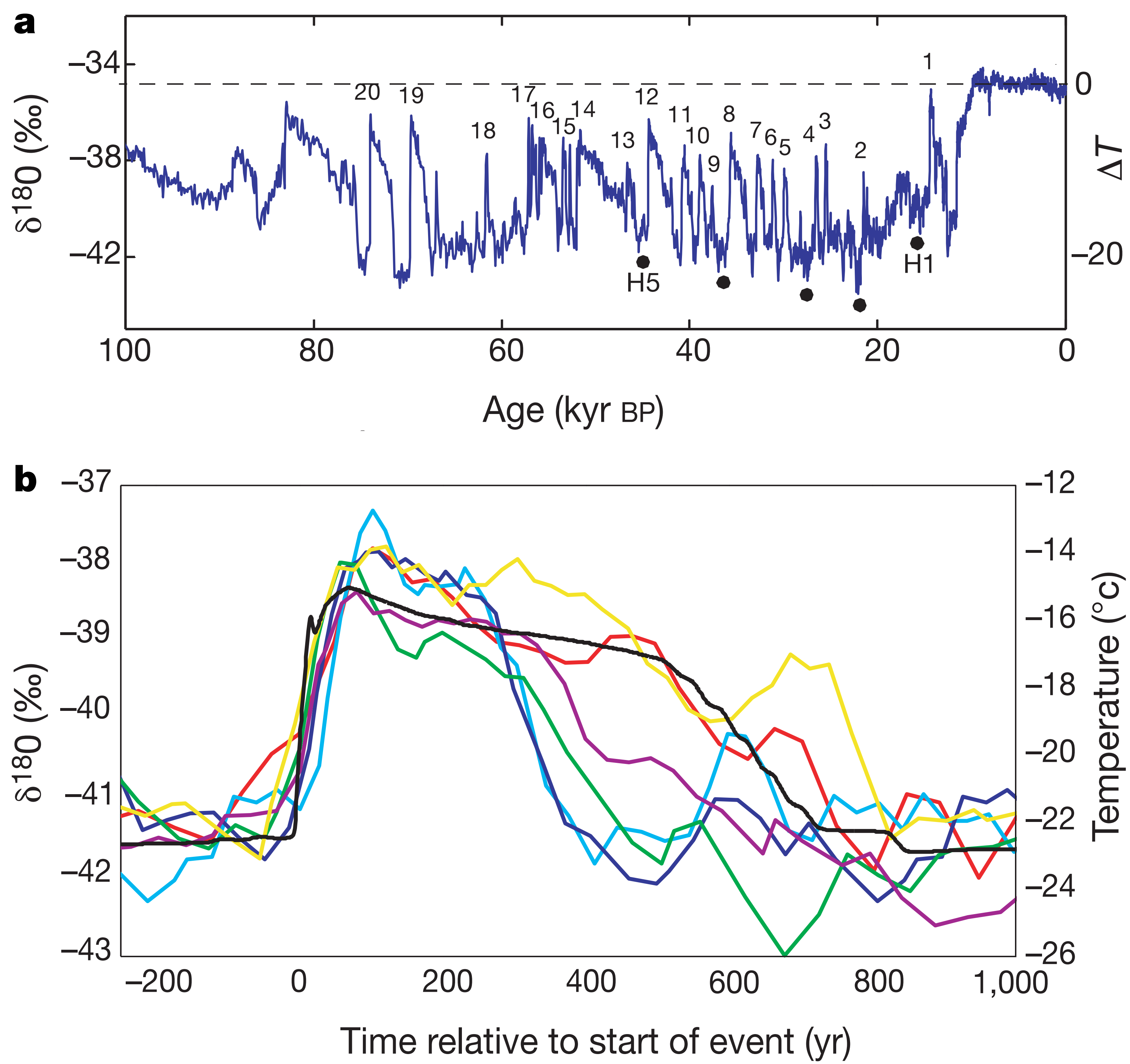

Figure 4 Abrupt climate changes in Greenland ice-core data. **a**, d[18]O from GRIP core, a proxy for atmospheric temperature over Greenland. Dansgaard±Oeschger (D/O) warm events (numbered). Heinrich events H1-H5 marked by black dots. **b**, Time evolution of recent D/O events taken from a (3, light blue; 4, dark blue; 5, purple; 6, green; 7, orange; 10, red). Many D/O events show the characteristic slow cooling phase after the initial warming, followed by a more abrupt temperature drop. Some events are much longer but still show this general characteristic (for example, nos 8, 12, 19, 20). A modeled D/O event in black (North Atlantic air temperature).

Ganopolski Rahmstorf 2001

Dansgaard-Oeschger events, outline

1. AMOC flushes/relaxation oscillations
2. sea ice amplification of the atmospheric signal
3. precise clock?
4. teleconnections

D/O-like AMOC oscillations, “flushes”

$$\frac{dS_l}{dt} = \frac{2M_{ld}}{hL}(S_d - S_l) + \frac{2M_{lh}}{hL}(S_h - S_l) + \frac{F_s}{h}$$

$$\frac{dS_h}{dt} = \frac{2M_{hd}}{hL}(S_d - S_h) + \frac{2M_{lh}}{hL}(S_l - S_h) - \frac{F_s}{h}$$

$$\frac{dS_d}{dt} = \frac{M_{ld}}{HL}\left(S_l - S_d\right) + \frac{M_{hd}}{HL}\left(S_h - S_d\right)$$

$$\frac{dT_d}{dt} = \frac{M_{ld}}{HL}\left(T_l - T_d\right) + \frac{M_{hd}}{HL}\left(T_h - T_d\right)$$

$$M_{\{l,h\}d} = C_{\{l,h\}} M_v$$

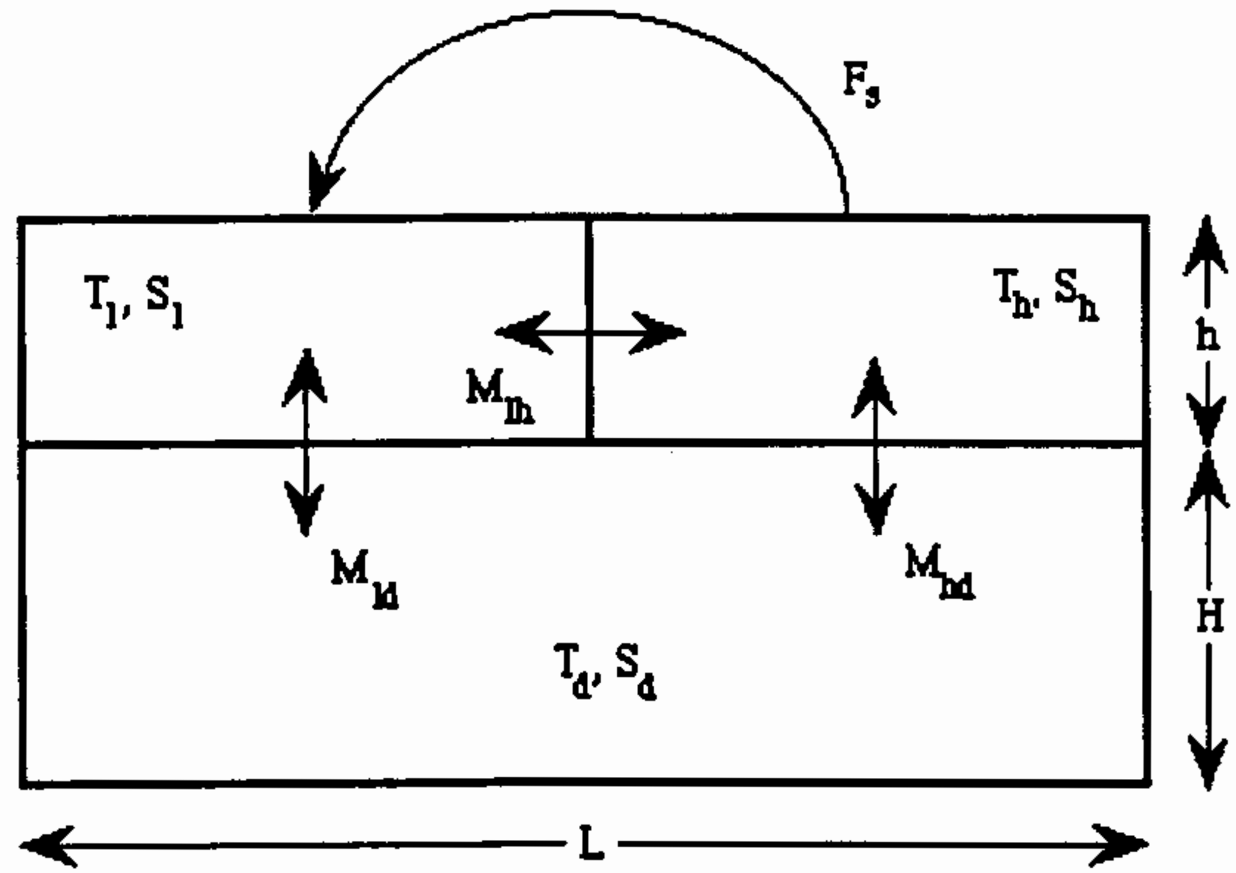

The convective parameters $C_{\{lh\}}$ are raised from 1 to 10 if $\rho(T_{\{lh\}},S_{\{lh\}})>\rho(T_d,S_d)$ where,

$$\rho(T,S)=0.79S-0.0611T-0.0055T^2.$$

Winton 1993

D/O-like AMOC oscillations, "flushes"

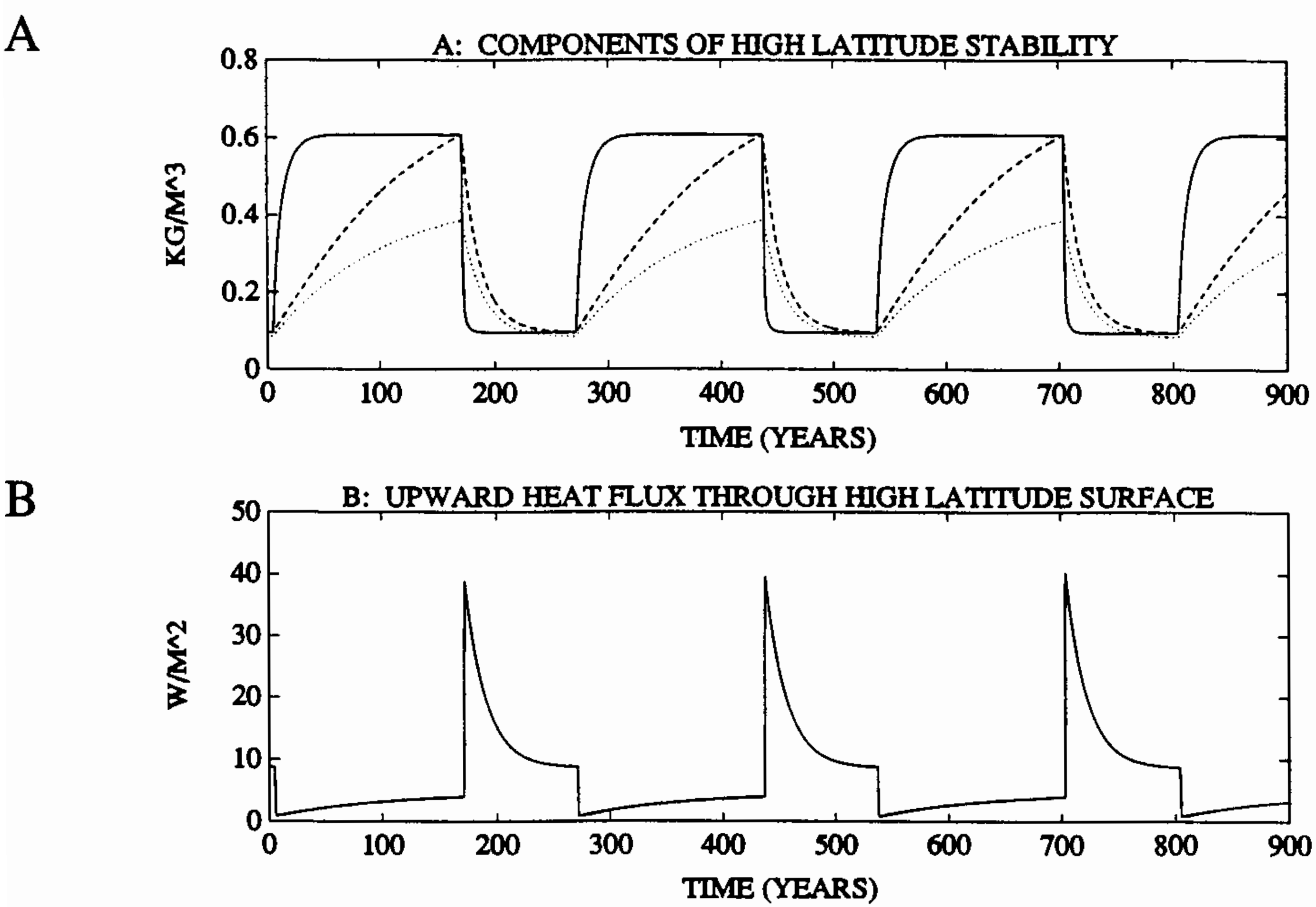

Figure 7: Three box model oscillations with F_s=(-35 kg·m^{-3})·(0.55 m·yr^{-1}). (a) High latitude stability due to the vertical salinity gradient (solid), destabilizing effect of the vertical temperature gradient (dashed), and linear destabilizing effect of temperature estimated with the thermal expansion coefficient for 0°C (dotted); all in kg·m^{-3}. (b) Upward heat flux through the high latitude surface (W·m^{-2}).

Winton 1993

D/O-like AMOC oscillations, “flushes”

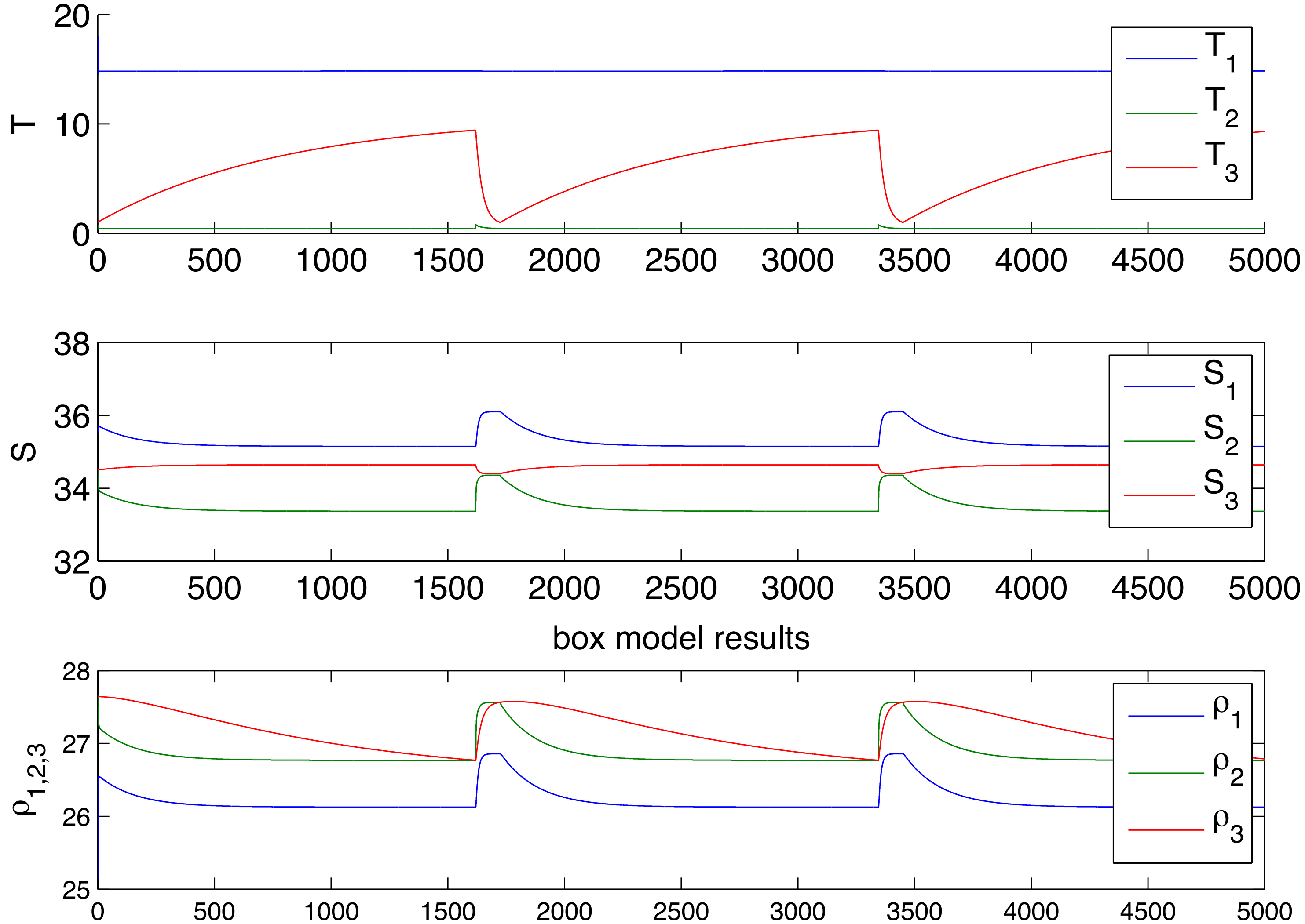

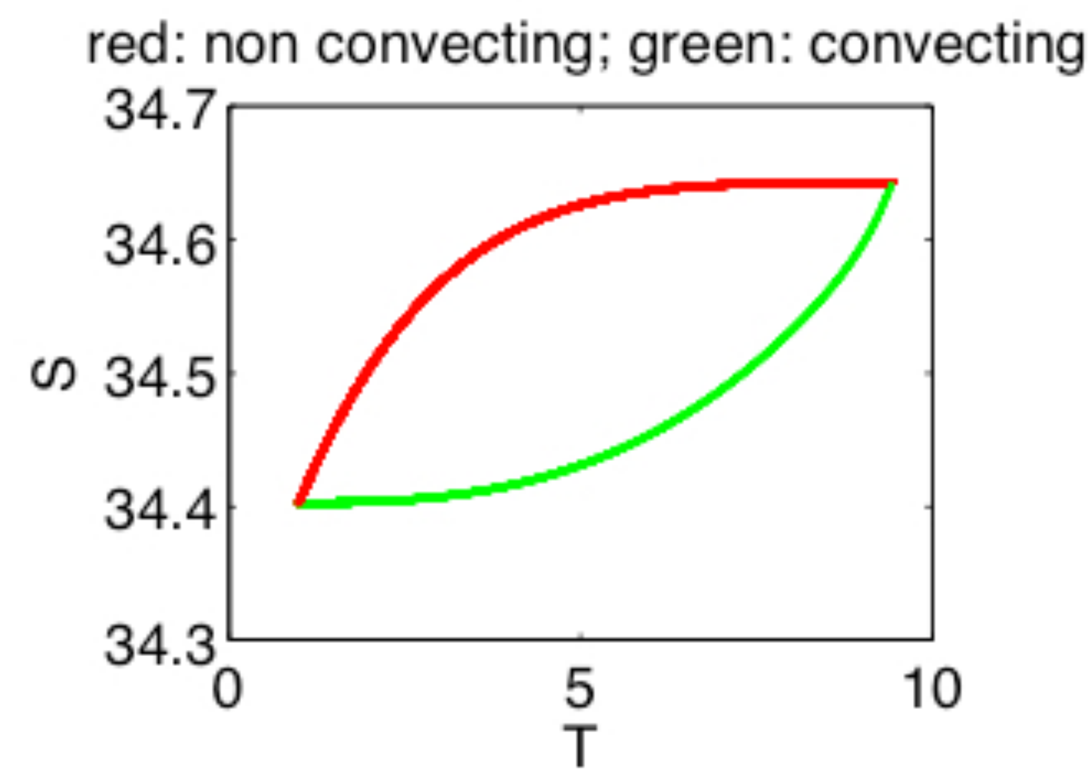

Temperature, salinity and density of all 3 boxes

T-S phase space

Winton 1993 model, based on Matlab code on course webpage

D/O-like AMOC oscillations, “flushes”

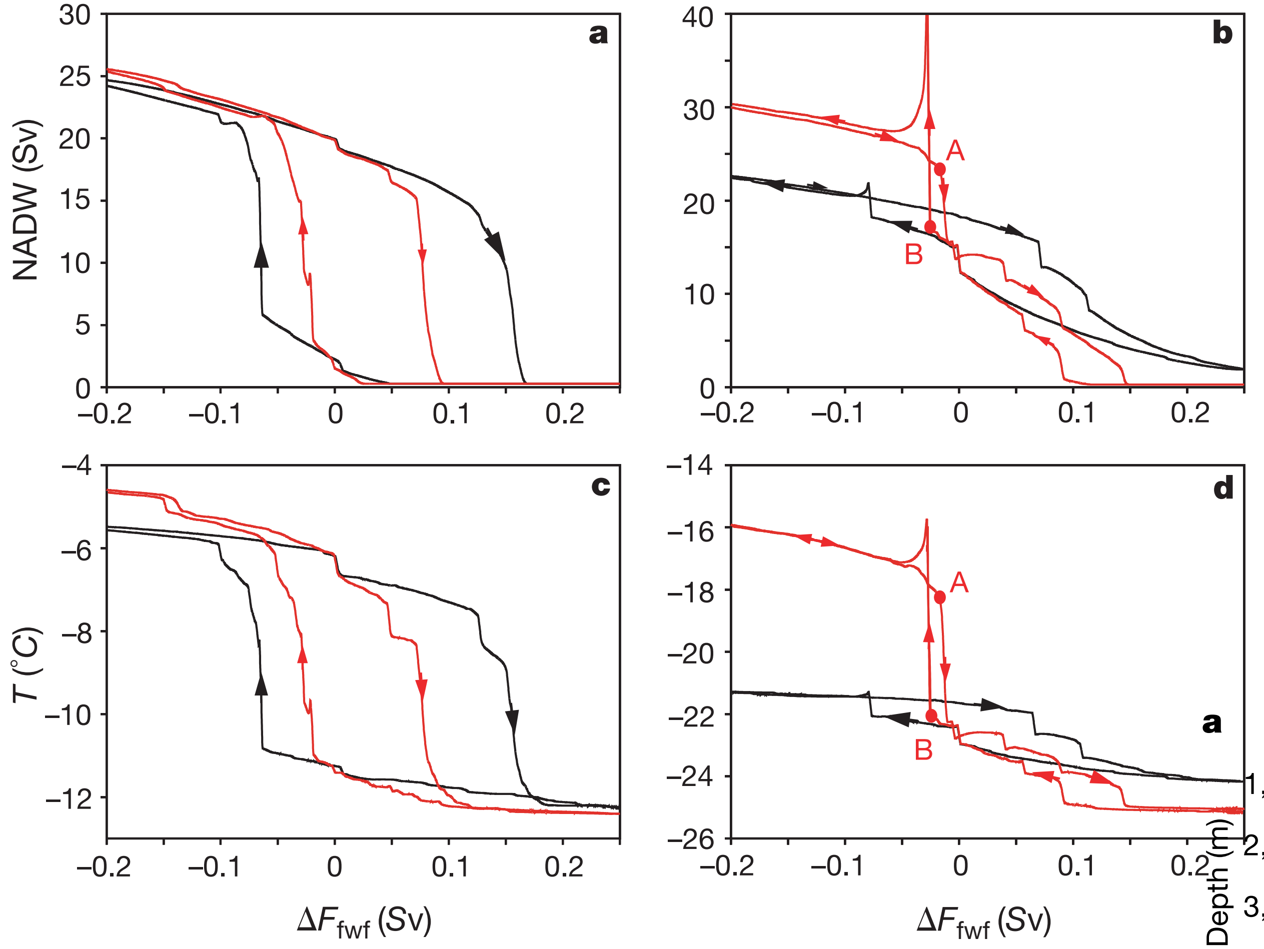

Figure 1. Stability diagrams for AMOC in a coupled model. present climate (left) differs substantially from the glacial climate (right). freshwater perturbation ΔF was added in 20–50N to obtain the black curves, and in 50–70N to obtain the red curves. a & b: AMOC. c & d: North Atlantic sector air temperature (60–70N).

present-day ‘on’

glacial warm

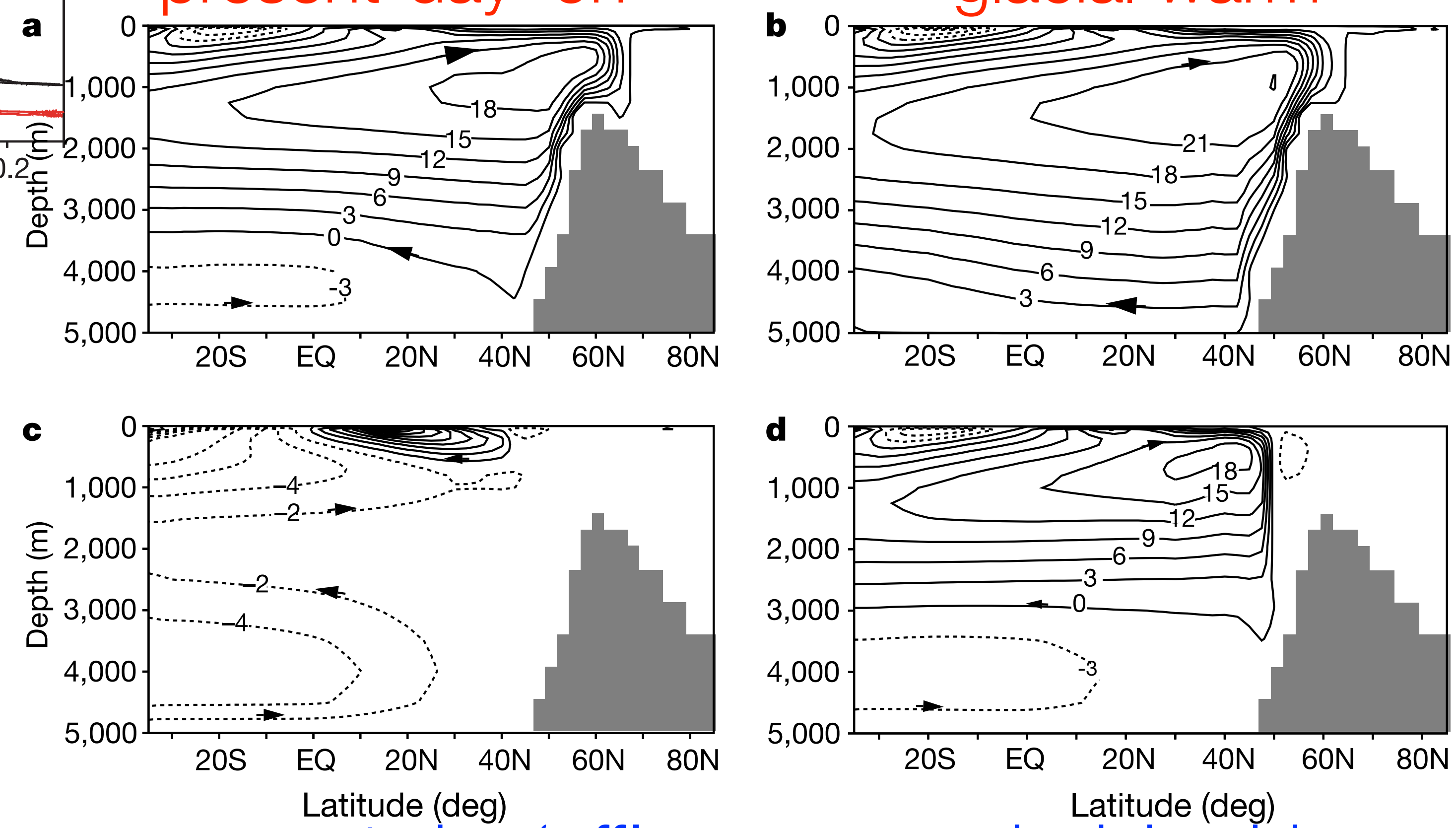

present-day ‘off’

glacial cold

Figure 2. Modes of AMOC in a coupled model. a, Holocene `warm' mode. b, Glacial `warm' (interstadial) mode. c, Holocene `off' mode. d, Glacial `cold' (stadial) mode. Shown: AMOC stream function (Sv)

Hysteresis diagrams for modern and glacial climates demonstrating the ease of making a transition between the two THC states in glacial climate;

Ganopolski & Rahmstorf 2001

D/O-like AMOC oscillations, “flushes”

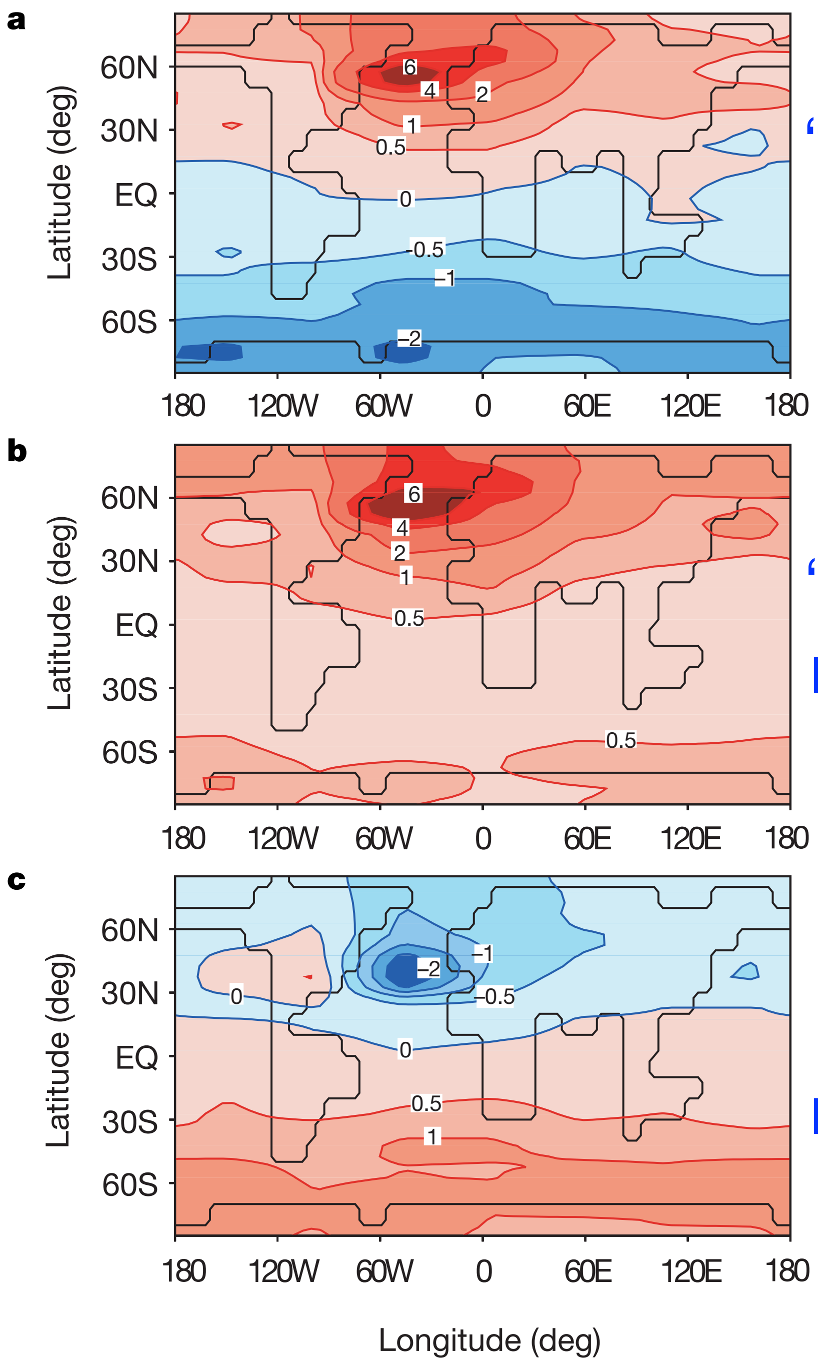

“glacial” warm minus cold

“DO” warm minus cold

“Heinrich” minus cold

Figure 3 Differences in model-simulated annual mean surface air temperature (C). a, Glacial `warm' mode (Fig. 2b) minus stadial (Fig. 2d) in equilibrium. b, Warmest phase of a D/O cycle minus stadia phase, 750 years apart (Fig. 5d). c, Heinrich event minus stadial (Fig. 5d).

Ganopolski and Rahmstorf 2001

D/O-like AMOC oscillations, “flushes”

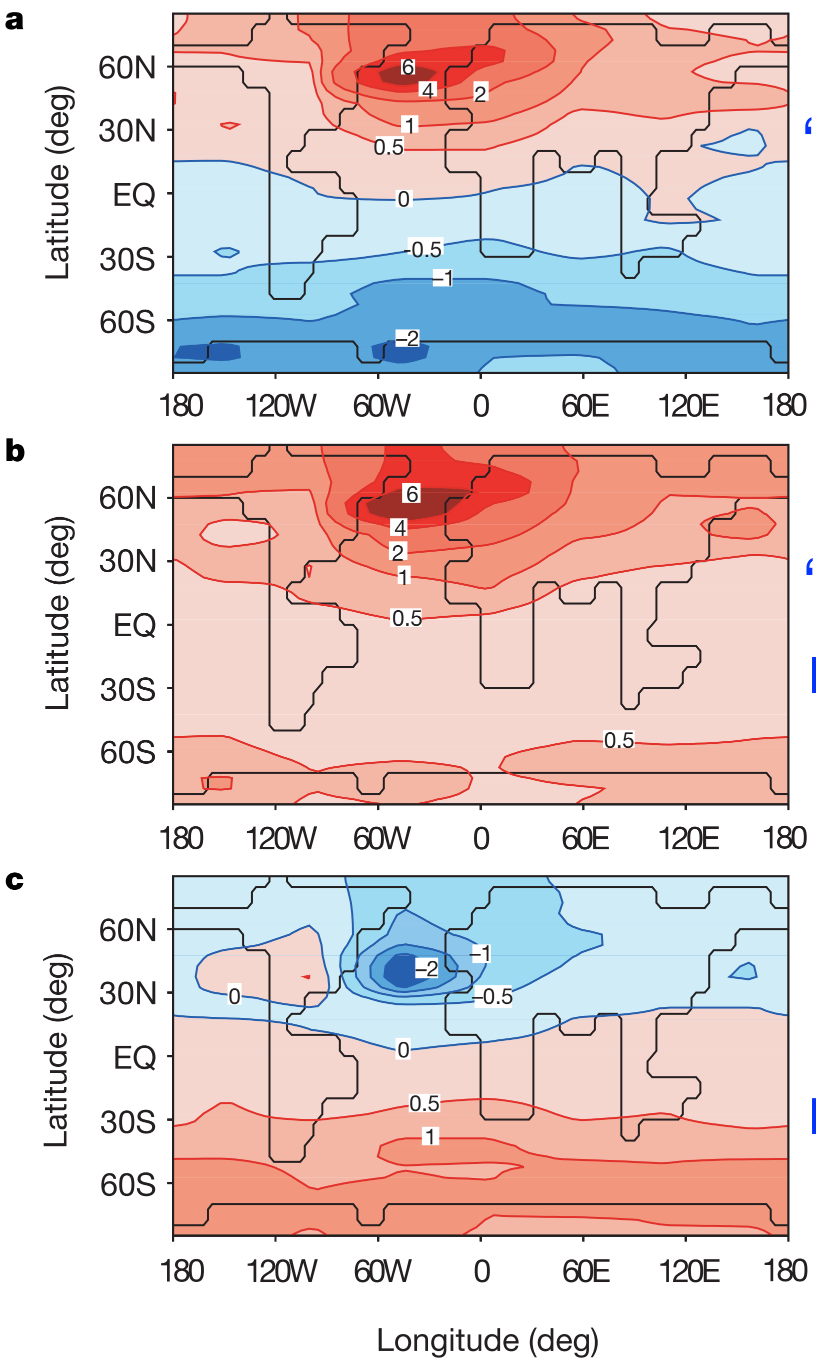

“glacial” warm minus cold

“DO” warm minus cold

“Heinrich” minus cold

Figure 3 Differences in model-simulated annual mean surface air temperature (C). a, Glacial `warm' mode (Fig. 2b) minus stadial (Fig. 2d) in equilibrium. b, Warmest phase of a D/O cycle minus stadia phase, 750 years apart (Fig. 5d). c, Heinrich event minus stadial (Fig. 5d).

AMOC

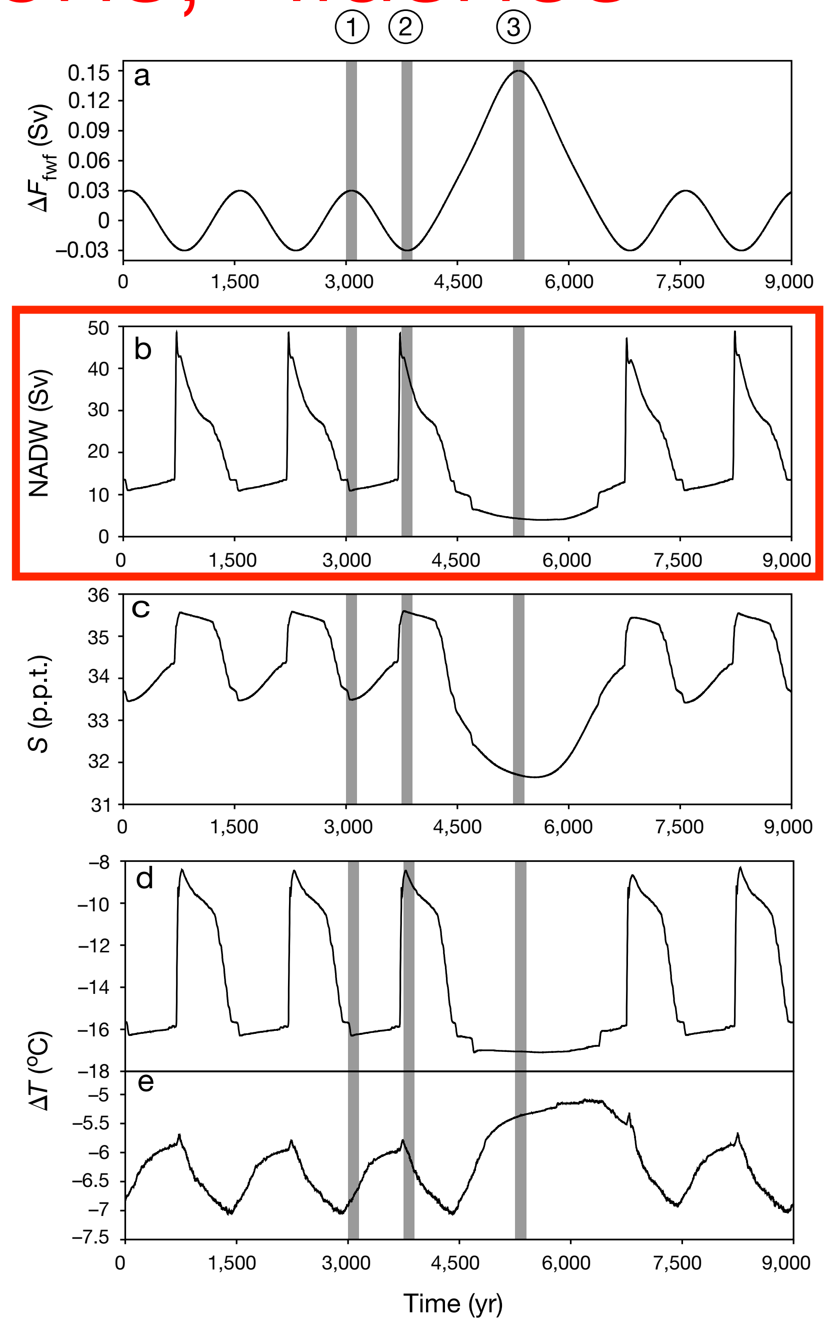

Figure 5 Simulated D/O & Heinrich events. a, Forcing, b, Atlantic overturning, c, Atlantic salinity (S) at 60N, d, air temperature in Atlantic (60-70N), & e, Antarctic temperature (difference from present-day). vertical bars: times of difference plot in Fig. 3b, c.

Ganopolski and Rahmstorf 2001

D/O-like AMOC oscillations, “flushes”

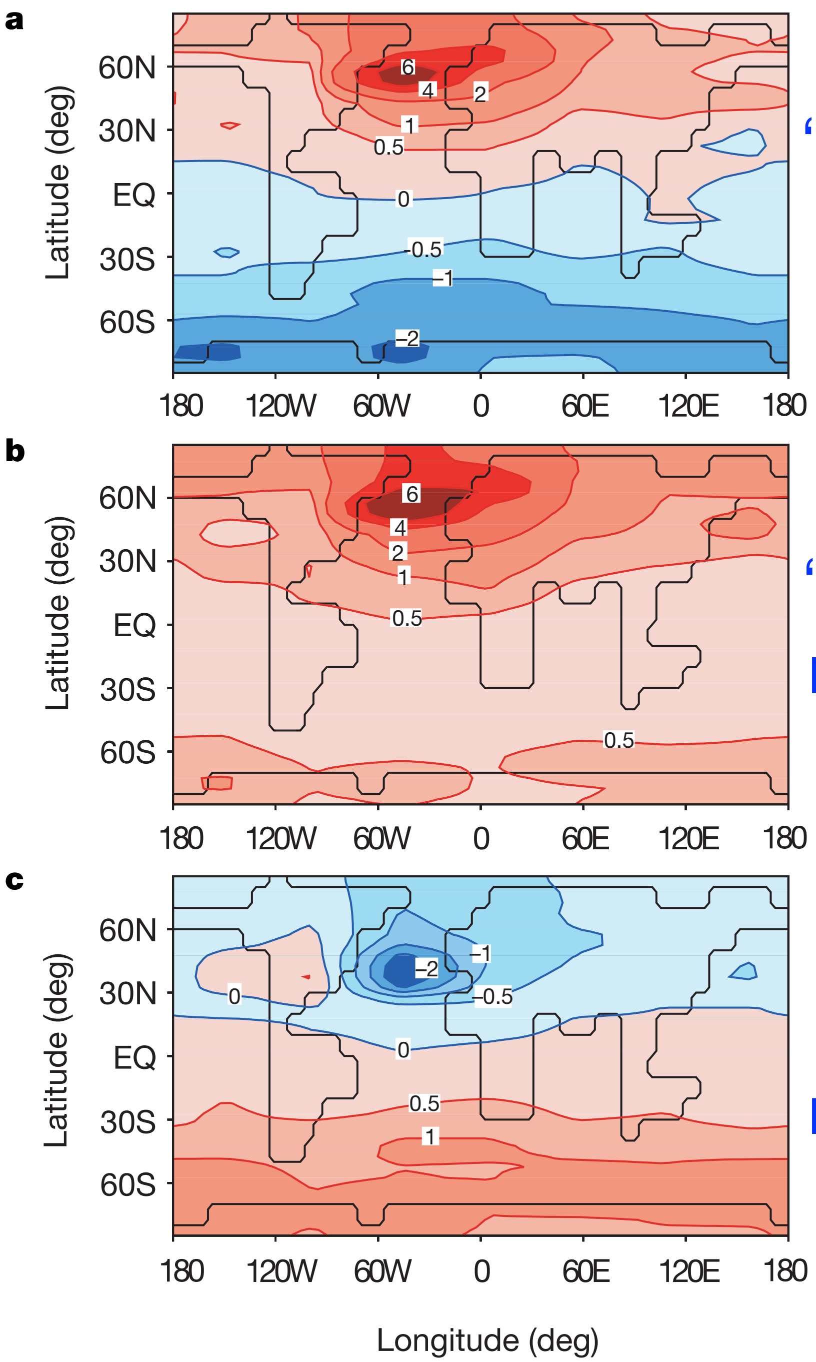

“glacial” warm minus cold

“DO” warm minus cold

“Heinrich” minus cold

AMOC

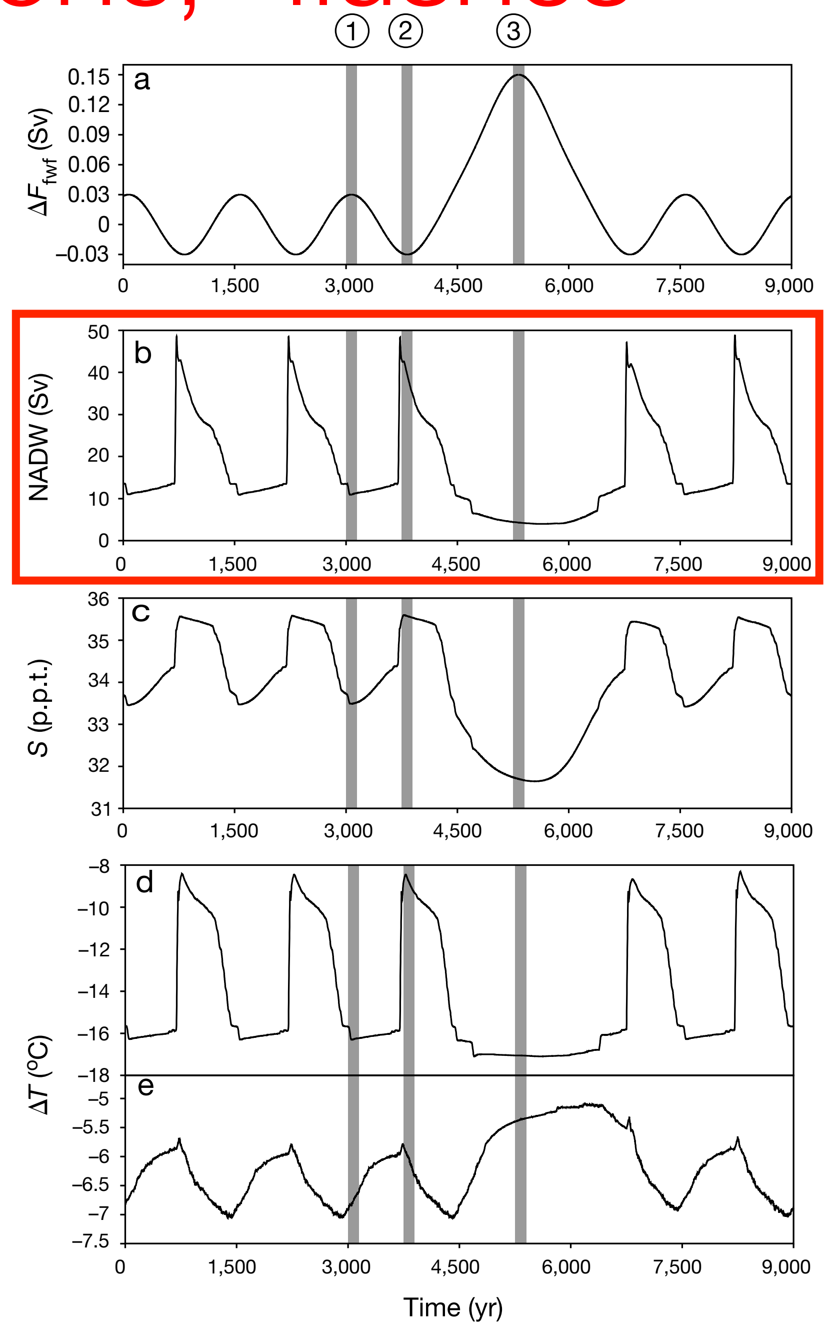

Figure 3 Differences in model-simulated annual mean surface air temperature (C). a, Glacial `warm' mode (Fig. 2b) minus stadial (Fig. 2d) in equilibrium. b, Warmest phase of a D/O cycle minus stadia phase, 750 years apart (Fig. 5d). c, Heinrich event minus stadial (Fig. 5d).

Figure 5 Simulated D/O & Heinrich events. a, Forcing, b, Atlantic overturning, c, Atlantic salinity (S) at 60N, d, air temperature in Atlantic (60-70N), & e, Antarctic temperature (difference from present-day). vertical bars: times of difference plot in Fig. 3b, c.

However: producing D/O signal requires a **very large (unrealistic?) AMOC response**

Ganopolski and Rahmstorf 2001

D/O due to weak AMOC variability amplified by sea ice changes?

Annual mean sea surface temperature boundary conditions for two atmospheric model runs

Surface air temperature difference between two runs

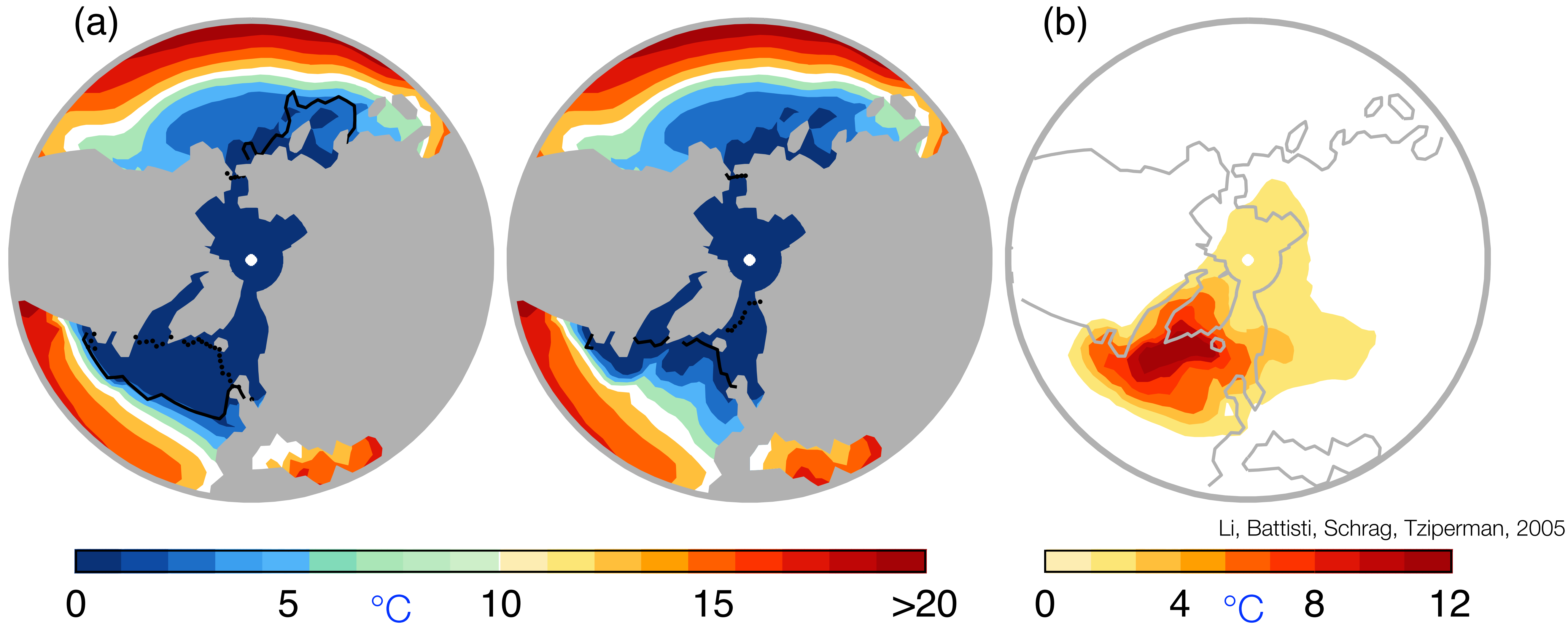

Comparison of LGM and reduced sea ice. **(a)** Annual mean SST boundary conditions (°C) for LGM (left) & reduced sea ice scenario (right). Maximum (February) and minimum (August) sea ice extents are indicated with the solid & dotted lines. The maximum sea ice extent is equivalent to LGM perennial ice cover, and the minimum to the modern day's. Ice thickness is 2 m, typical for today's Arctic. **(b)** Difference in surface air temperature between the two simulations (°C).

A modest sea ice changes can trigger a DO-like response!

D/O due to weak AMOC variability amplified by sea ice changes?

example equations for sea ice in a simple model

$$H_{\mathrm{air-sea}}(y) = \frac{\rho_o C_p^{\mathrm{water}} \Delta_{\mathrm{top}}}{\tau} [\theta(y) - T(y)] \cdot \left[f_{\mathrm{open\ ocean}}(y) + f_{\mathrm{SI}}(y) \frac{\gamma}{D_{\mathrm{SI}}(y) + 1.7\mathrm{m}} \right], \quad (3)$$

air-sea heat flux

$$H_{\mathrm{SI}\leftrightarrow\mathrm{ocean}}(y) = \frac{\rho_o C_p^{\mathrm{water}}}{\tau_{\mathrm{SI}}} \frac{V_s(y)}{\rho_{\mathrm{sea\ ice}} L_f^{\mathrm{SI}}} [T_{\mathrm{SI}} - T(y)], \quad (18)$$

heat exchange between sea ice and ocean

$$H_{\mathrm{SI}}^{\mathrm{SW}}(y) = S_{\odot}[s_1 + s_2 \cos(y)](1 - \alpha_{\mathrm{atm}}^{\mathrm{SW}}) \cdot (1 - \alpha_{\mathrm{sea\ ice}}^{\mathrm{SW}}) \frac{L_x \Delta y f_{\mathrm{SI}}(y)}{\rho_{\mathrm{sea\ ice}} L_f^{\mathrm{SI}}}. \quad (19)$$

SW absorption by sea ice

$$\frac{\partial V_{\mathrm{SI}}(y)}{\partial t} = P_{\mathrm{sea\ ice}}(y) + H_{\mathrm{SI}\leftrightarrow\mathrm{ocean}}(y) - H_{\mathrm{SI}}^{\mathrm{SW}}(y)\alpha_{\mathrm{melting}} + K_{\mathrm{SI}} \frac{\partial^2 D_{\mathrm{SI}}(y)}{\partial y^2} L_x \Delta y f_{\mathrm{SI}}(y), \quad (20)$$

sea ice volume equation given all of the above

Sayag, Tziperman & Ghil 2004

D/O due to weak AMOC variability amplified by sea ice changes?

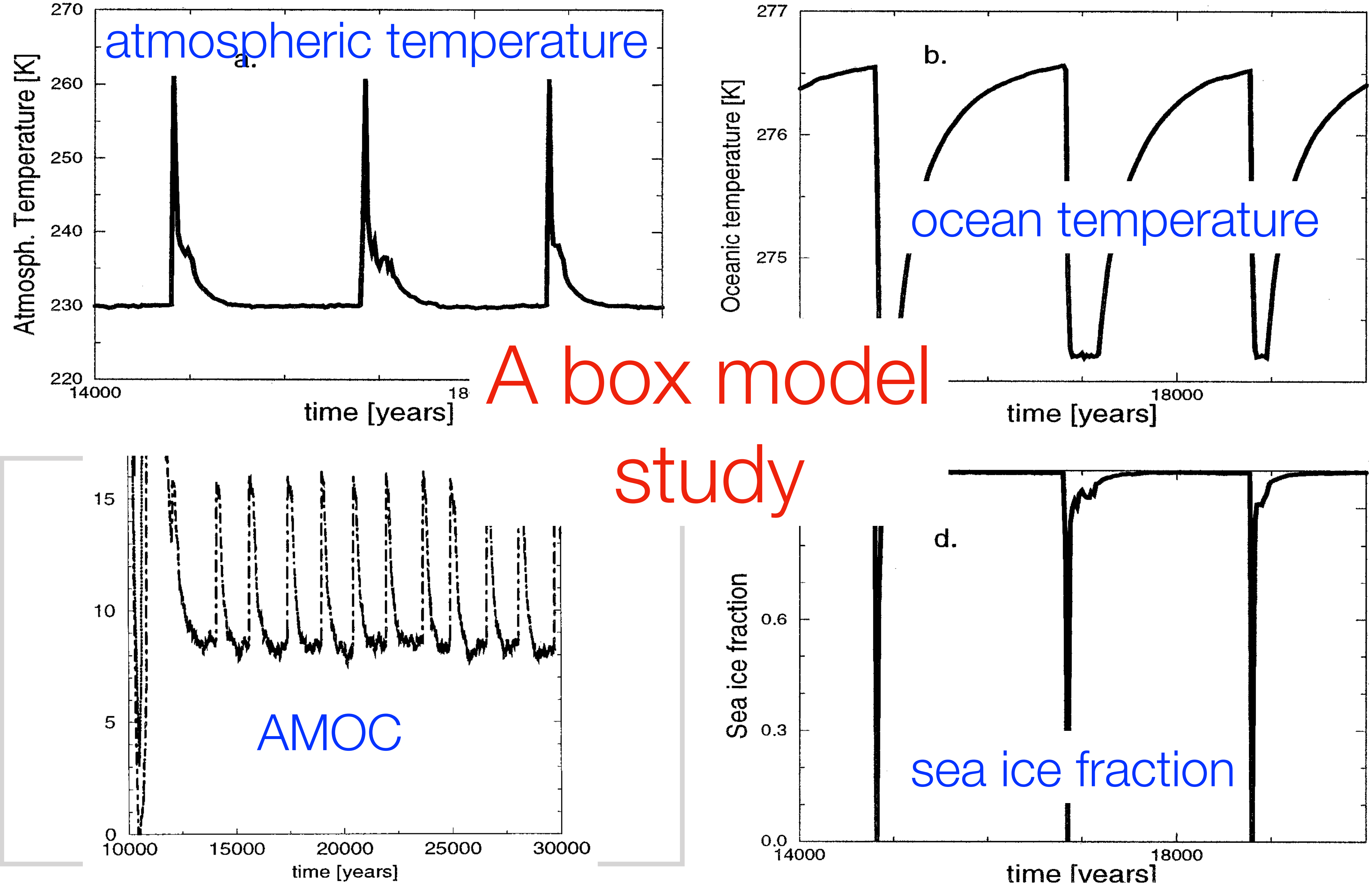

A box model study

FIG. 3. Jan atmospheric and oceanic variables corresponding to the stochastically forced meltwater experiment in Fig. 2 using a maximum freshwater anomaly of 0.45 Sv. (a) Atmospheric temperature, (b) oceanic subsurface temperature, (c) surface (solid) and subsurface (dashed) density, and (d) sea ice fraction in the northernmost box.

Weak AMOC variability ➨ sea ice ➨ large atmc temperature signal

Timmermann, Gildor, Schultz, Tziperman 2003

D/O due to weak AMOC variability amplified by sea ice changes?

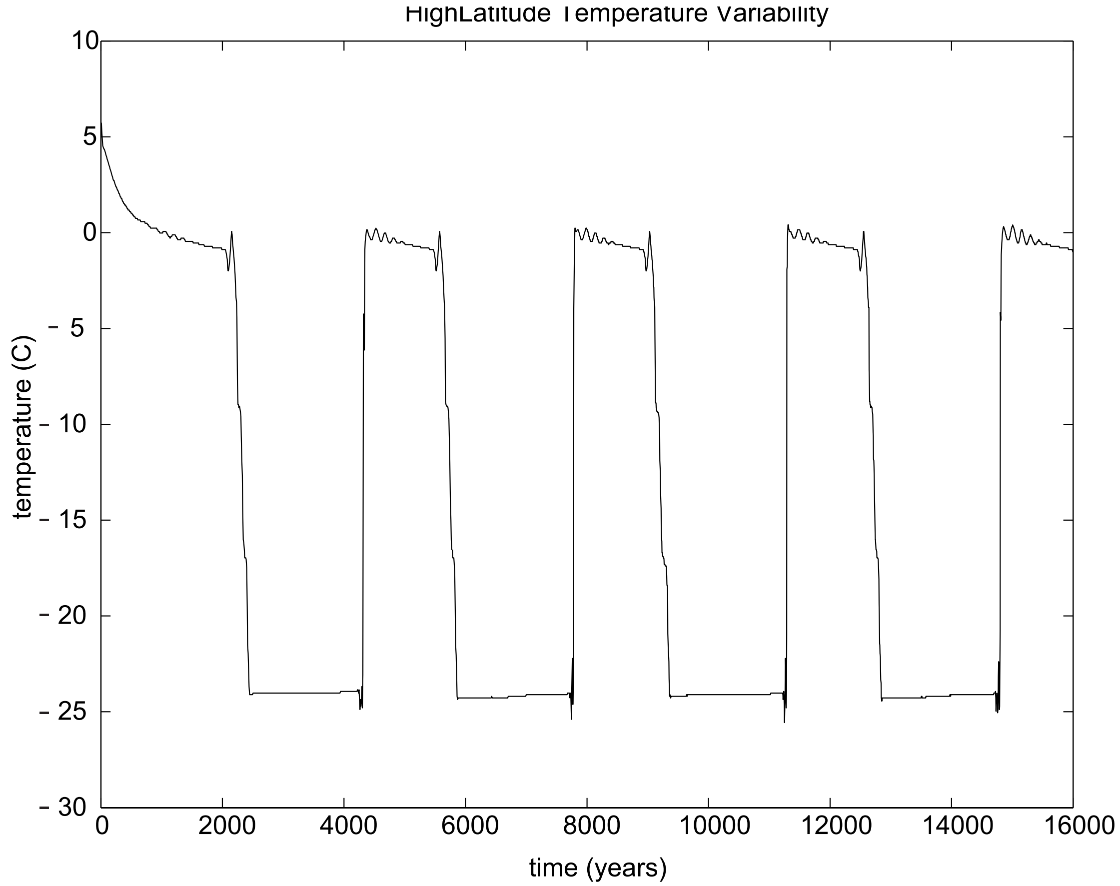

Figure 13. Time series of atmospheric temperature in the e = 0.73 experiments without stochastic forcing. There is less variability in the amplitude and period of the temperature oscillations when no stochastic forcing is applied compared to oscillations with stochastic forcing.

Figure 8. Time series of oceanic (red) and atmospheric (blue) meridional heat transport at (top) 50°N and (center) 40°N. (bottom) Maximum overturning circulation in sverdrups (red) and sea ice thickness (blue). The oceanic heat transport (red) increases over both warming cycles at 40°N, and the atmospheric heat transport (blue) decreases. (top) The increase in meridional heat transport by the ocean is accompanied by (bottom) an increase in mass transport by the ocean. The reduction in heat transport by the atmosphere is associated with a reduction in the atmospheric temperature gradient (Figure 6). The (top) 50°N location is near the sea ice edge where the meridional temperature gradient in the atmosphere is very large.

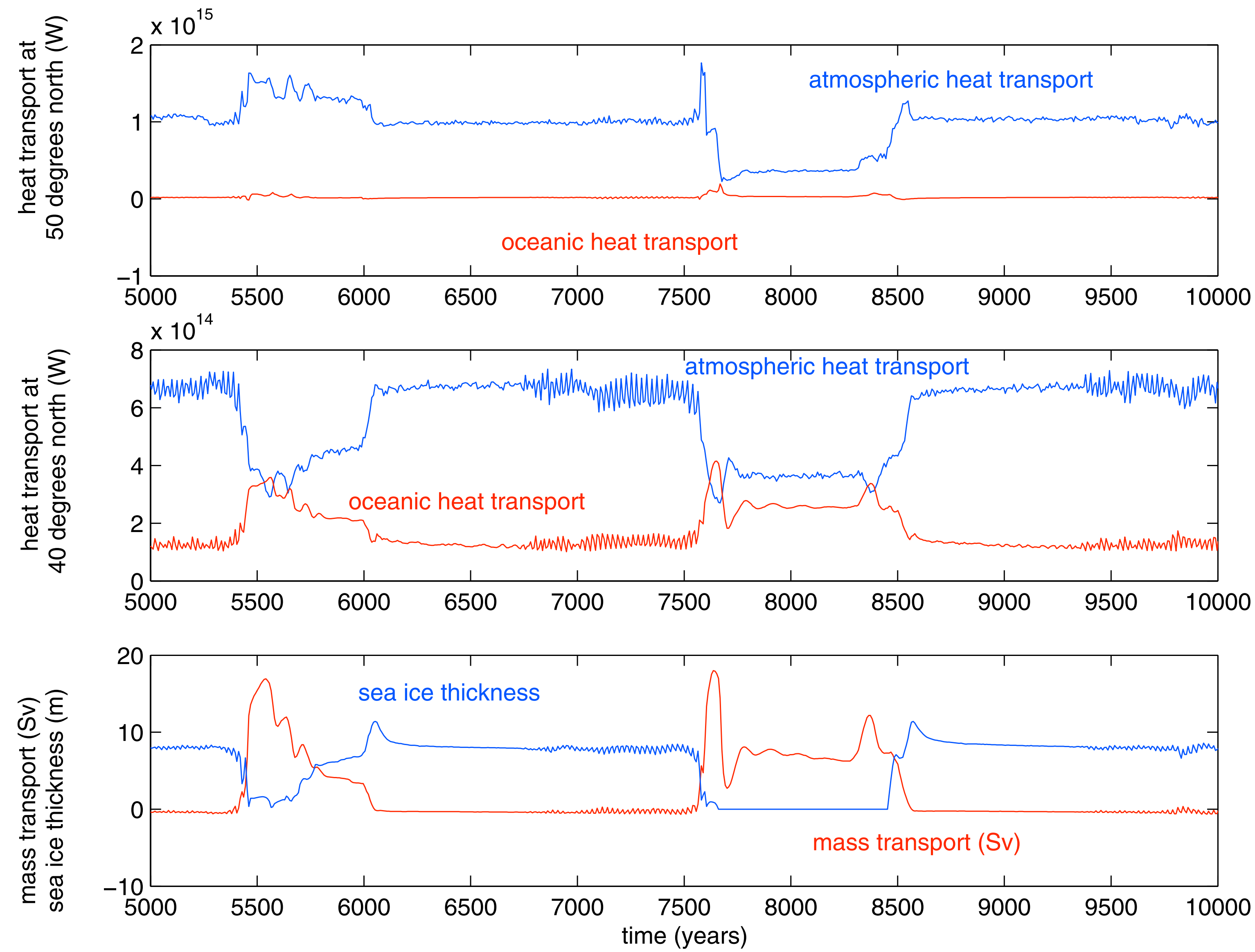

A GCM study

Weak AMOC variability ➨ sea ice ➨ large atmc temperature signal

Loving, Vallis 2005

Precise D/O clock?! Every 1470 years?

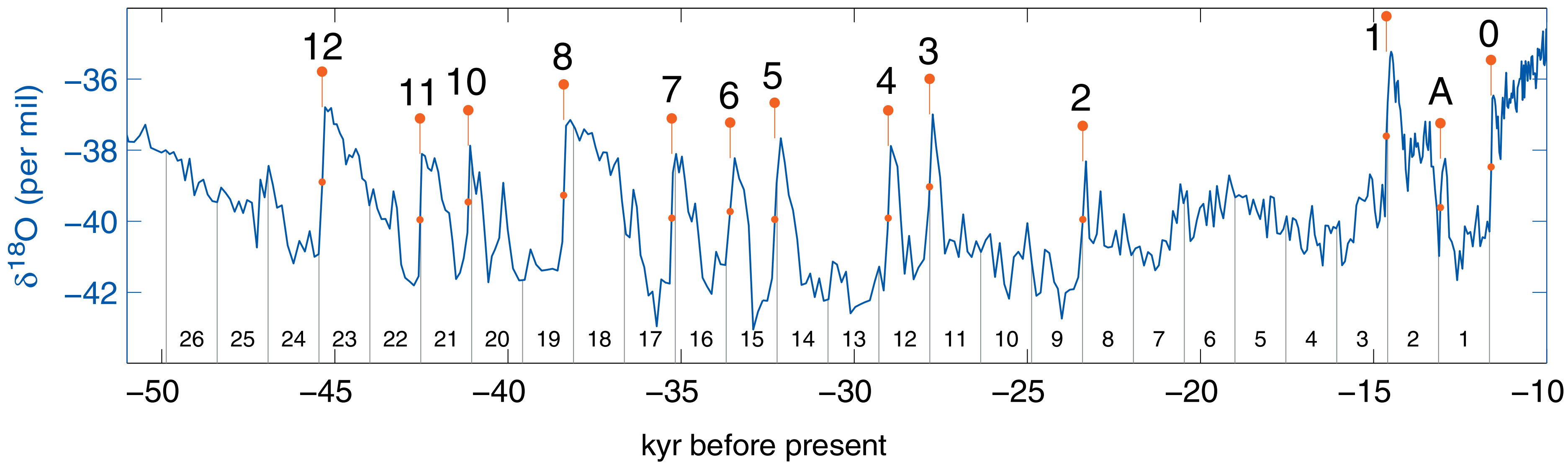

Figure 1. The GISP2 climate record for the second half of the glacial. Dansgaard-Oeschger warming events found by the objective detection algorithm are labeled with red flags. The grey vertical lines show 1,470-year spacing, small numbers at the bottom count the number of 1,470-year periods from DO event 0.

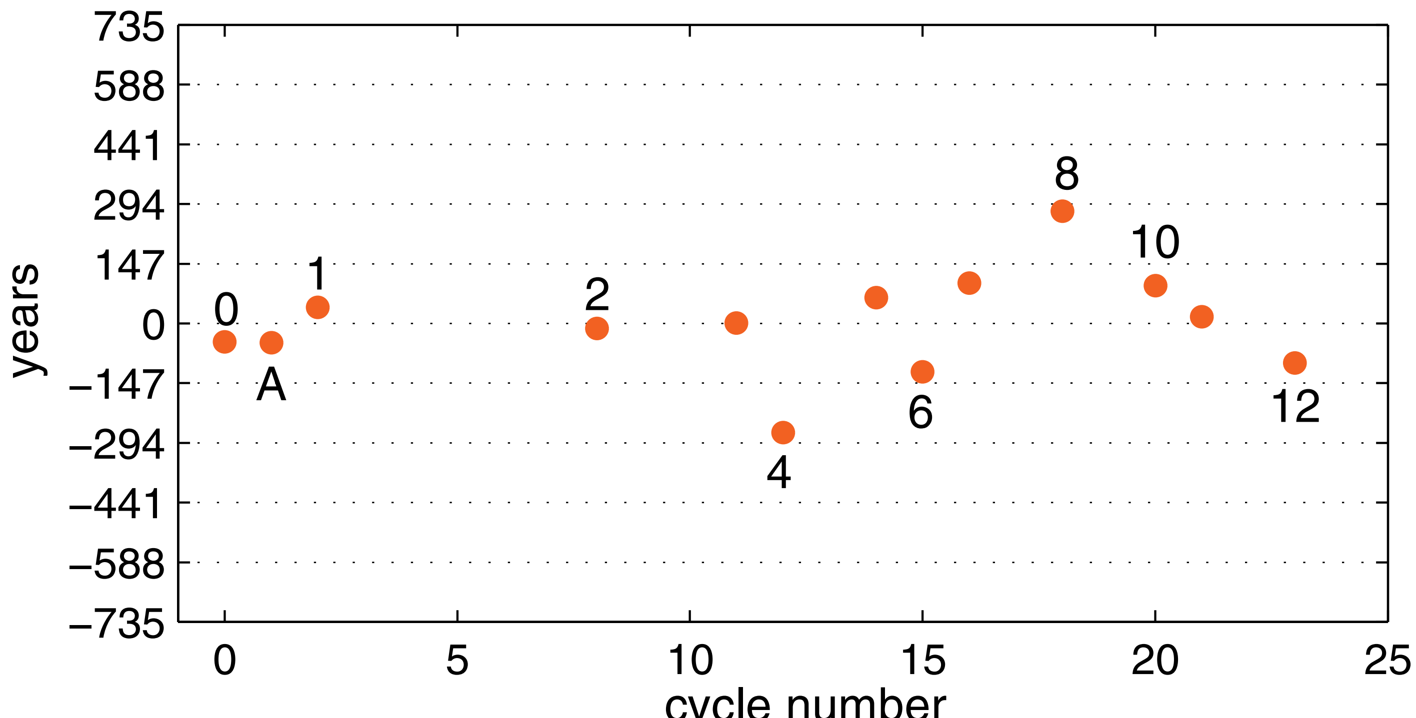

Figure 2. Time deviation δ_i for each DO event from the grey lines in Figure 1, labelled with event number.

Rahmstorf 2003

reminder: AMOC variability: stochastic resonance

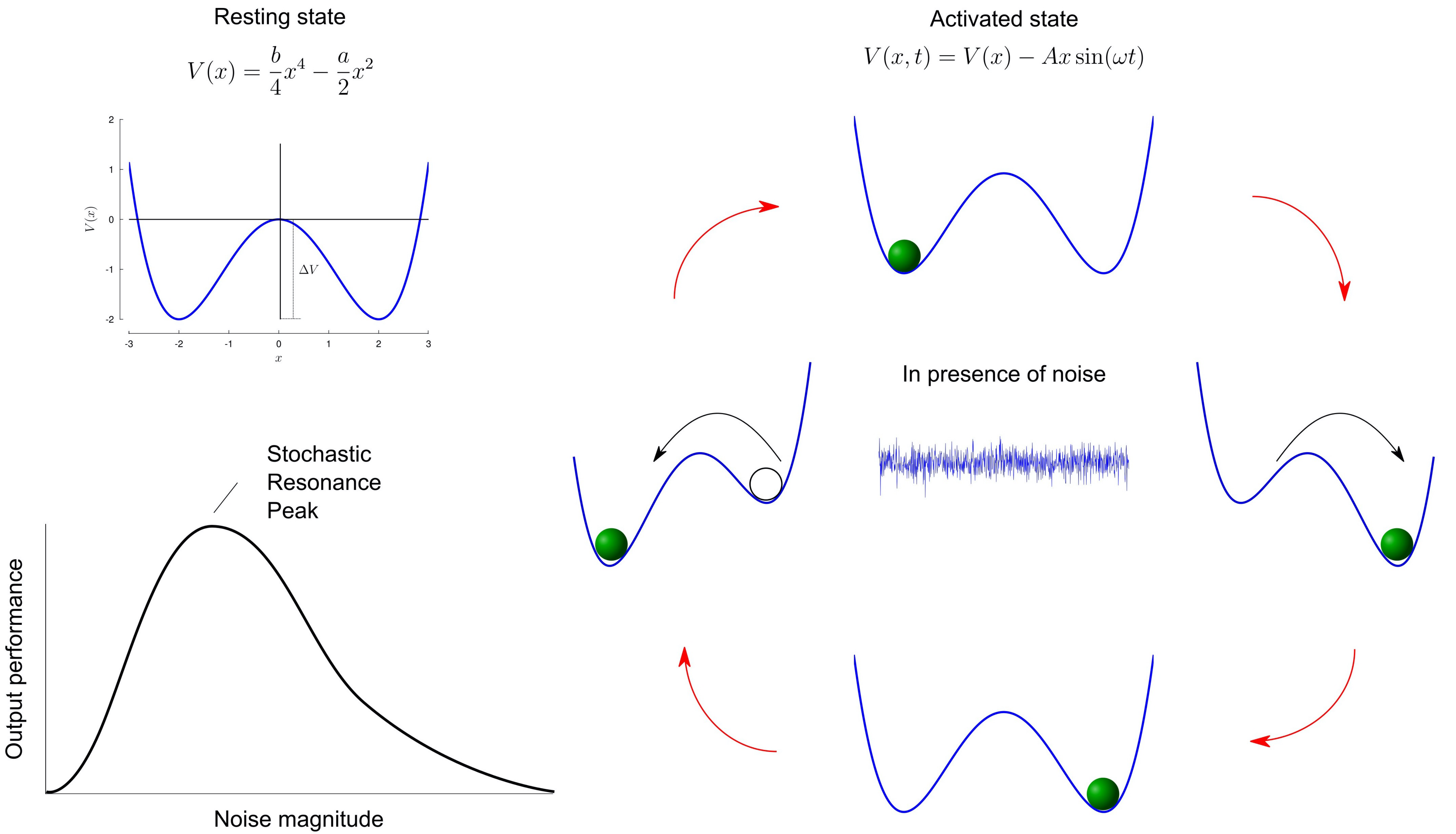

FIGURE 1 | Mechanism of stochastic resonance. **(A)** Sketch of a double well potential V(x). In this example, the values a and b are set to 2 and 0.5, respectively. The minima are located at $x = \pm\sqrt{\frac{a}{b}}$ and are separated by a barrier potential $\Delta V = \frac{a^2}{4b}$. **(B)** In the presence of periodic driving, the height of the potential barrier oscillates through an antiphase lowering and raising of the wells. The cyclic variations are depicted in the cartoon. A suitable dose of noise (represented by the central white noise plot) will allow the marble to hop to the globally stable state. **(C)** Typical curve of output performance versus input noise magnitude, for systems capable of stochastic resonance. For small and large noise, the performance metric is very small, while some intermediate non-zero noise level provides optimal performance. Panels **A,B** adapted from Gammaitoni et al. (1998).

White et al, 2019, doi:10.3389/fphys.2018.01865

reminder: AMOC variability: stochastic resonance

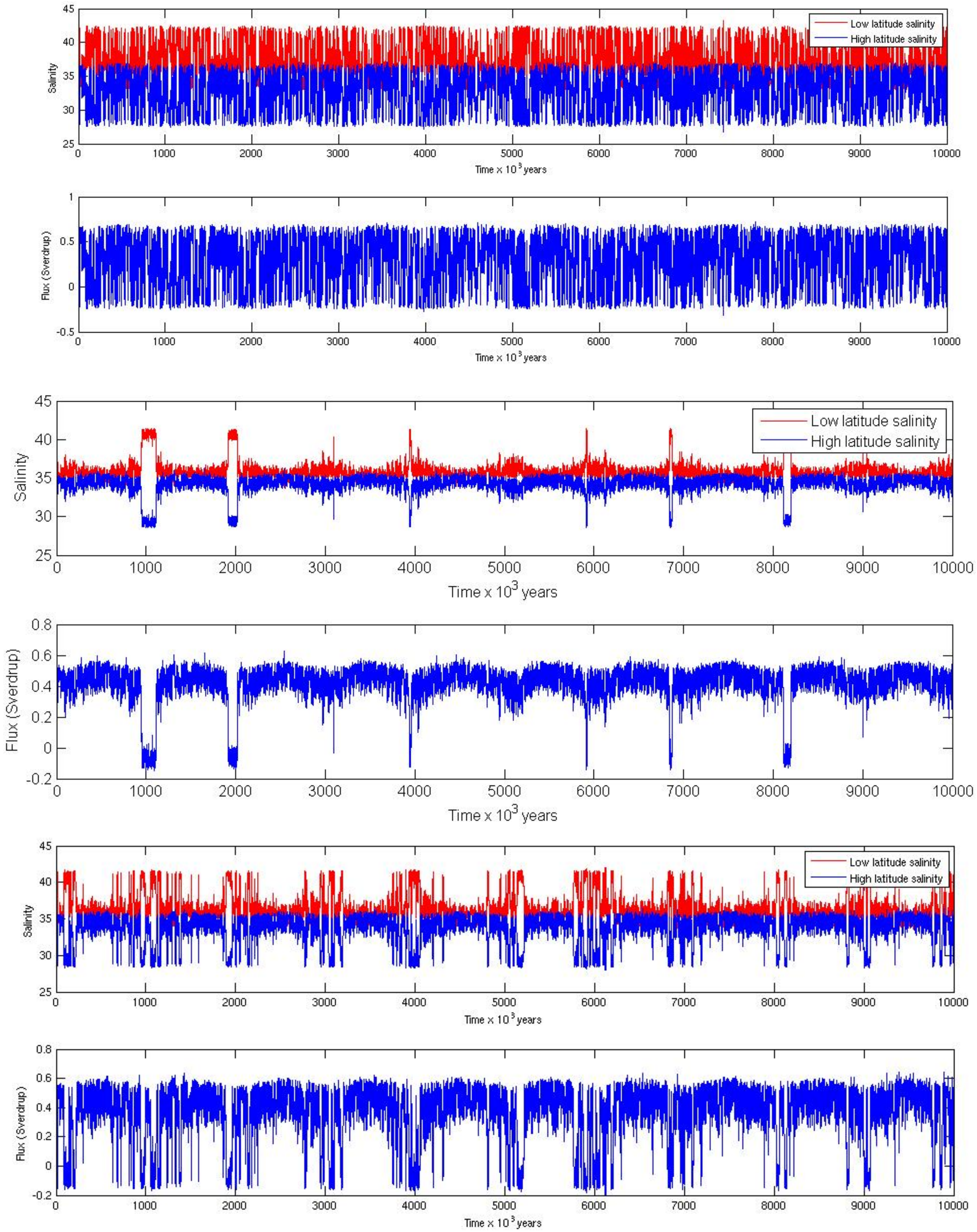

strong forcing, frequent transitions

weak forcing, rare transitions

‘optimal’ forcing, periodic transitions

Stommel model under periodic+stochastic FW forcing based on code on course webpage

D/O = perfect clock due to stochastic resonance?

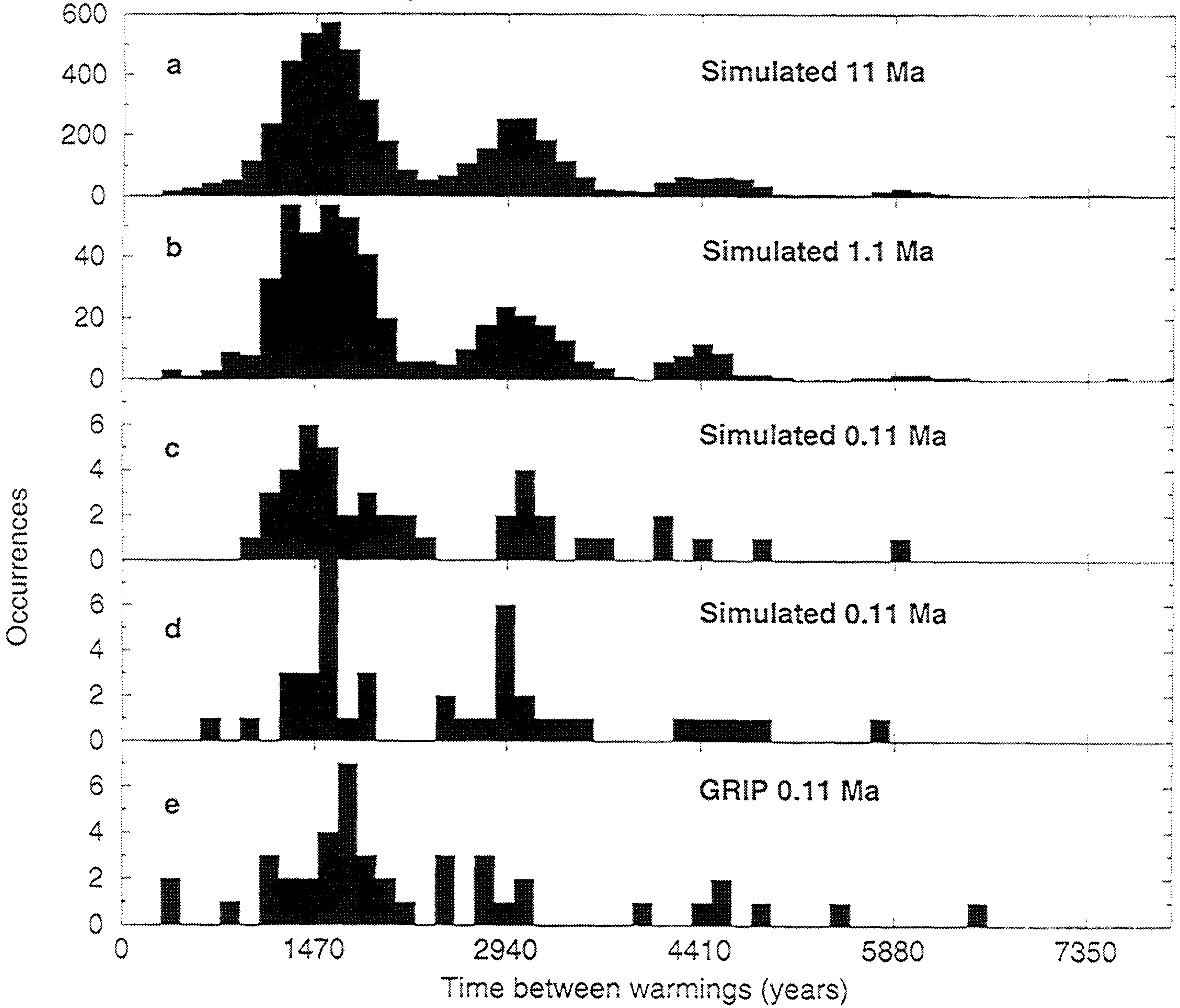

Figure 2. Number of occurrences of different waiting times between warmings for: (figure 2a) a simulated stochastically resonant time series 100 times longer than the GRIP data; (2b-d) subsets of that simulated time series that are 10x longer than GRIP (figure 2b) and of the same length as GRIP (figures 2c and 2d,); and (figure 2e) the observed GRIP ice-core data (150-year samples, high-pass cutoff of 7000 years, and d=0.25 or ~20% of the standard deviation of the resampled and high-pass-filtered data). The long-simulated series has the expected stochastically resonant pattern. The shorter subsets display deviations from this pattern related to the smaller sample size. The GRIP data are more similar to the long-simulated series than one of the two shorter subsets shown and than about one quarter of all GRIP-length subsets examined, based on chi-square testing.

Alley et al 2001

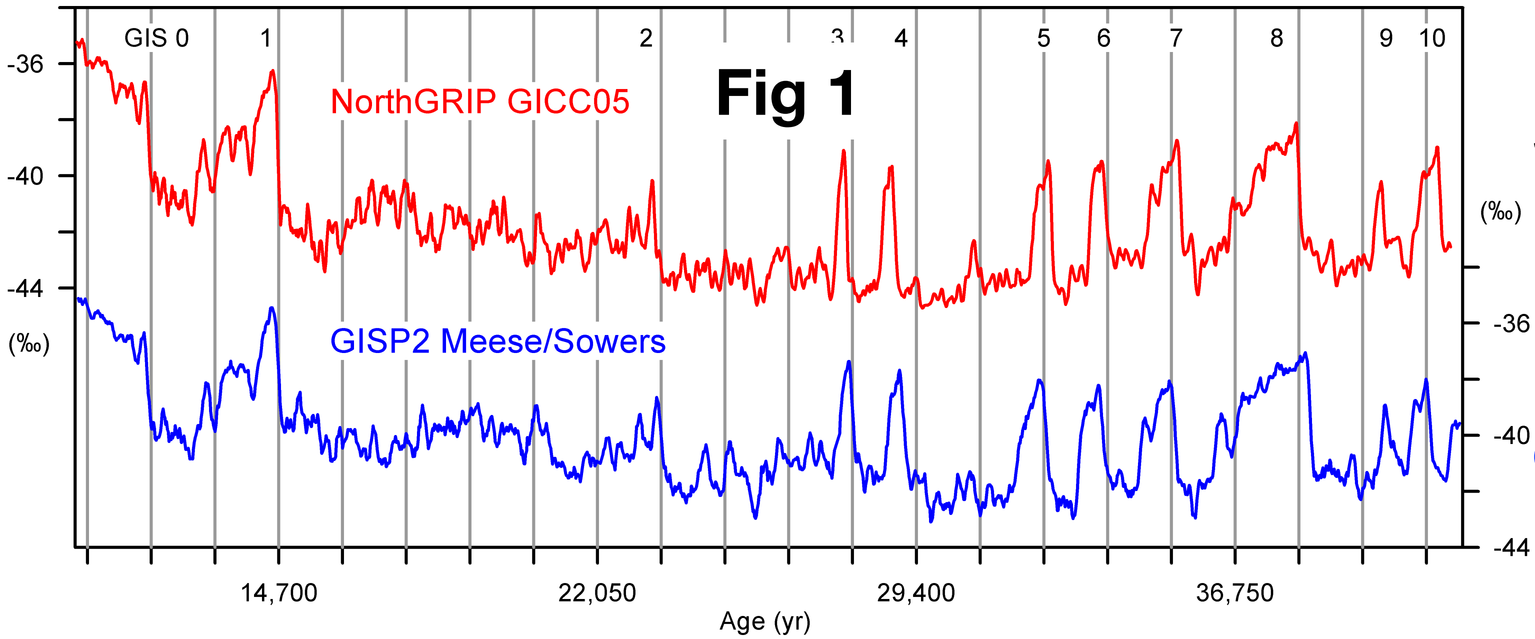

problem 1: new dating/ data does not seem to have 1470 periodicity

(‰) new

old

Ditlevsen et al 2007

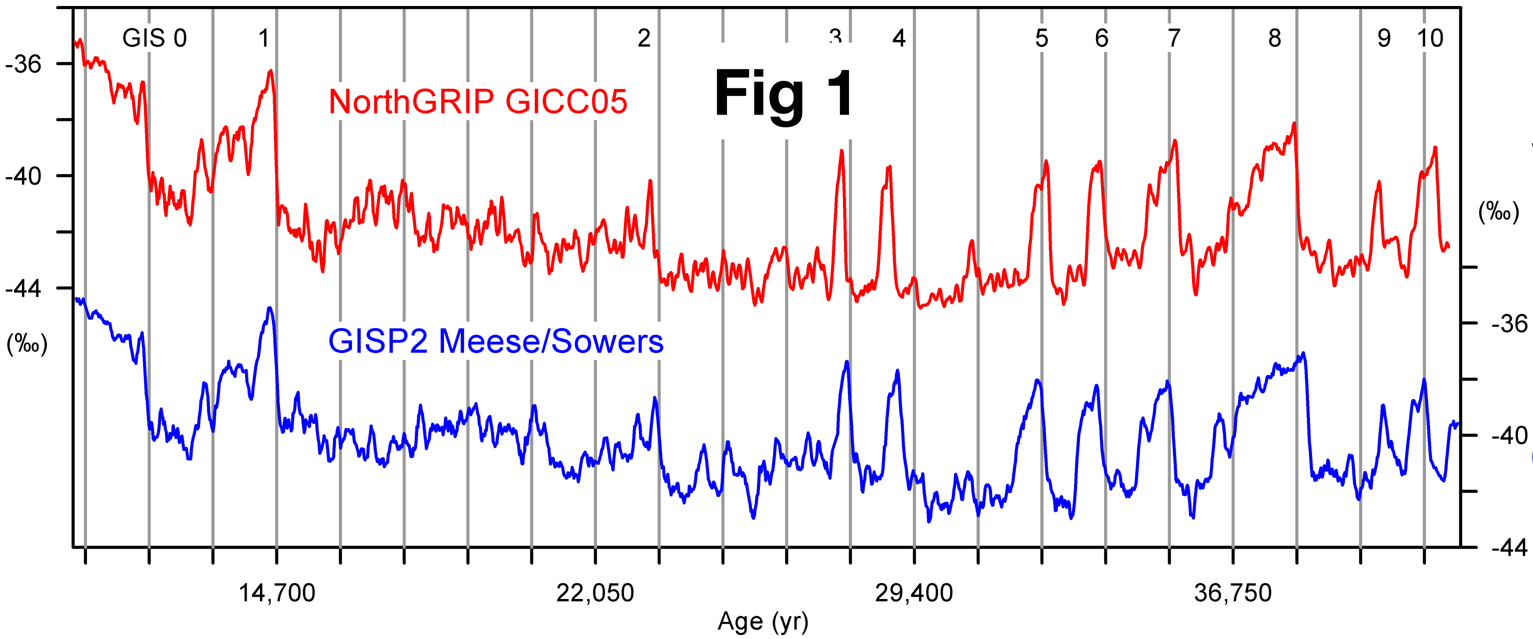

problem 1: new dating/ data does not seem to have 1470 periodicity

new

old

Problem 2: even older data do not satisfy Rayleigh test for periodicity

$$R(\tau) = (1/N)\,|\,\Sigma_j \cos(2\pi t_j/\tau) + i\sin(2\pi t_j/\tau)\,|$$

t_j = DO times

red dots: old NGRIP dating
blue: new GISP2 dating

The period τ is selected to maximize $R(\tau)$

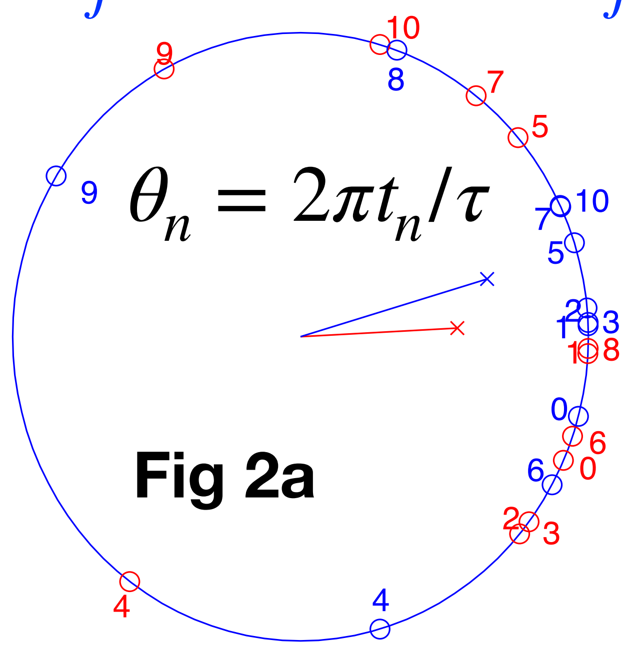

Ditlevsen et al 2007

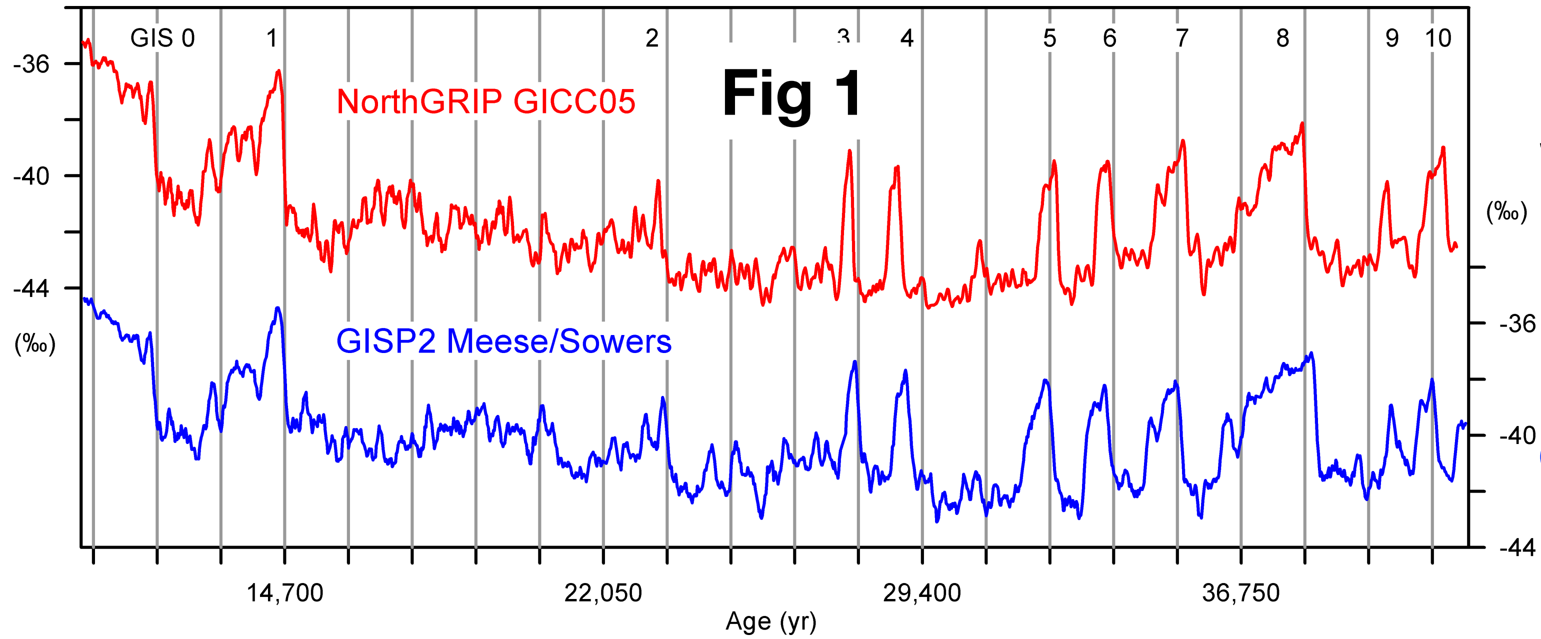

Fig 1

problem 1: new dating/ data does not seem to have 1470 periodicity

new

old

Problem 2: even older data do not satisfy Rayleigh test for periodicity

$$R(\tau) = (1/N)\,|\,\Sigma_j \cos(2\pi t_j/\tau) + i\sin(2\pi t_j/\tau)\,|$$

t_j = DO times

red dots: old NGRIP dating

blue: new GISP2 dating

The period τ is selected to maximize $R(\tau)$

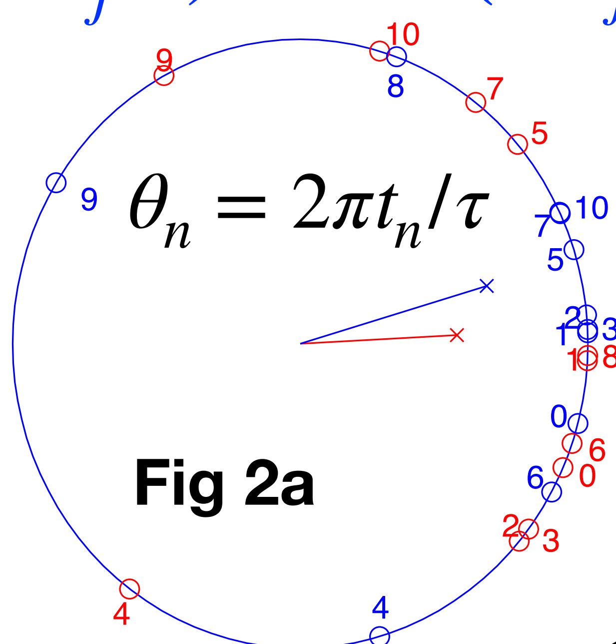

Fig 2a

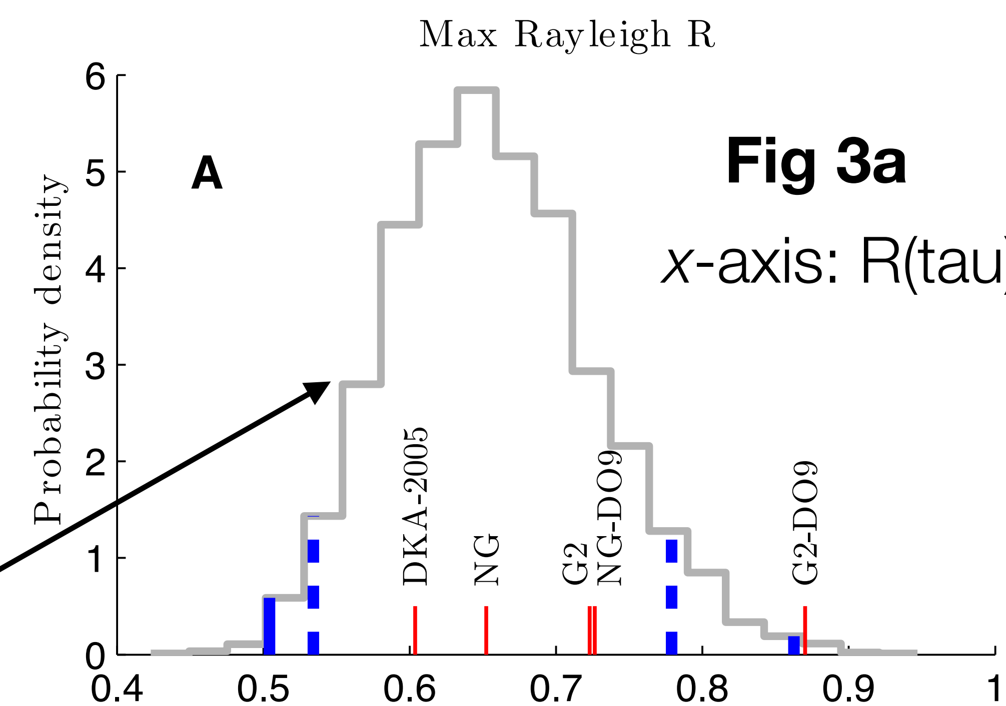

Fig 3a

x-axis: R(tau)

1. gray: random simulations: an exponential distribution w/avg wait time of 2800 yrs
2. blue: (dash) 90% and (solid) 99% of random simulations
3. red: Greenland data, different date models; also: G2-D09: removing event #9

Ditlevsen et al 2007

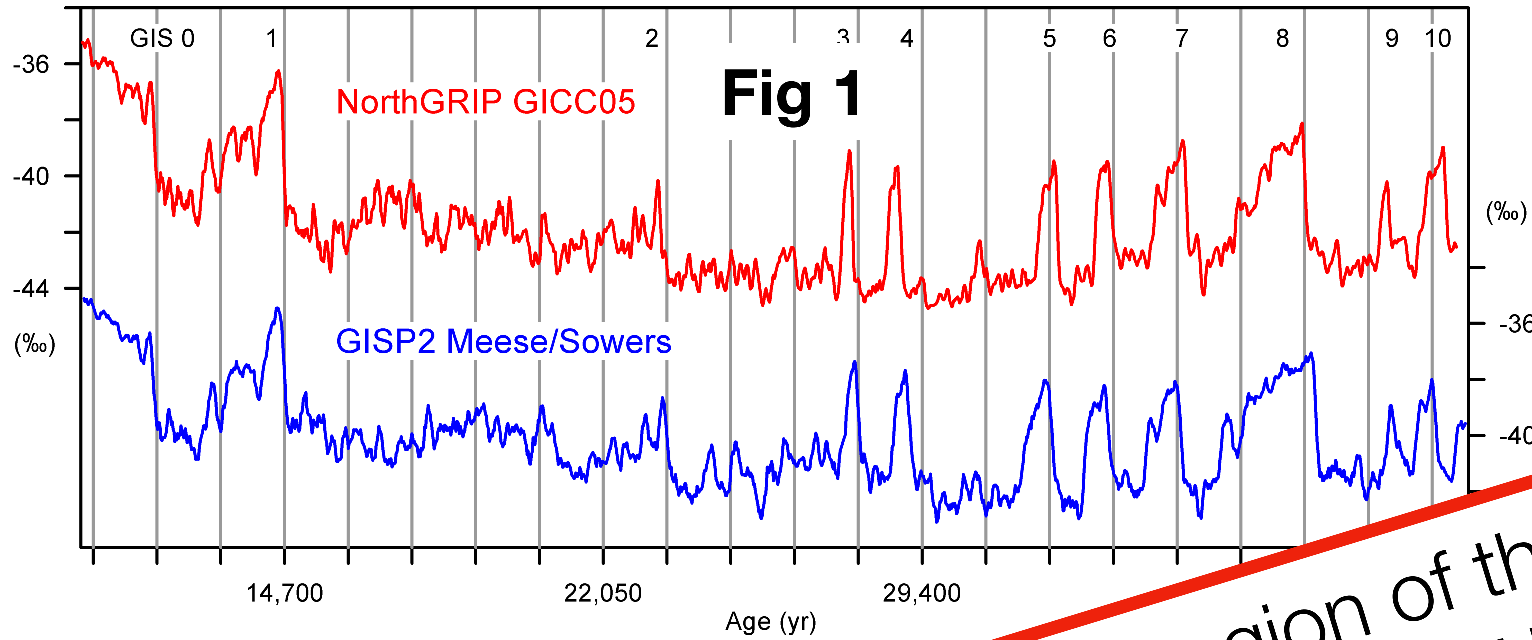

problem 1: new dating/ data does not seem to have 1470 periodicity

(‰) new

-36

-40 old

Problem 2: ev

$R(\tau) = (1/N)$

“Data fall within high likelihood region of the exponential distribution. Thus no basis for rejecting hypothesis of [random] data. An exception is the **curious** case of GISP2 dating w/o [event] DO9, where random model can be rejected at the 99% confidence level.”

re

blu ting

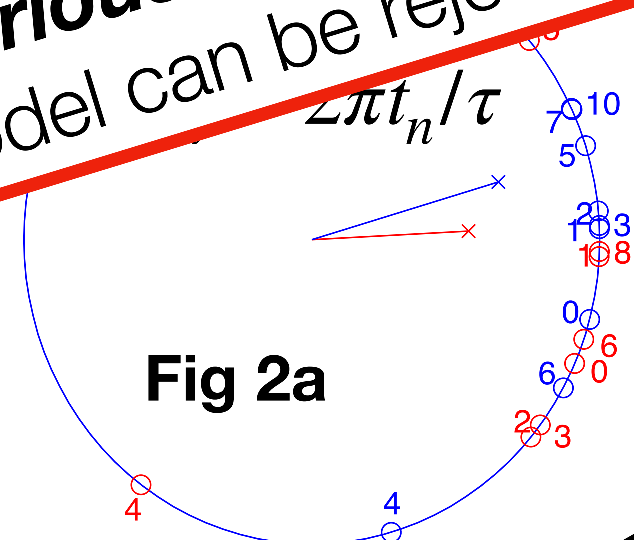

The period τ is selected to maximize $R(\tau)$

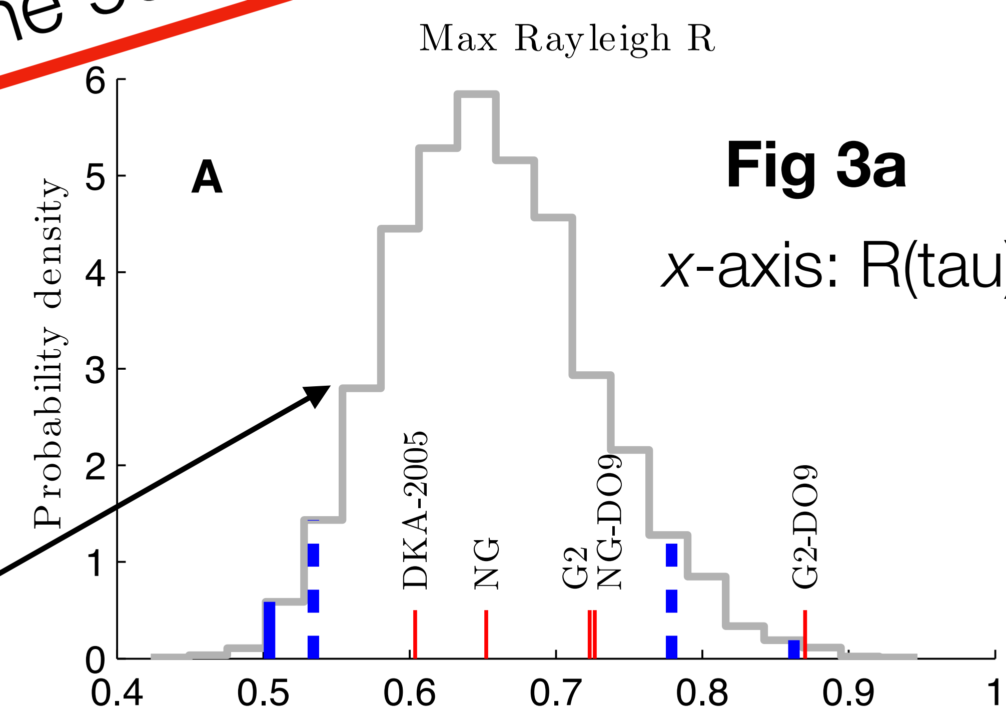

1. gray: random simulations: an exponential distribution w/avg wait time of 2800 yrs
2. blue: (dash) 90% and (solid) 99% of random simulations
3. red: Greenland data, different date models; also: G2-D09: removing event #9

Ditlevsen et al 2007

Precise D/O clock?! Every 1470 years?

captions for figures on previous slide

Fig. 1. The δ^{18}O isotope records from NGRIP and GISP on their stratigraphic time scales (Alley et al., 1997; Andersen et al., 2006). The vertical bars are separated by 1470 years. The analysis focus on the well defined fast onsets of DO events, which are the transitions from the stadial to the interstadial states. Beginning at GIS0 the onset for the DO events are for the NGRIP GICC05 (GISP2) time scale: 11 700 (11 660); 13 130 (13 180); 14 680 (14 700); 23 340 (23 560); 27 780 (27 920); 28 900 (29 100); 32 500 (32 400); 33 740 (33 700); 35 480 (35 360); 38 220 (38 480); 40 160 (40 280); 41 460 (41 240). Ages are b2k=BP+50 years.

Fig. 2. The Rayleigh R test for the two records. The maximum is obtained for the period τ=1470 years. Left panel shows the timing of the onsets t_n plotted on the unit circle using the transformation $\theta_n = 2\pi t_n/\tau$. The red dots represents the NGRIP dating (NG) while the blue dots represents the GISP2 dating (G2). The segments of radians points at the mean phase, corresponding to the vertical bars in Fig. 1 (for NGRIP dating).

Fig. 3. Panels **(A)** and **(B)**: By Monte Carlo an ensemble of 1000 realizations of waiting times in a 40 kyr period has been generated from an exponential distribution with mean waiting time of 2800 years, corresponding to 14 DO-events in 40 kyr. This gives probability densities for the maximal Rayleigh's $R(\tau)$ in the range 500 yr$<\tau<$5000 yr and for the "Standard deviation of residual" (see text). The red bars give the values for the ice-core records (see text). The blue bars are 90% (dashed) and 99% (full) confidence levels. Panels **(C)** and **(D)**: Same as panels (A) and (B), where now the distribution functions are obtained for a perfect 1470 year periodic signal subject to a dating error taken to be a gaussian with standard deviation of 100 years. Panels **(E)** and **(F)**: Same as panels (A) and (B), with distribution functions obtained from stochastic resonance models with period of 1470 years. From light to dark green the model parameters are: a=0.1, 0.2, 0.4 and σ=0.38, 0.35, 0.27 (see text), which generates on average 11 DO-events in 31 kyr. The important difference from the case shown in the panels above is that the Rayleigh's R and Std. dev. of residual in this case are calculated for the fixed period of 1470 yr. The red bars are ice-core data as above. The gray curves are the distributions for the exponential model repeated from the top panels. This shows that the SR model with a=0.1 cannot be identified in a sample, since spurious coincidental periodicities will give a better match to the data than the 1470 yr cycle.

Ditlevsen et al 2007

D/O teleconnections: observations

Remote relationships with DO events: test for covariance between time-uncertain series

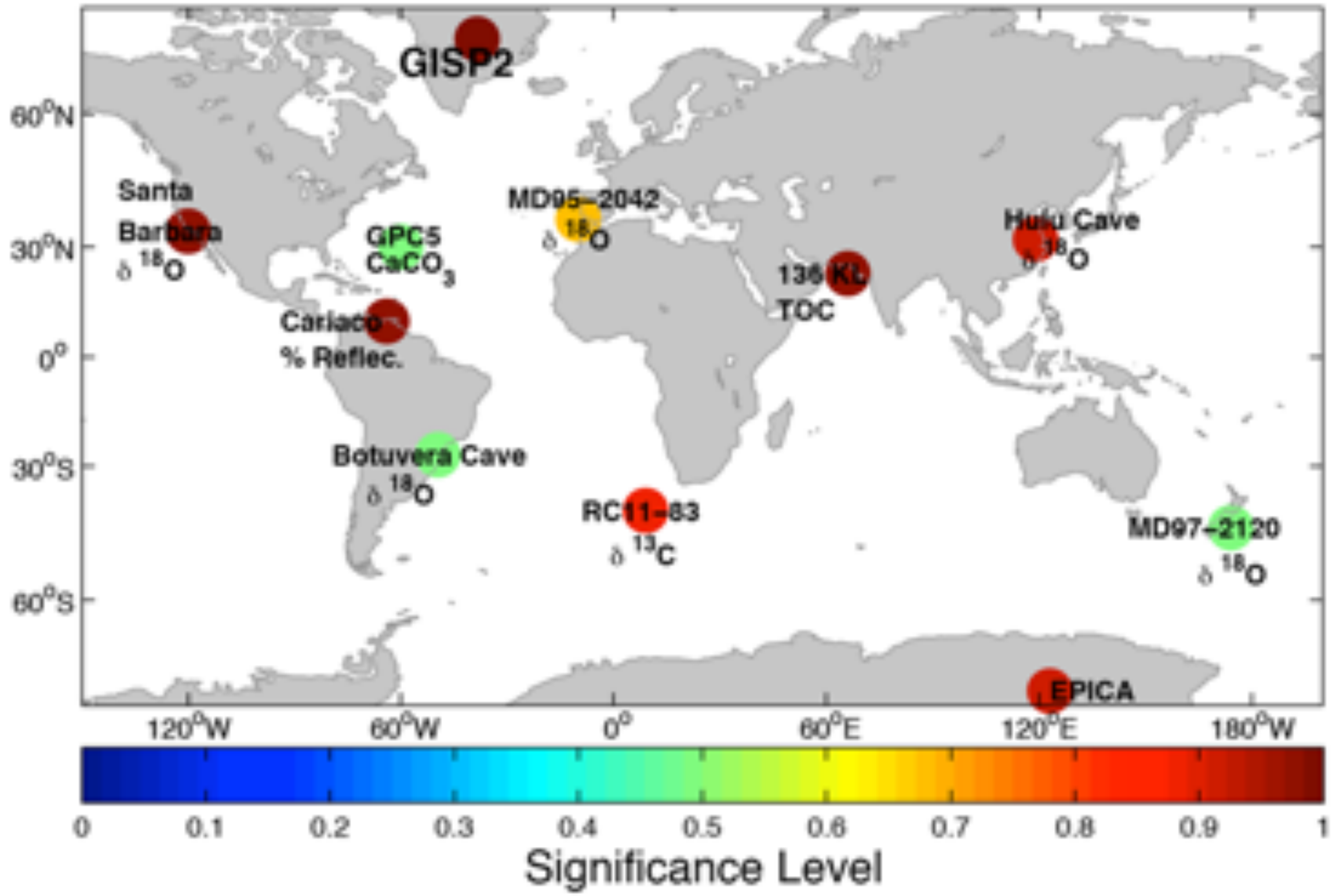

Significance of covariance between GISPII and remote proxies of climate, accounting for time uncertainty.

D/O teleconnections: observations

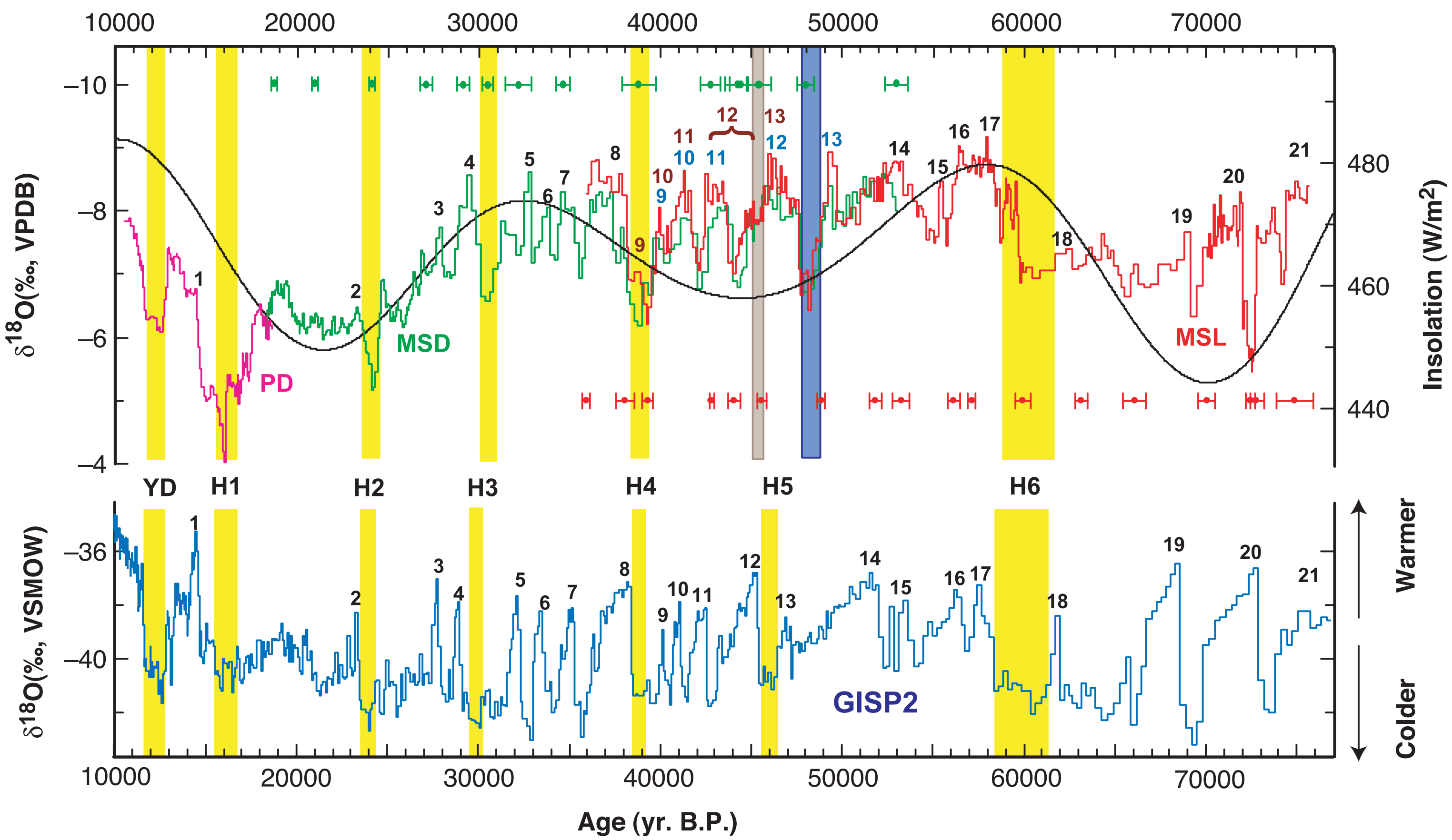

delta^{18}O of Hulu Cave (China) stalagmites (purple, green, and red) and Greenland Ice (dark blue) and insolation at 33°N averaged over June, July, August (black)

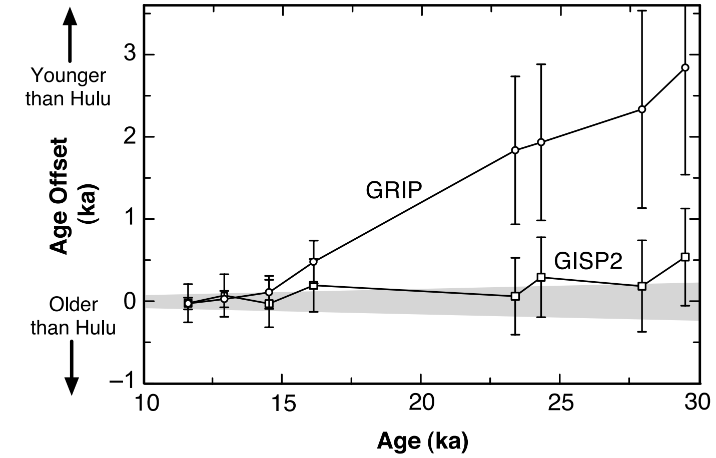

Difference in age between Hulu & Greenland ice core time scales [GRIP, GISP2] vs Hulu age.

A High-Resolution Absolute-Dated Late Pleistocene Monsoon Record from Hulu Cave, China

Y. J. Wang,[1,3] H. Cheng,[2] R. L. Edwards,[2]* Z. S. An,[3] J. Y. Wu,[4] C.-C. Shen,[5] J. A. Dorale[6]

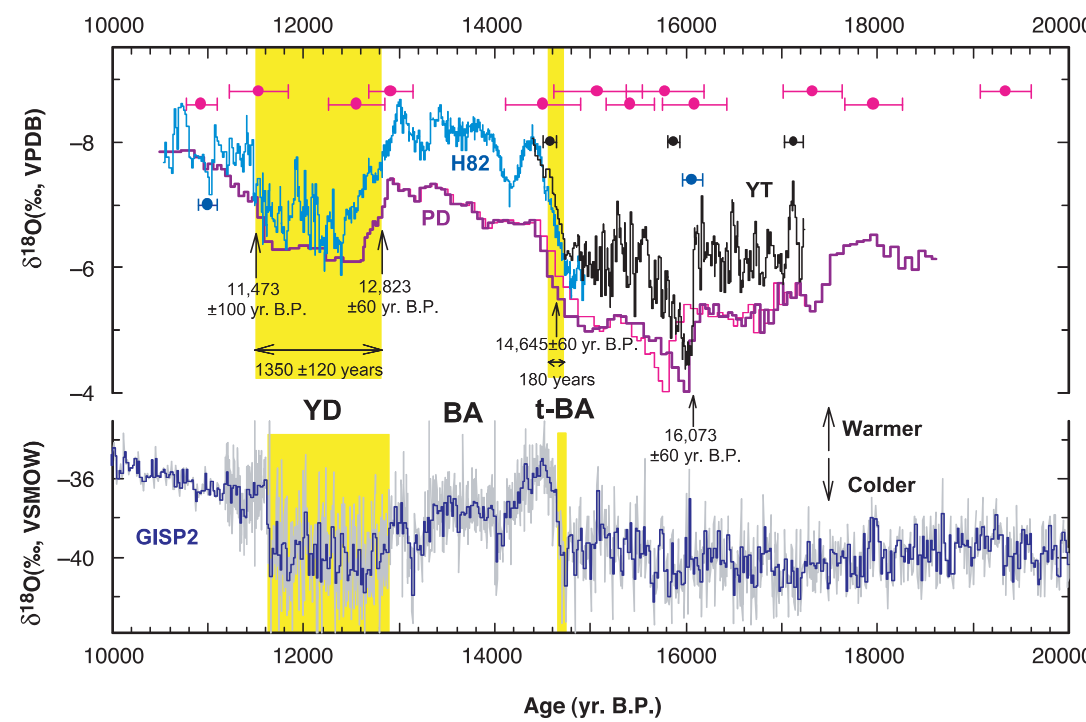

delta^{18}O of Hulu stalagmites (purple, black, and blue) and Greenland Ice (dark blue: 20-year avg; gray: 3-yr avg) vs time. Yellow bands: timing and duration of YD and transition into the Bolling-Allerod.

D/O teleconnection mechanism 1: AMOC/“thermal seesaw”

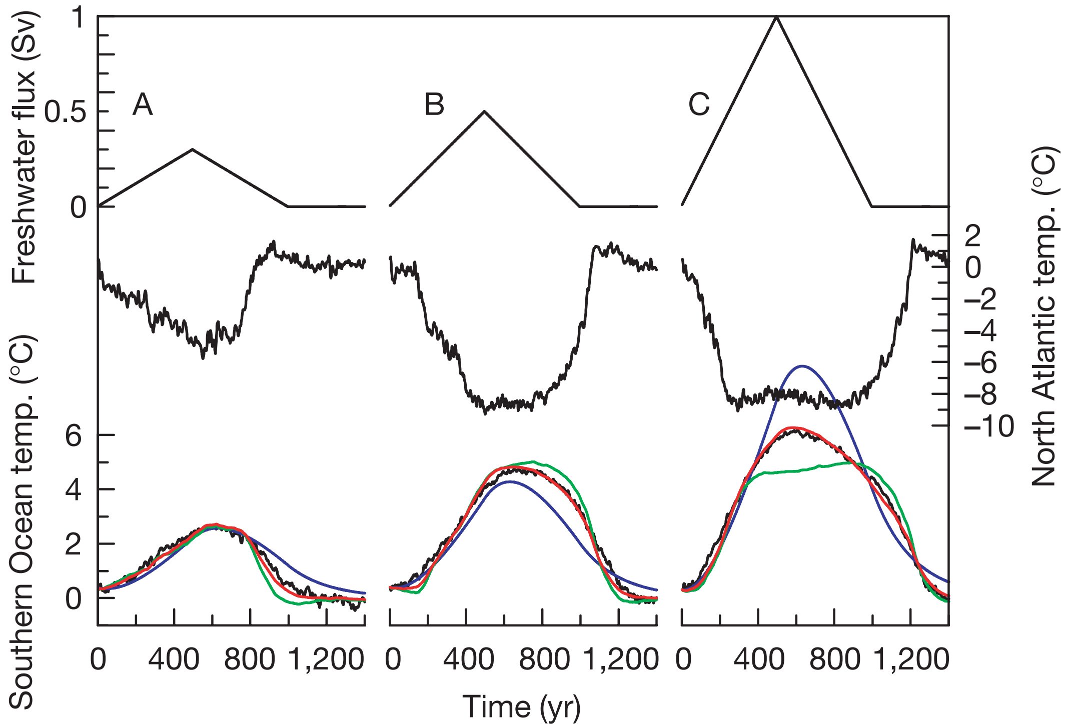

Temperature response to 3 scenarios of freshwater discharge into North Atlantic. Freshwater (top), 10-yr running mean of NA near-surface air temperature (middle), Southern Ocean (bottom). partial THC shutdown in A, complete shutdown in B & C.

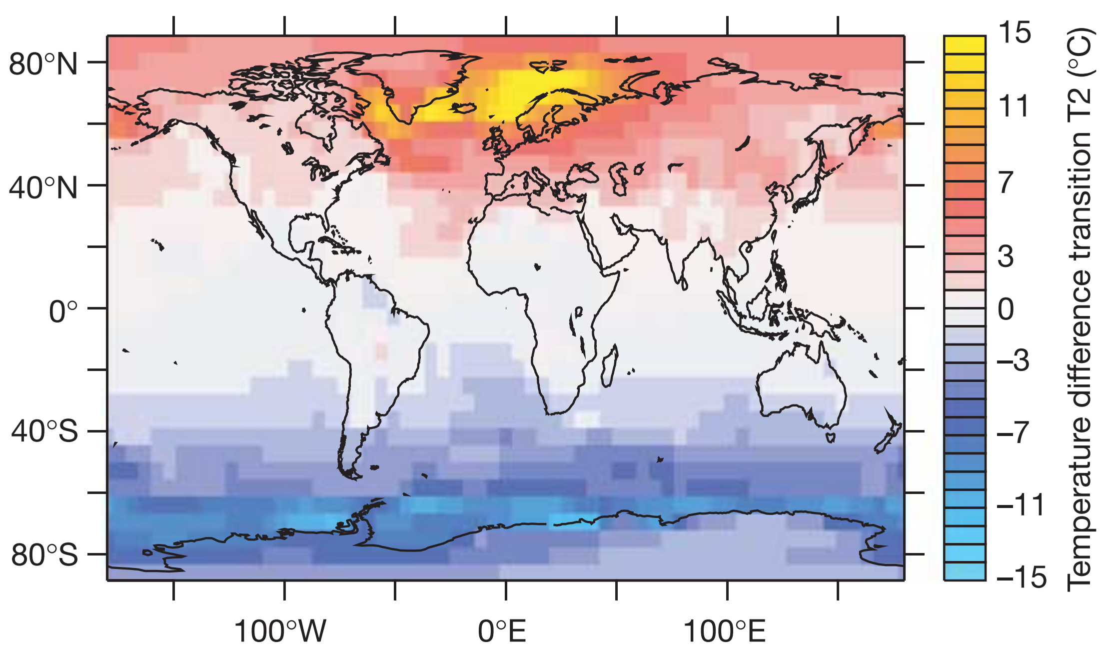

Strong hemispheric coupling of glacial climate through freshwater discharge and ocean circulation

Knutti, Fluckiger, Stocker & Timmermann 2004

D/O teleconnection mechanism 1: AMOC/“thermal seesaw”

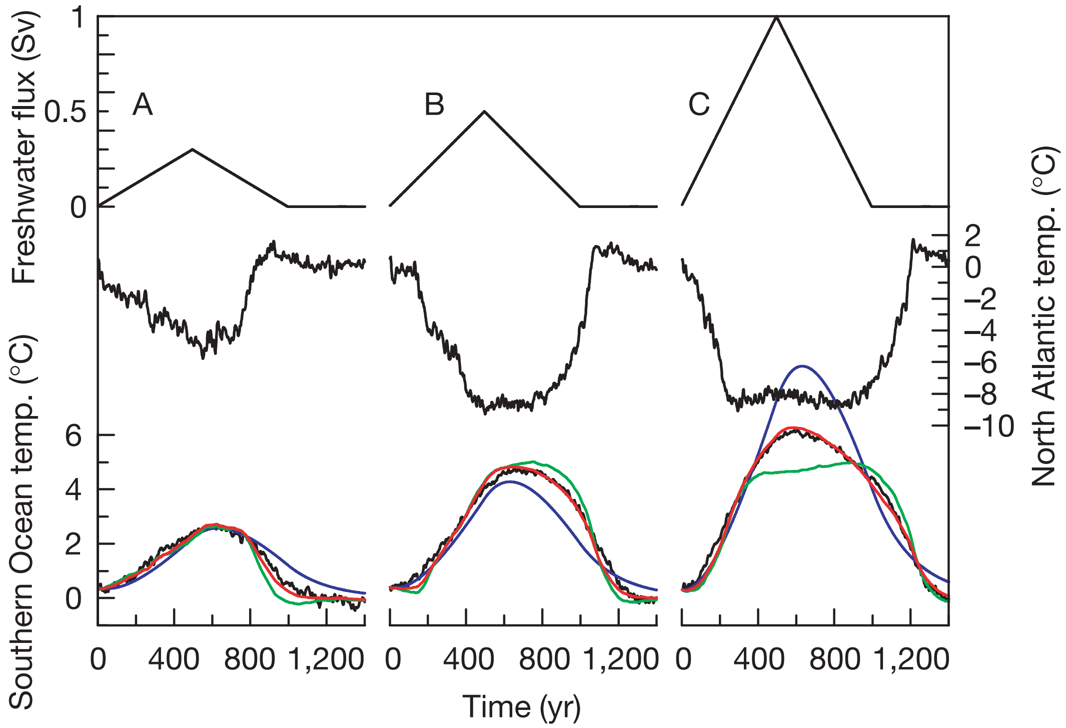

Temperature response to 3 scenarios of freshwater discharge into North Atlantic. Freshwater (top), 10-yr running mean of NA near-surface air temperature (middle), Southern Ocean (bottom). partial THC shutdown in A, complete shutdown in B & C.

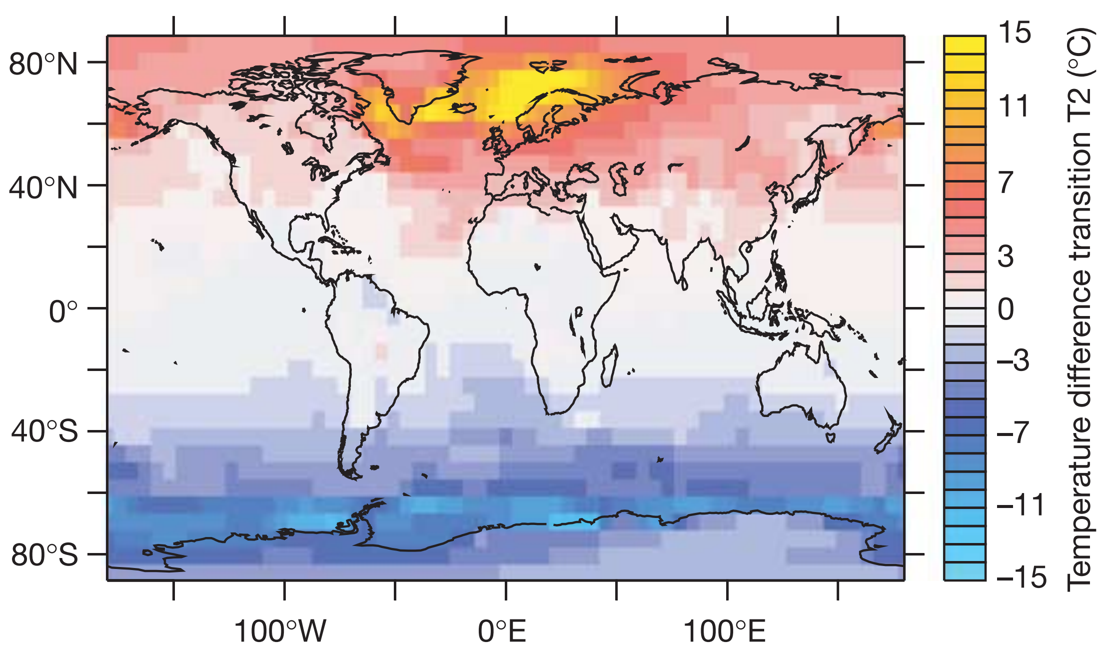

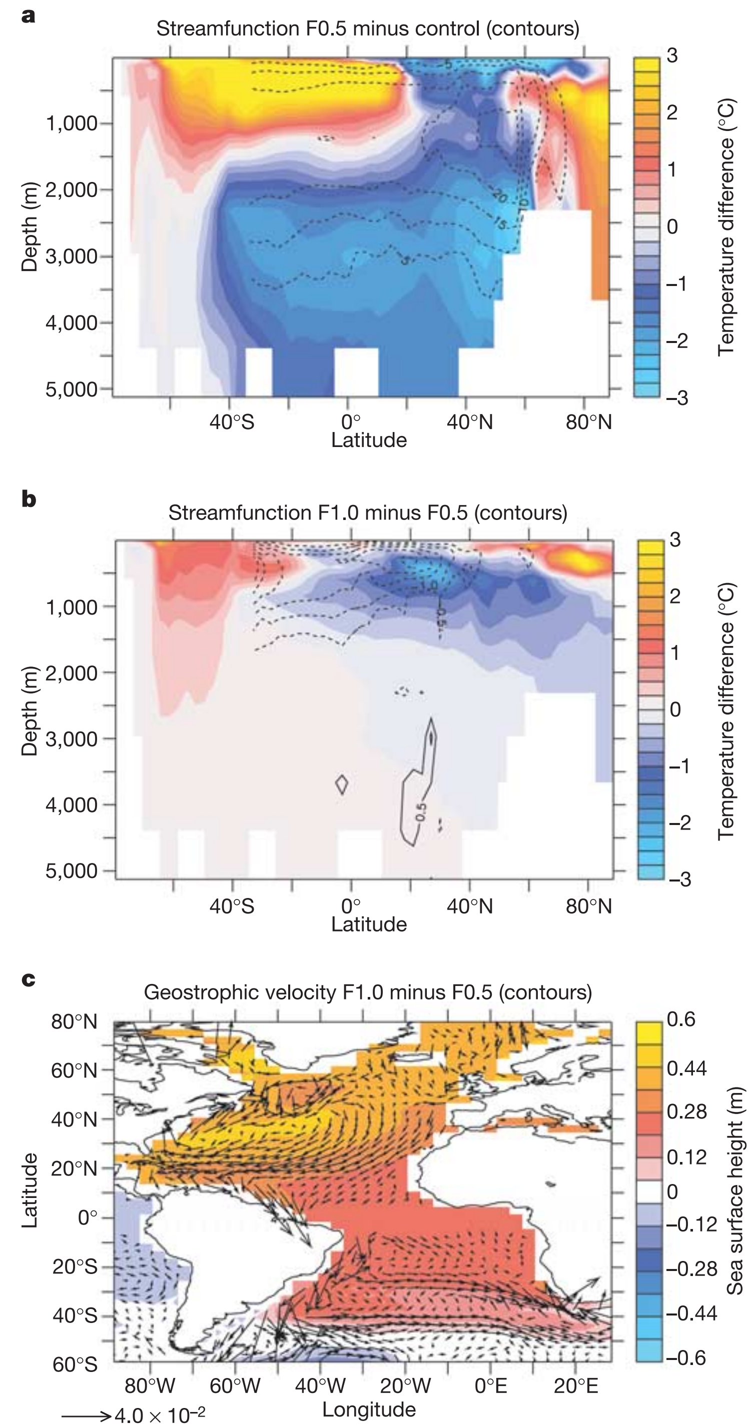

(a,b) Temperature and MOC response to freshwater forcing of **sustained** 1.0 Sv & 0.5 Sv sustained; (c) sea level & velocities

Strong hemispheric coupling of glacial climate through freshwater discharge and ocean circulation

Knutti, Fluckiger, Stocker & Timmermann 2004

D/O teleconnection mechanism 1: AMOC/“thermal seesaw”

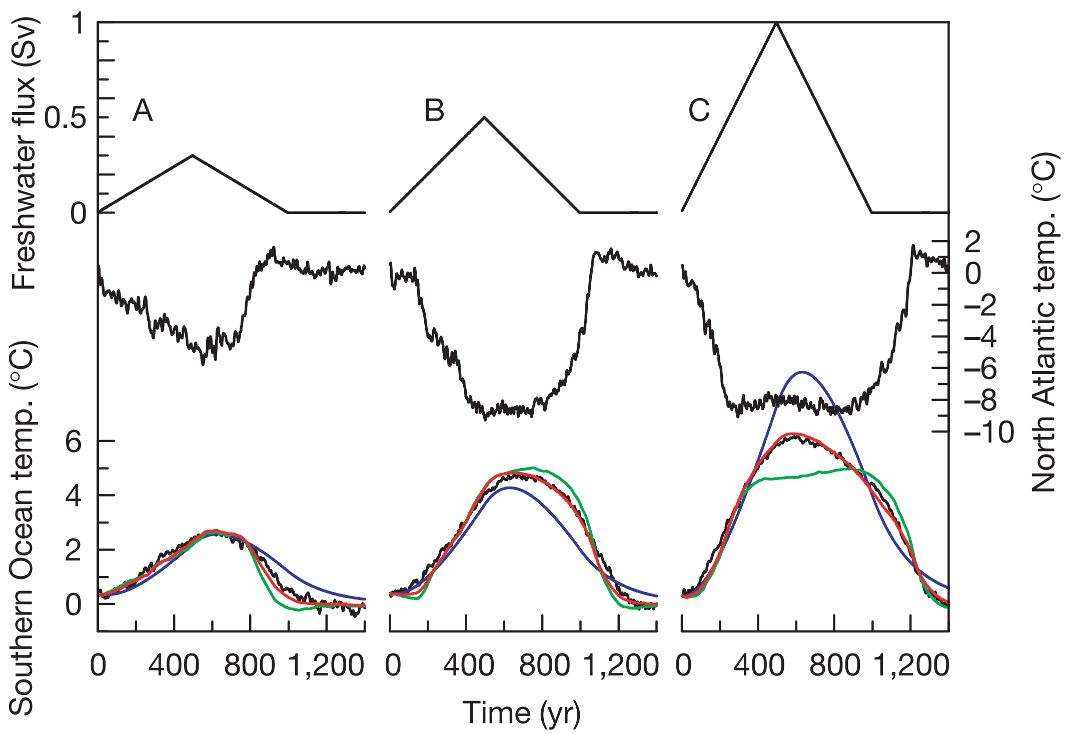

Temperature response to 3 scenarios of freshwater discharge into North Atlantic. Freshwater (top), 10-yr running mean of NA near-surface air temperature (middle), Southern Ocean (bottom). partial THC shutdown in A, complete shutdown in B & C.

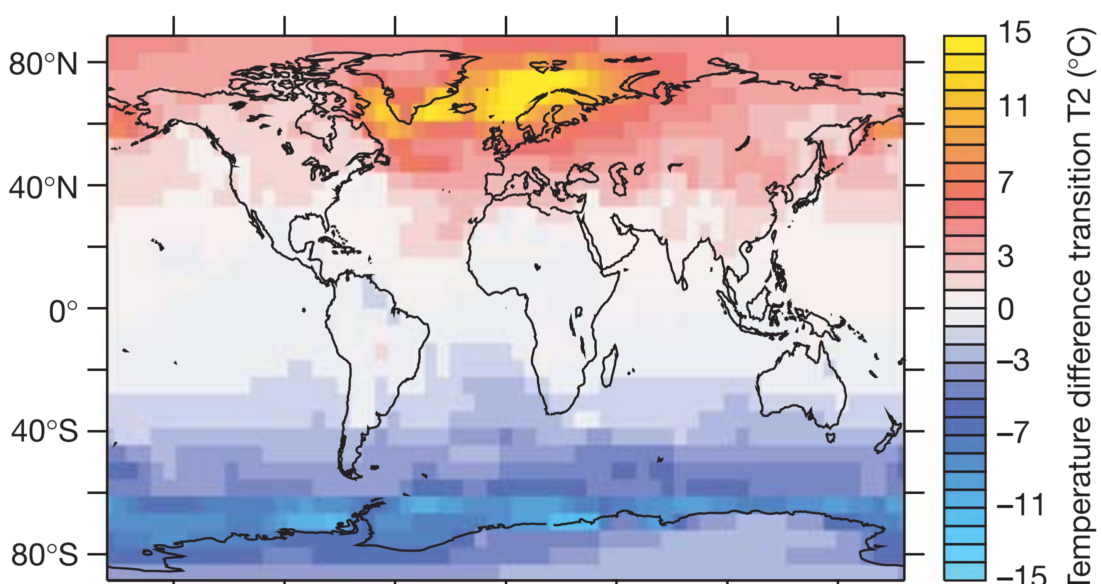

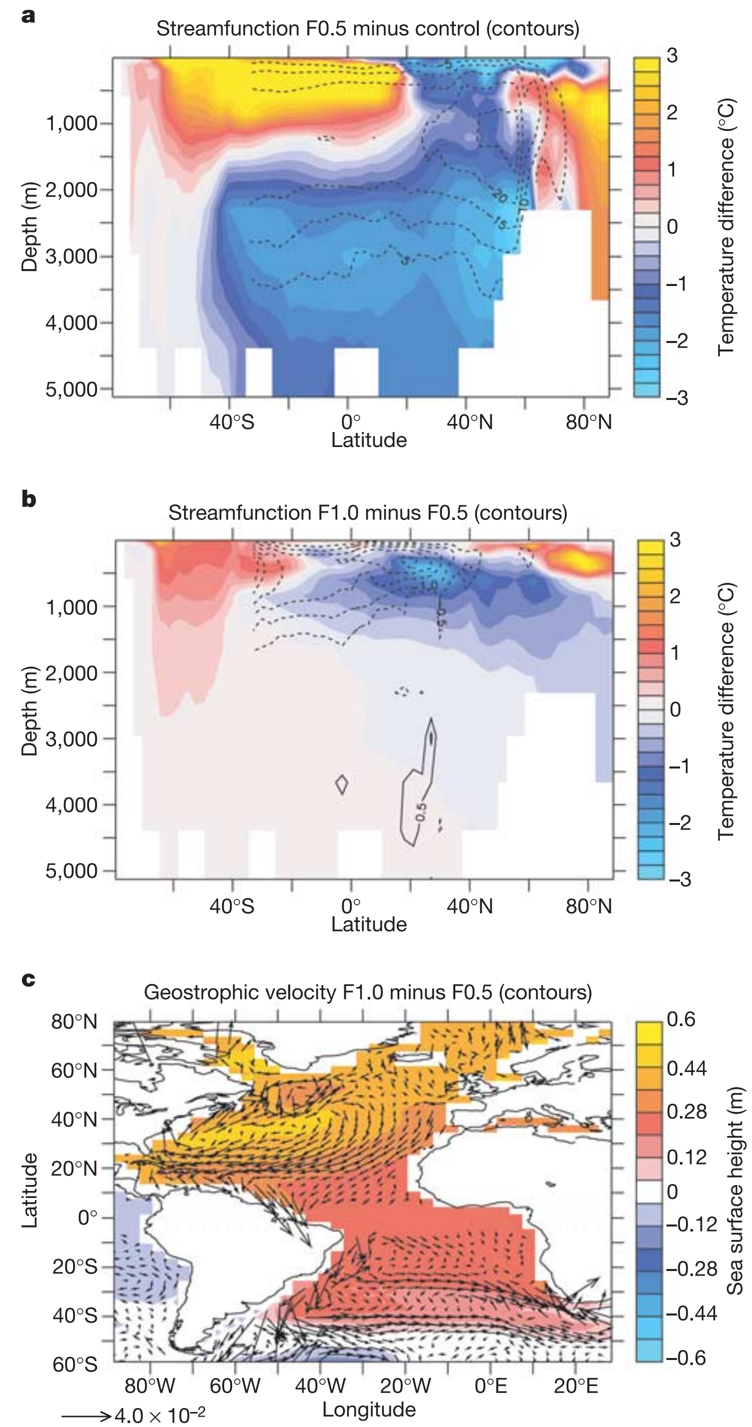

(a,b) Temperature and MOC response to freshwater forcing of **sustained** 1.0 Sv & 0.5 Sv sustained; (c) sea level & velocities

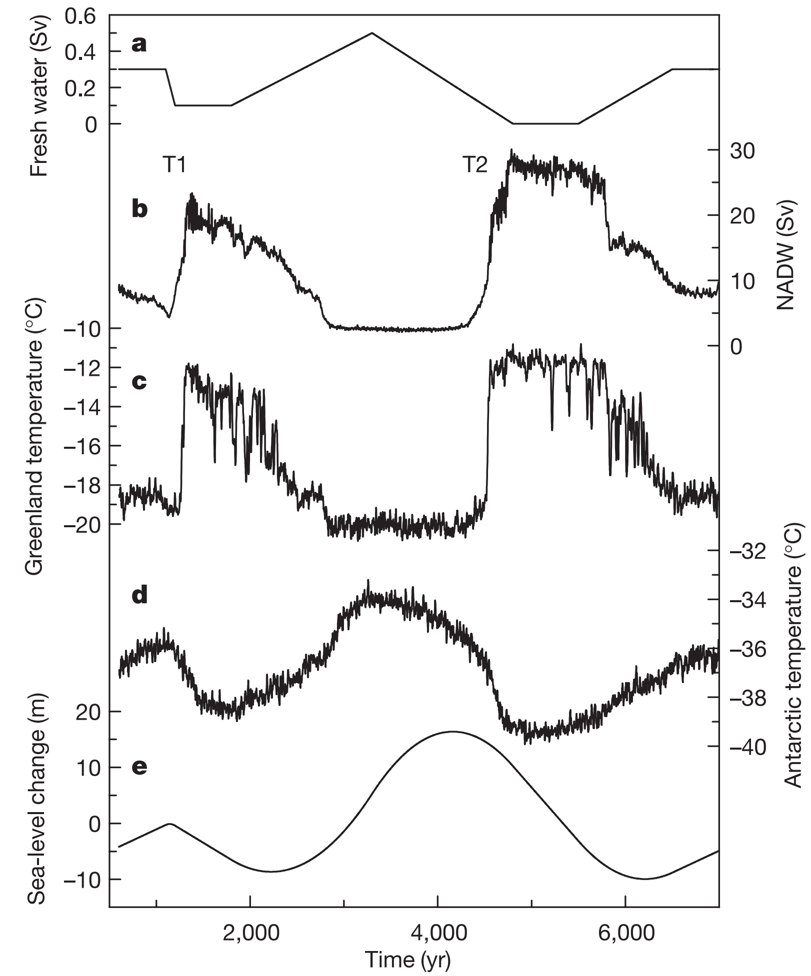

response to strong (30 m sea level) fresh water forcing

Strong hemispheric coupling of glacial climate through freshwater discharge and ocean circulation

Knutti, Fluckiger, Stocker & Timmermann 2004

D/O teleconnection mechanism 2: ocean waves

Global Teleconnections of Meridional Overturning Circulation Anomalies

HELEN L. JOHNSON* AND DAVID P. MARSHALL 2004

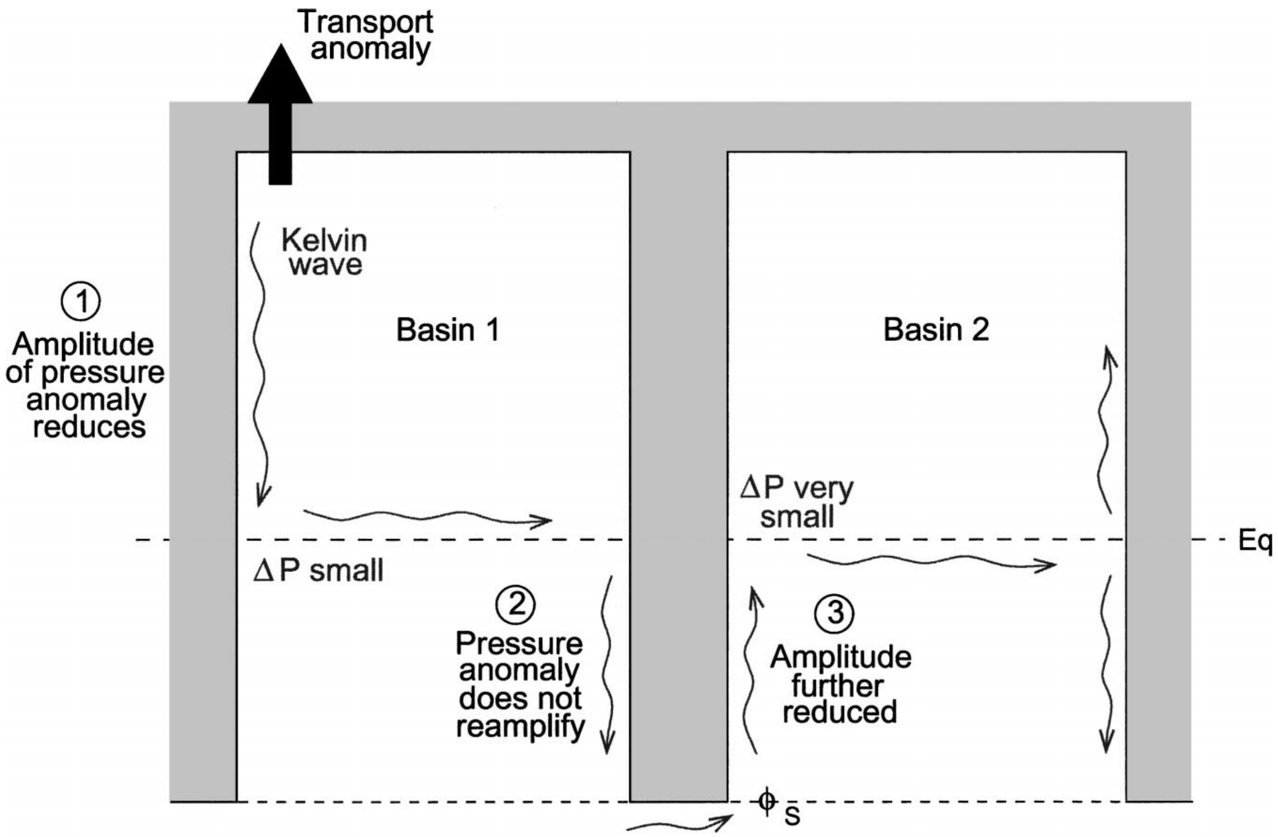

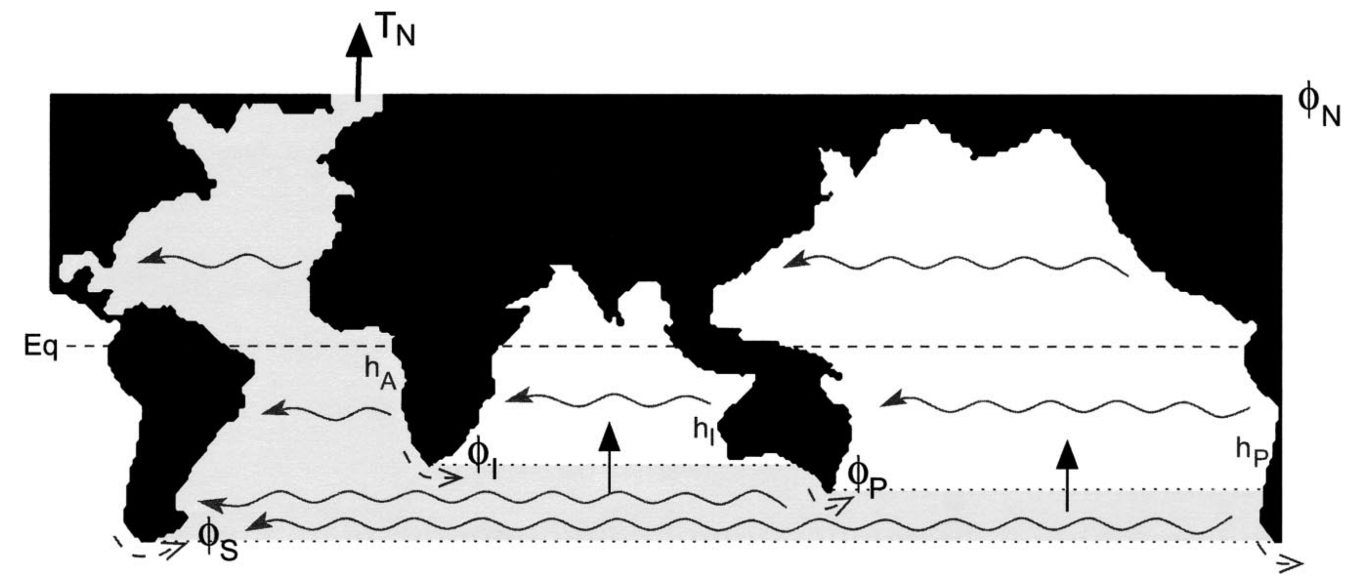

Schematic of Kelvin wave response to a prescribed anomaly in thermohaline overturning on the northern boundary of basin 1. The associated pressure anomaly is in geostrophic balance and consequently reduces in amplitude as it propagates southward as a Kelvin wave along the western boundary (1). The resulting small thermocline displacement is transmitted across the equator but does not reamplify as the Kelvin wave travels poleward on the eastern side of basin 1 (2). Having propagated around the cape separating the two basins, the Kelvin wave is further reduced in amplitude as it travels equatorward along the western boundary of basin 2 (3). The response on the eastern boundary of basin 2 is therefore smaller than that on the eastern boundary of basin 1 and depends upon the latitude f_S. Rossby waves communicate the reduced pressure anomaly into the interior of each basin.

Heinrich events

Heinrich Events: Observations

Typical N. Atlantic marine sediment core

Typical marine sediment (Forams, etc.)

Ice rafted debris (IRD)

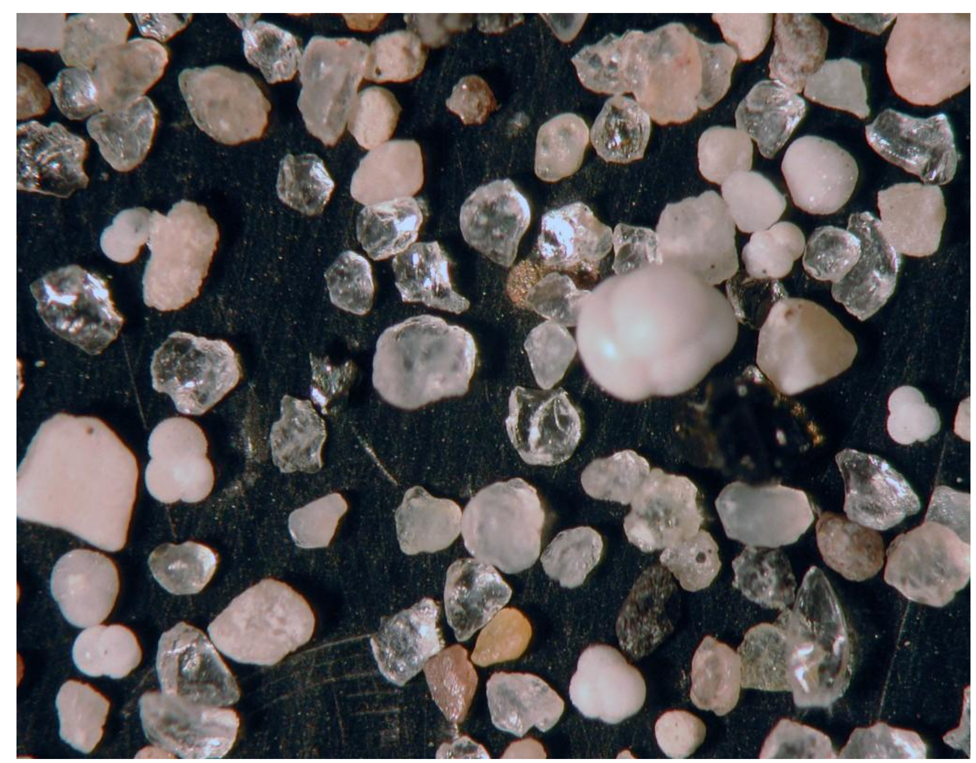

Heinrich Events: Observations

Ice rafted debris layers marking Heinrich events: major glacier discharge events from the Laurentide ice sheet to the North Atlantic, every 7–10,000 years (http://www/ncdc.noaa.gove/paleo/slides/

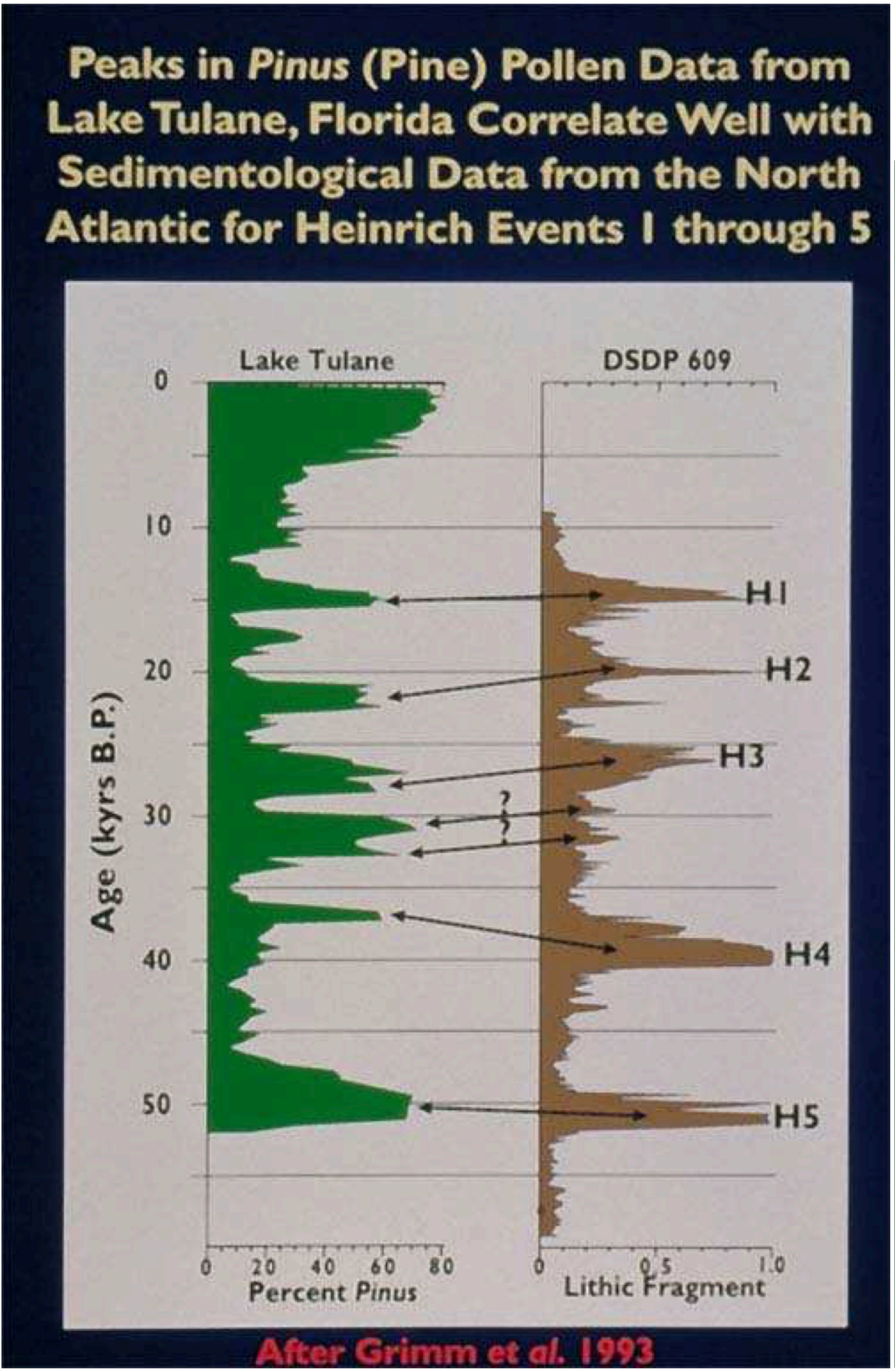

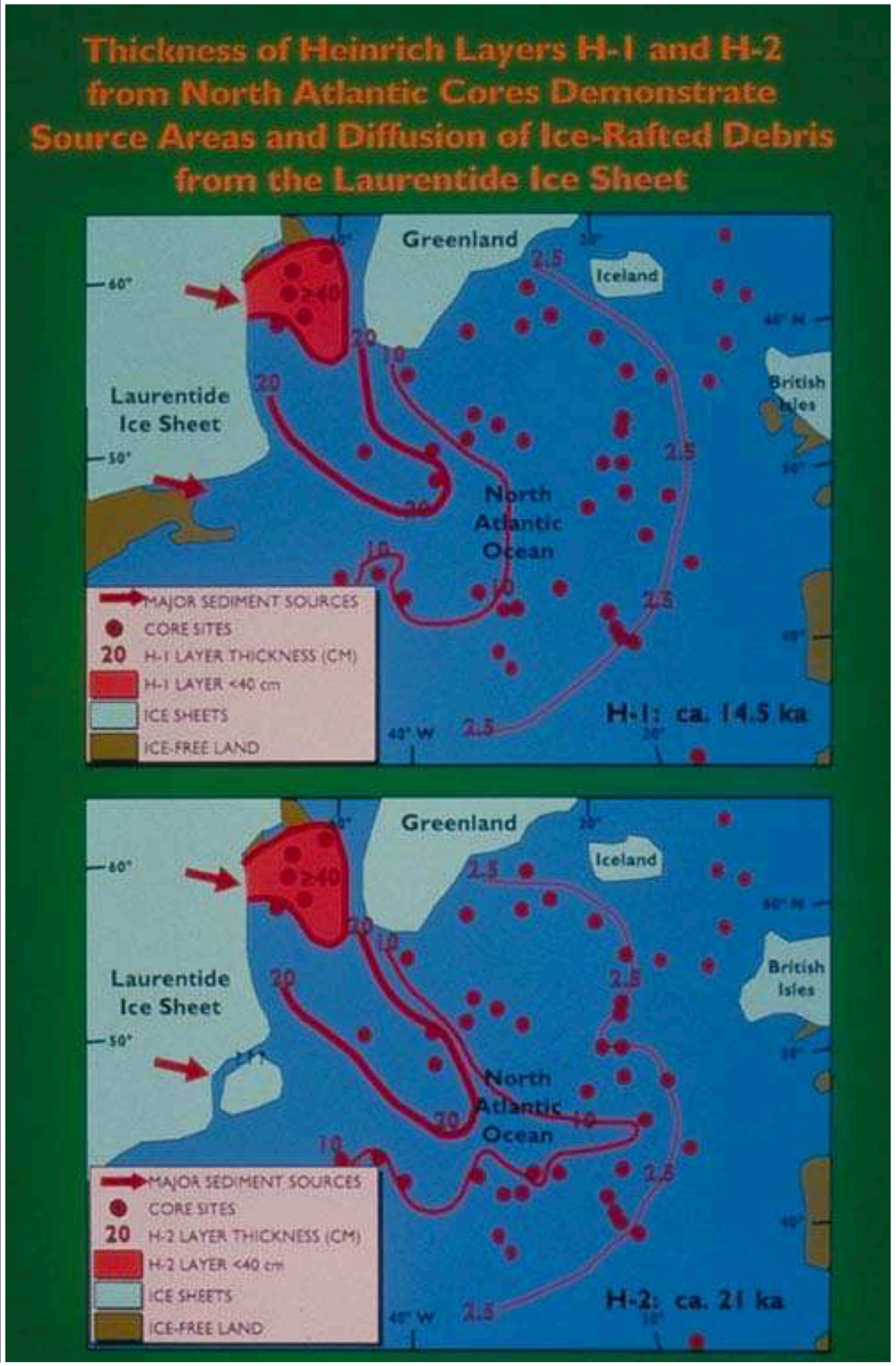

https://en.wikipedia.org/wiki/Heinrich_event

Heinrich events, three hypotheses

1. Binge-purge, time scale, isolated basal conditions. BUT: moulins
2. ice shelf collapse, hydrofracturing
3. MISI

Heinrich Events: Observations, vs DO events

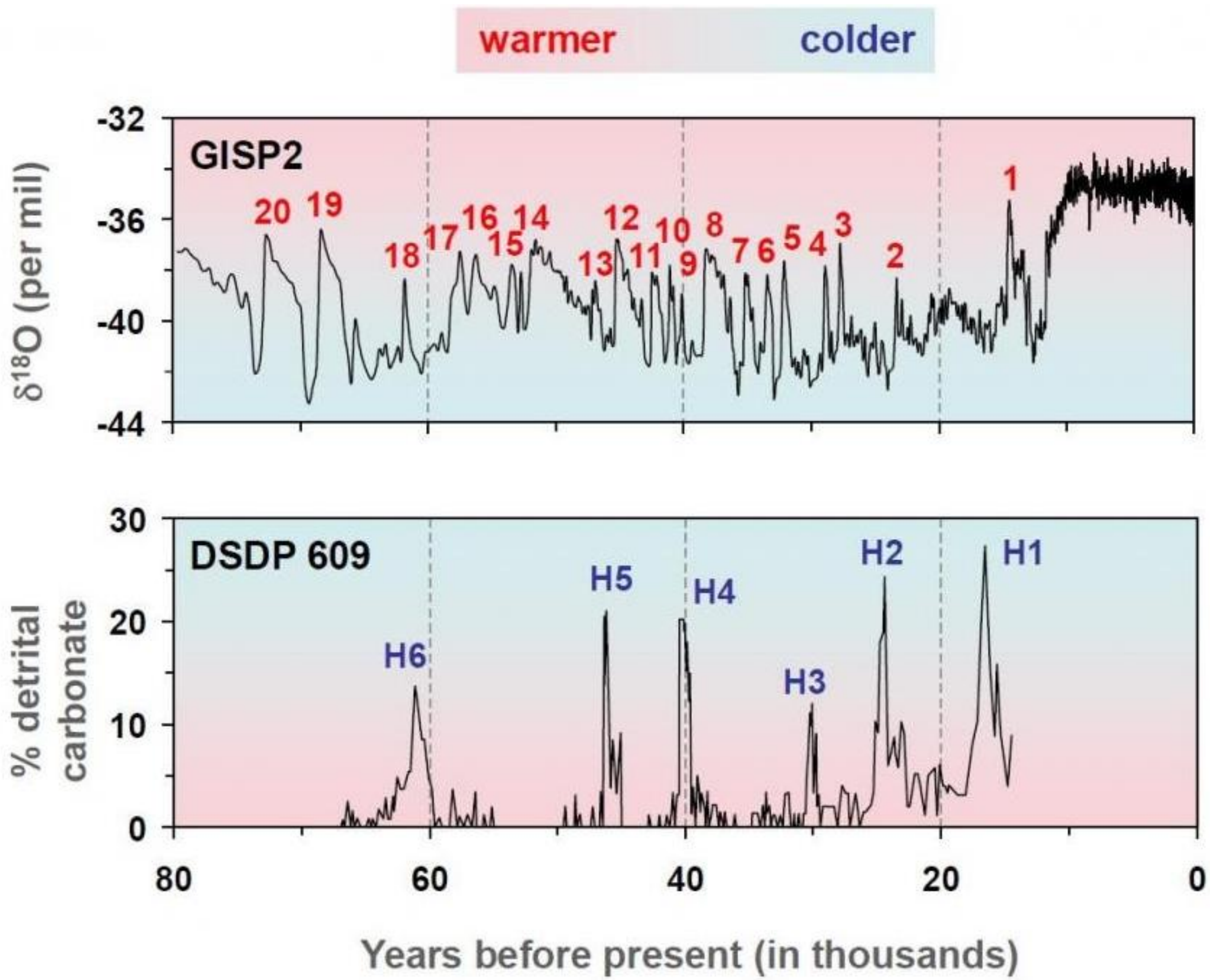

Comparison of percent abundance of detrital carbonate in the coarse fraction of Deep Sea Drilling Program Site 609 to the $\delta^{18}O$ of the Greenland Ice Sheet Project 2 ice core (Modified from Grootes et al., 1993).

https://scholarship.claremont.edu/cgi/viewcontent.cgi?article=2920&context=scripps_theses

McIlvaine, Ava, "Influence of Iceberg-Discharge Events on the Climate and Circulation of the Central North Atlantic Ocean During the Last Glaciation" (2021). Scripps Senior Theses. 1903. https://scholarship.claremont.edu/scripps_theses/1903

Heinrich Events: Observations

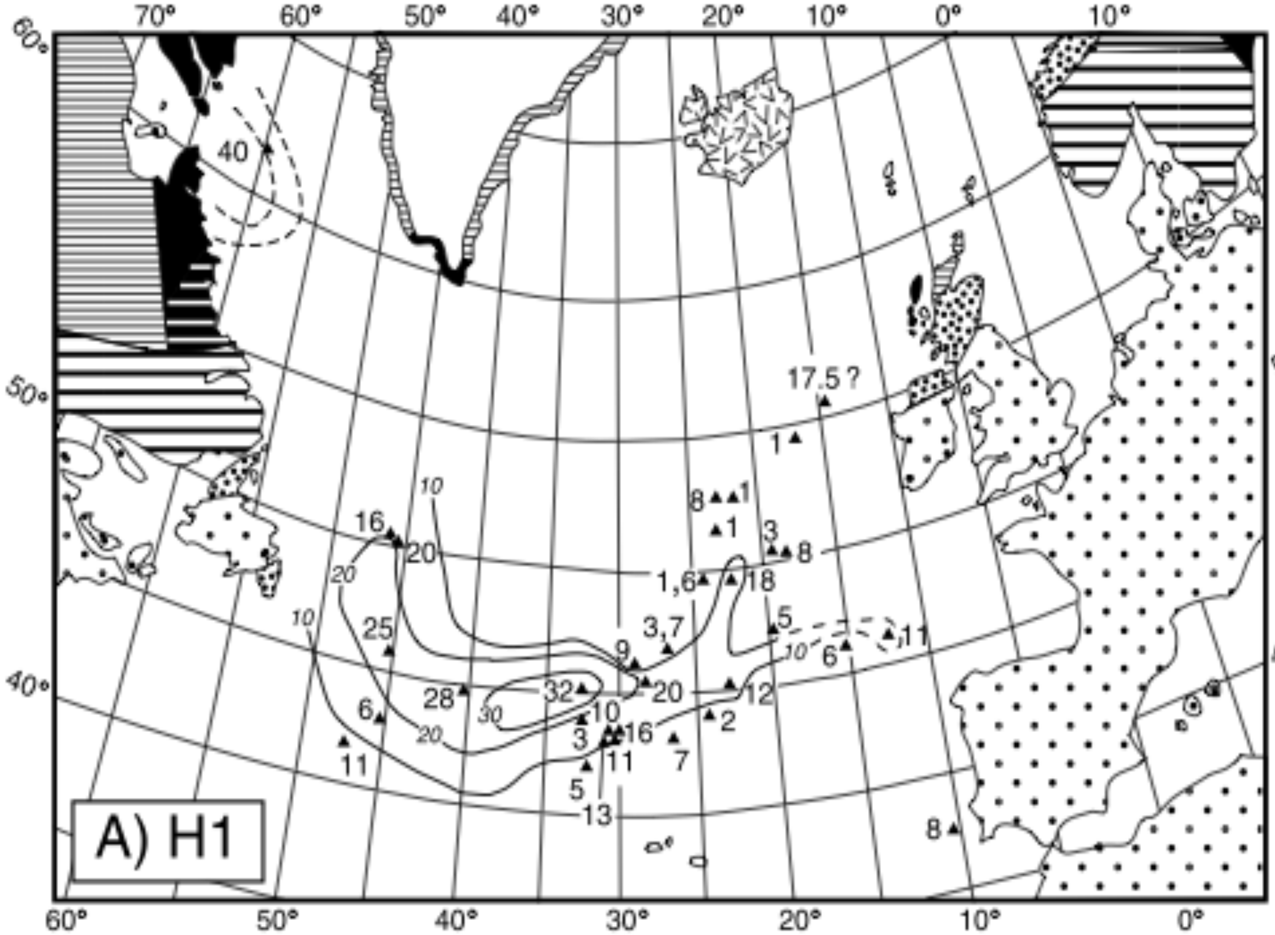

Isotach maps of the Heinrich layers in the North Atlantic: (a) H1, (b) H2, (c) H4, and (d) H5. Contour intervals are 10 cm. Data and data sources are given in Table 1.

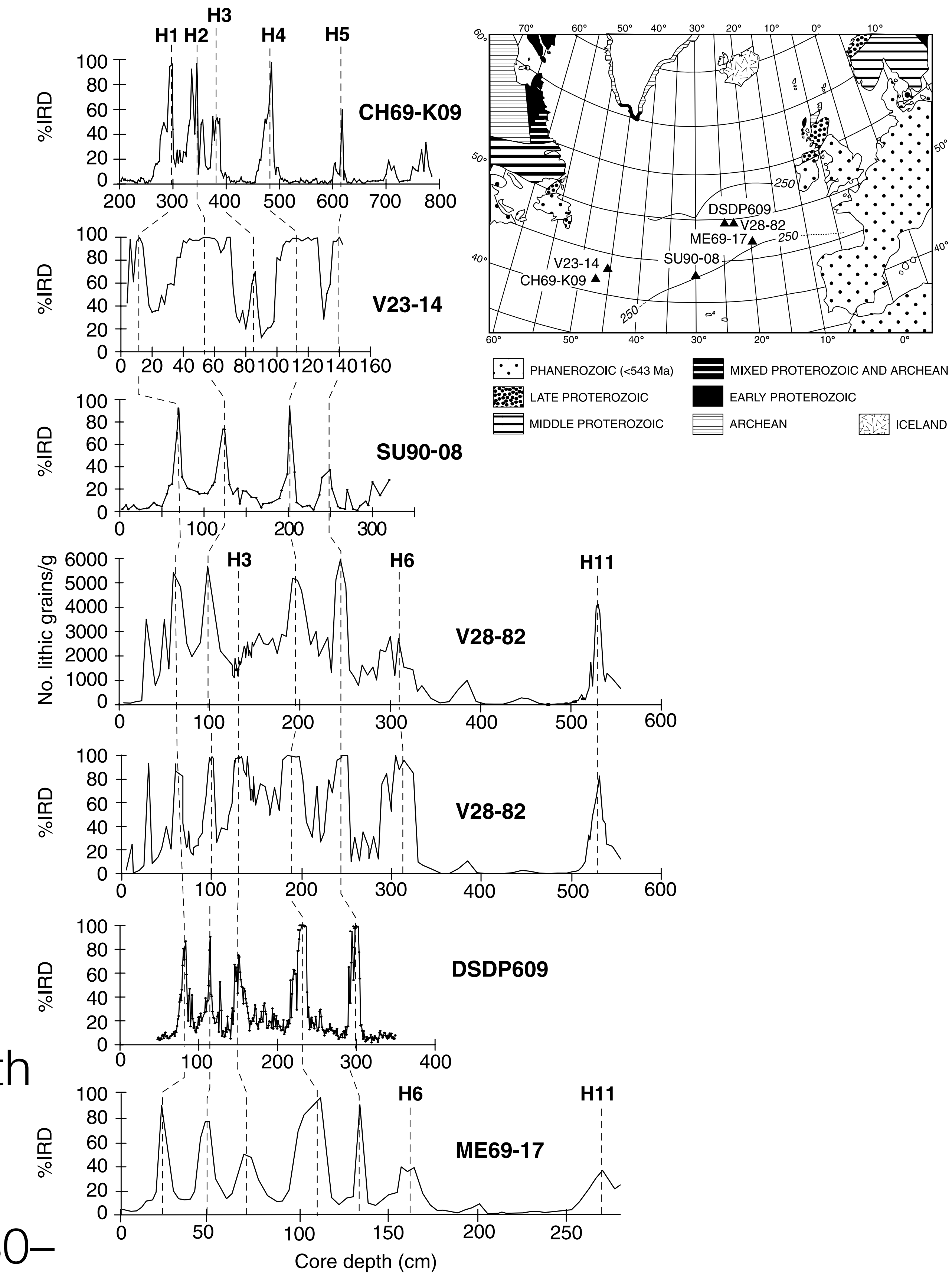

Figure 1. Ice-rafted detritus (IRD) data for North Atlantic sediment cores with Heinrich layers. showing % of lithic grains in the >150 mm fraction; ME69-17 : % of lithic grains in the 180–3000 mm fraction. map: location of cores.

(Hemming 2004)

Global-mean sea level rise associated with Heinrich events

0.4 m–4 m sea level rise (H1 and H2, Dowdswell,1995)

~3 m sea level rise (Alley and MacAyeal,1993)

0.1 m–20 m sea level rise (Hemming, 2004)

Heinrich events: summary of observations

- Glacier discharges every 7,000–10,000 years (Heinrich 1988; Broecker et al. 1992; Bond et al. 1992)

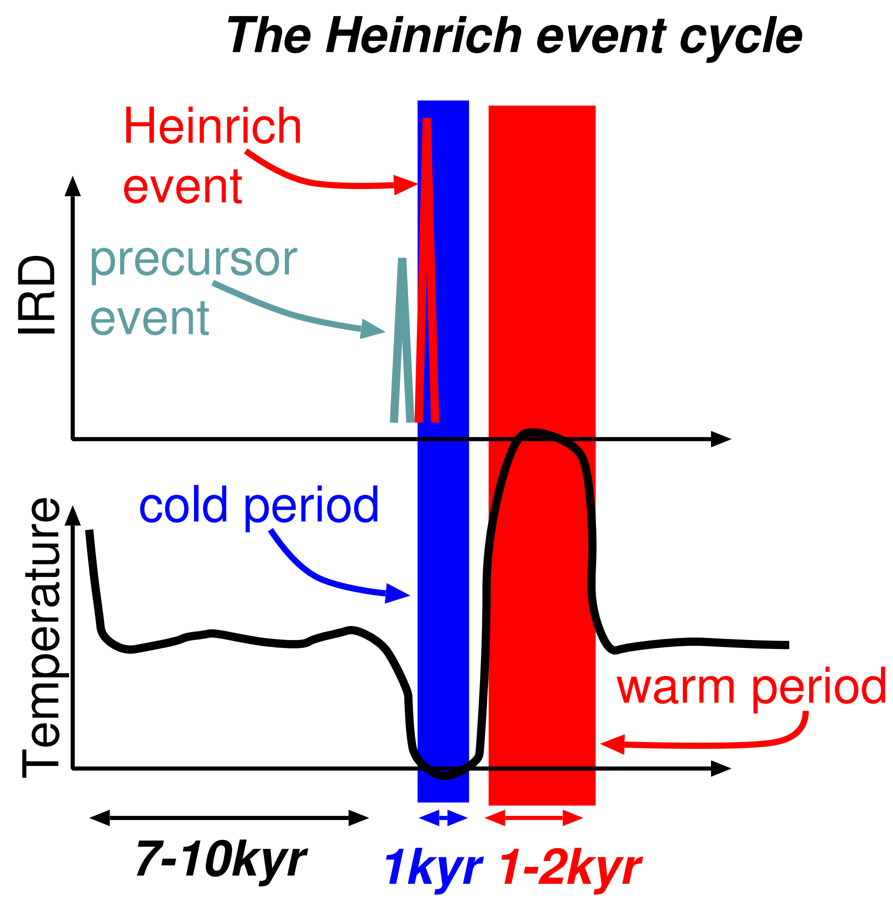

Heinrich events: summary of observations

- Glacier discharges every 7,000–10,000 years (Heinrich 1988; Broecker et al. 1992; Bond et al. 1992)
- Colder NA temperatures during glacier discharges (Bard et al. 2000)

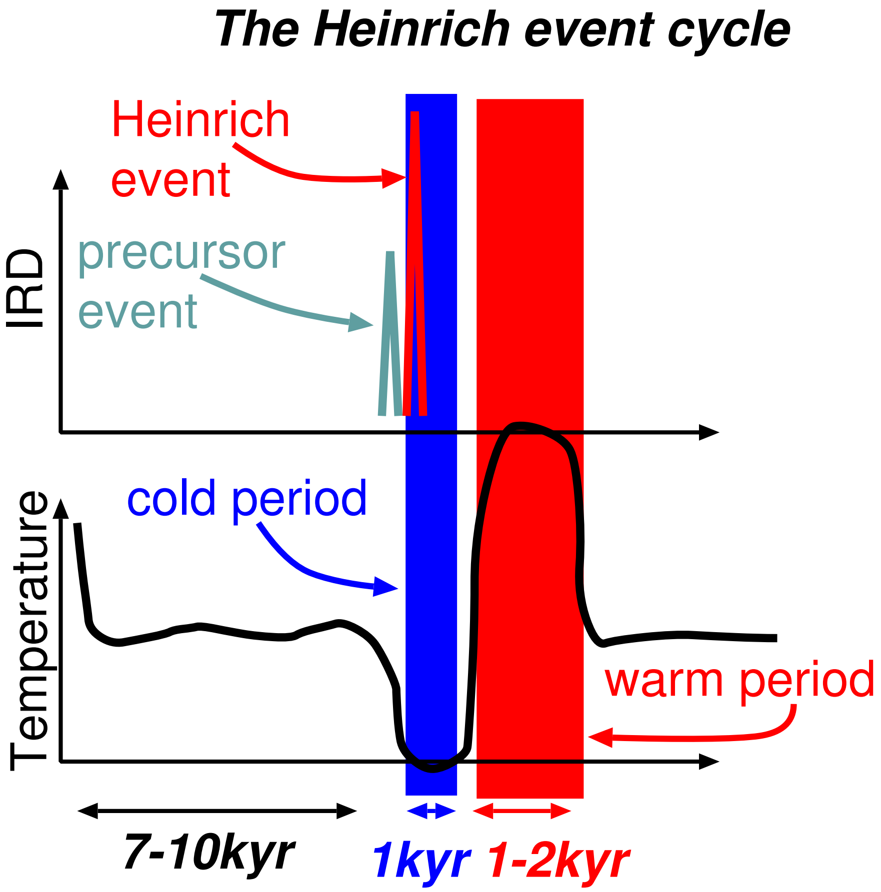

Heinrich events: summary of observations

- Glacier discharges every 7,000–10,000 years (Heinrich 1988; Broecker et al. 1992; Bond et al. 1992)
- Colder NA temperatures during glacier discharges (Bard et al. 2000)
- Abrupt warming to interglacial temperatures for ~1–2 kyr, starting <1 kyr after discharge (Dansgaard et al. 1993; Bond et al. 1993)

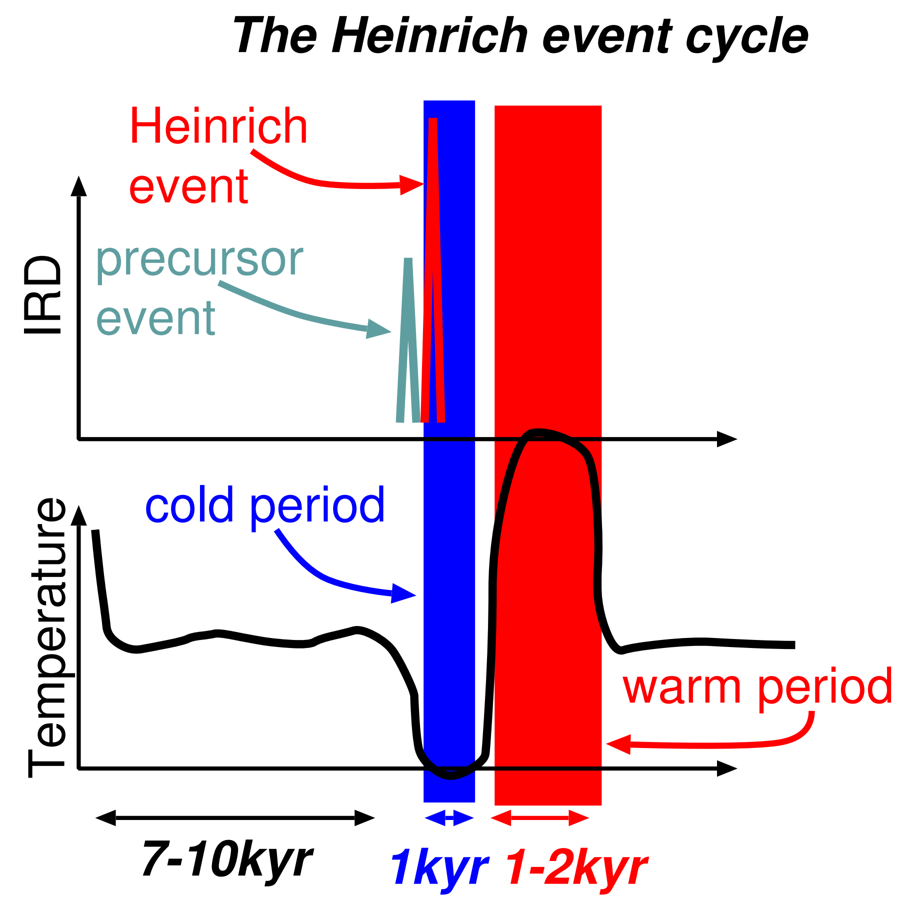

Heinrich events: summary of observations

- Glacier discharges every 7,000–10,000 years (Heinrich 1988; Broecker et al. 1992; Bond et al. 1992)
- Colder NA temperatures during glacier discharges (Bard et al. 2000)
- Abrupt warming to interglacial temperatures for ~1–2 kyr, starting <1 kyr after discharge (Dansgaard et al. 1993; Bond et al. 1993)
- Simultaneous/ related glacier discharges from ice sheets around the North Atlantic (Bond & Lotti 1995; Elliot et al. 1998; Fronval et al. 1995): Hudson Bay, Icelandic, Gulf of St. Lawrence, British, Barents-Sea ice sheets.

The Heinrich event cycle

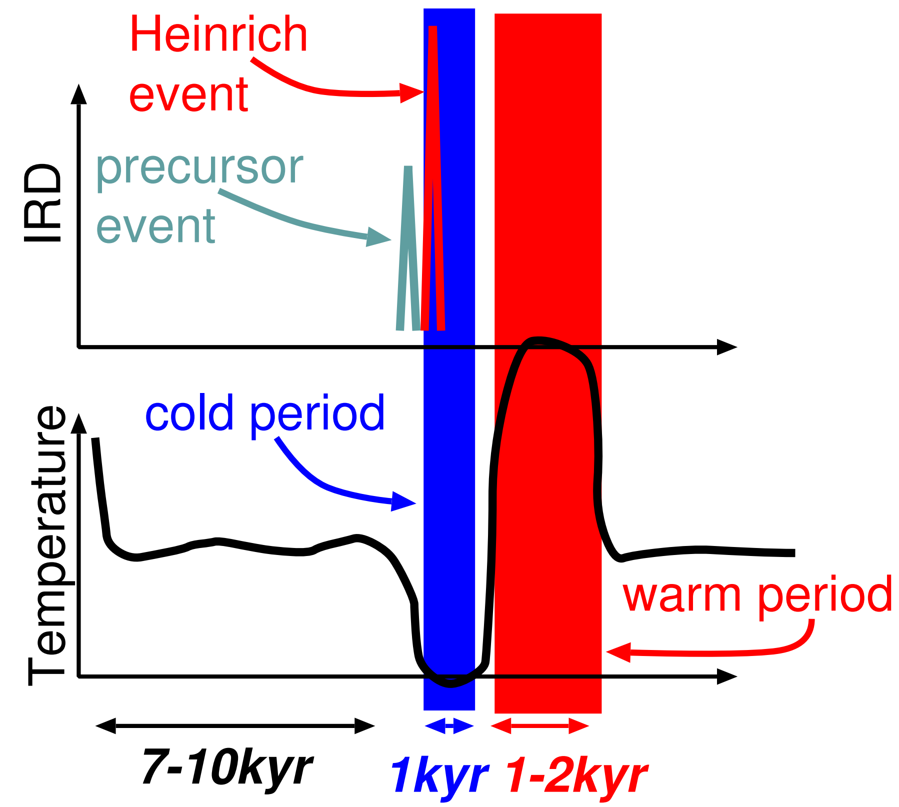

Heinrich events: summary of observations

- Glacier discharges every 7,000–10,000 years (Heinrich 1988; Broecker et al. 1992; Bond et al. 1992)
- Colder NA temperatures during glacier discharges (Bard et al. 2000)
- Abrupt warming to interglacial temperatures for ~1–2 kyr, starting <1 kyr after discharge (Dansgaard et al. 1993; Bond et al. 1993)
- Simultaneous/ related glacier discharges from ice sheets around the North Atlantic (Bond & Lotti 1995; Elliot et al. 1998; Fronval et al. 1995): Hudson Bay, Icelandic, Gulf of St. Lawrence, British, Barents-Sea ice sheets.
- "Precursor" events: smaller ice sheets (e.g., Icelandic) discharge glaciers just prior to LIS (Bond, Lotti 1995; Bond et al. 1999)

The Heinrich event cycle

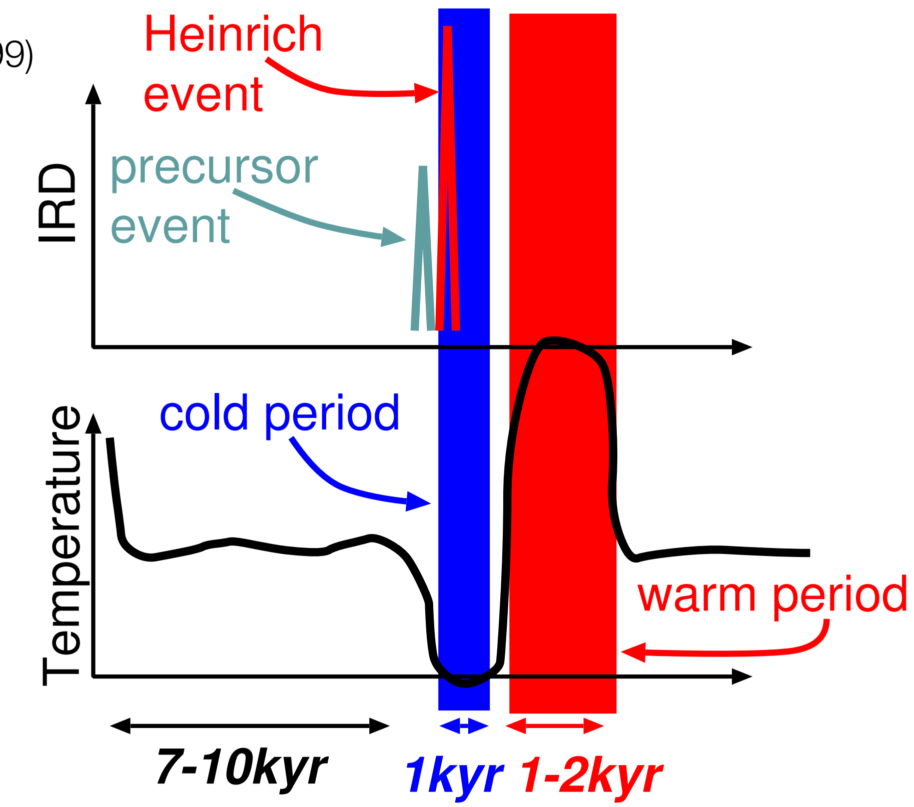

Heinrich events: summary of observations

- Glacier discharges every 7,000–10,000 years (Heinrich 1988; Broecker et al. 1992; Bond et al. 1992)
- Colder NA temperatures during glacier discharges (Bard et al. 2000)
- Abrupt warming to interglacial temperatures for ~1–2 kyr, starting <1 kyr after discharge (Dansgaard et al. 1993; Bond et al. 1993)
- Simultaneous/ related glacier discharges from ice sheets around the North Atlantic (Bond & Lotti 1995; Elliot et al. 1998; Fronval et al. 1995): Hudson Bay, Icelandic, Gulf of St. Lawrence, British, Barents-Sea ice sheets.
- “Precursor” events: smaller ice sheets (e.g., Icelandic) discharge glaciers just prior to LIS (Bond, Lotti 1995; Bond et al. 1999)
- Sea level signal: 0.1–20 m

The Heinrich event cycle

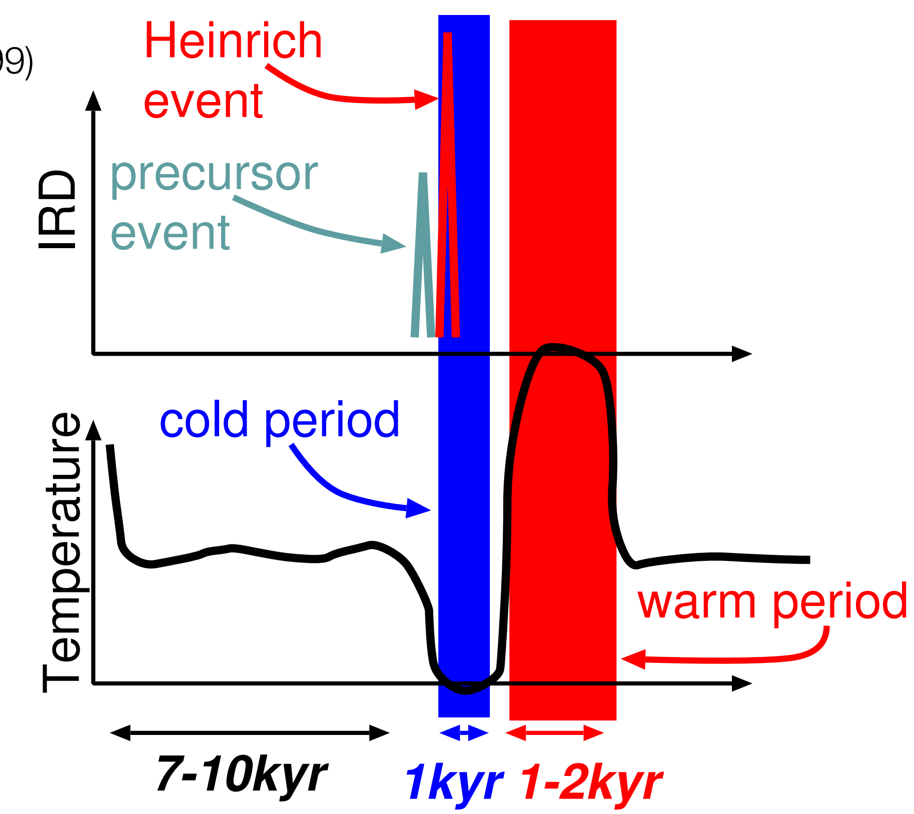

Ice streams: Ice Velocities for the Antarctic Ice Sheet

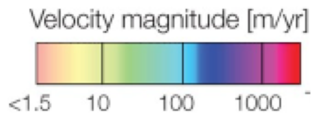

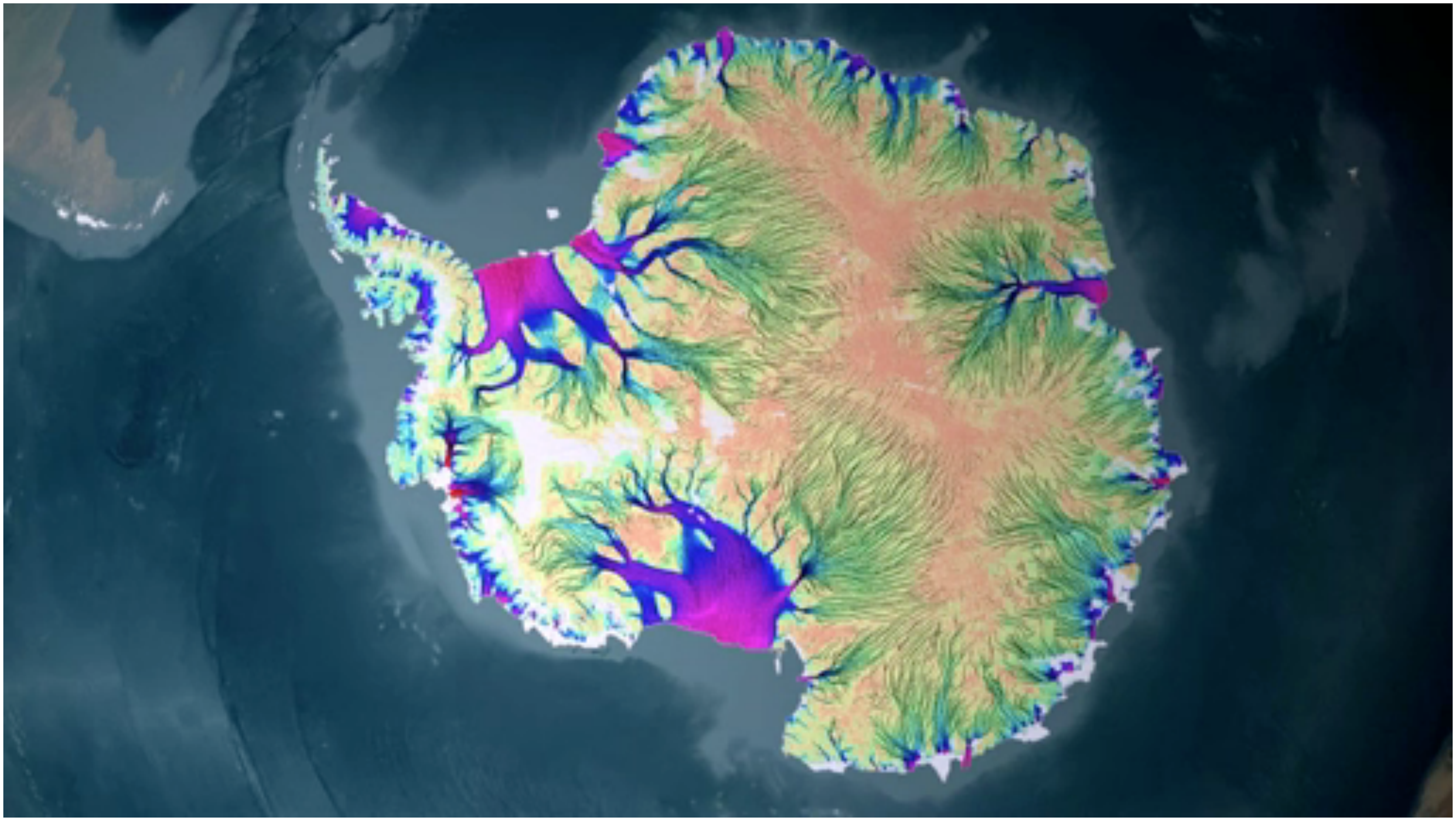

Rignot et al. 2011

Ice streams: Ice Velocities for the Antarctic Ice Sheet

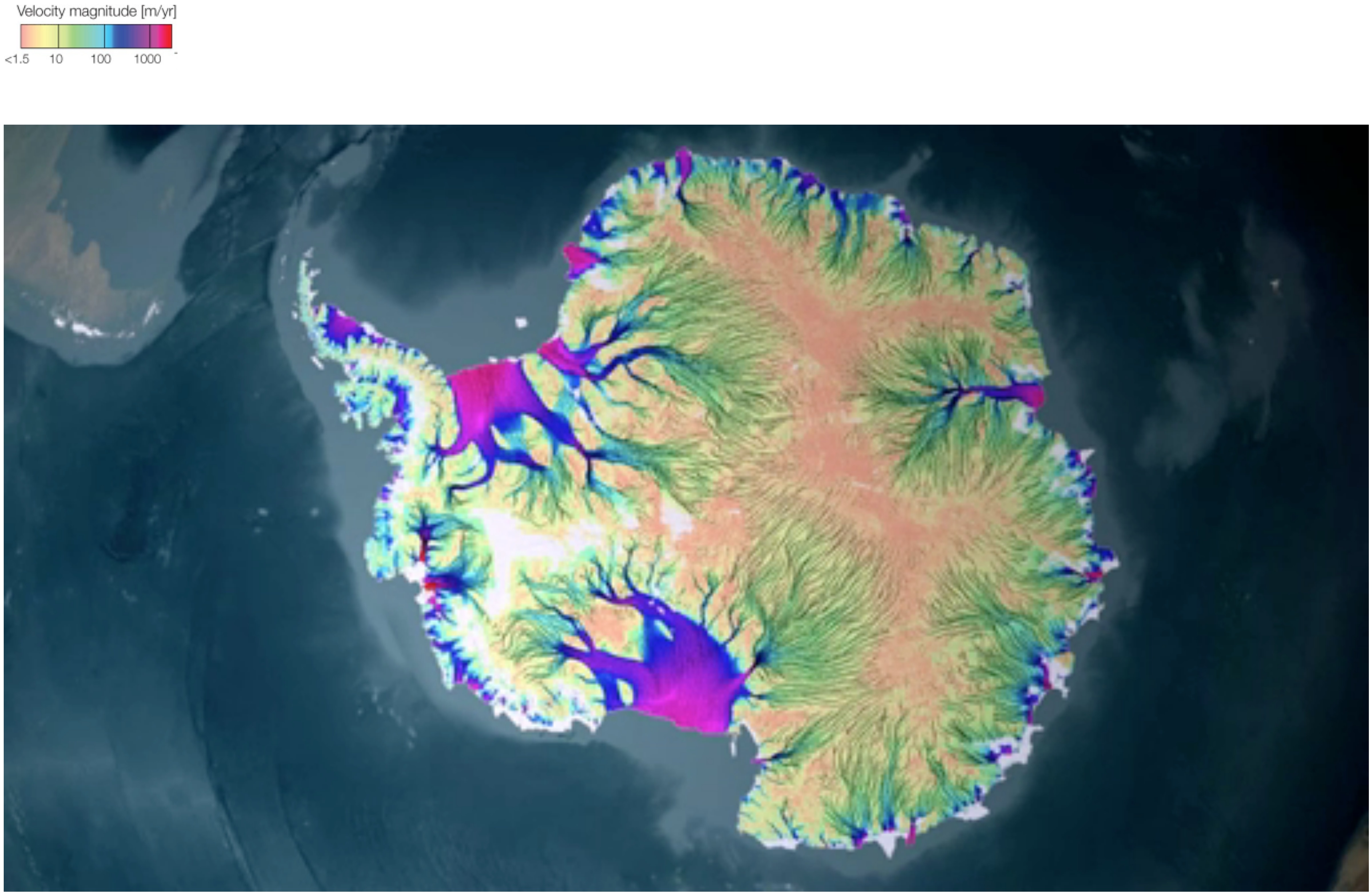

Rignot et al. 2011

Ice streams: Ice Velocities for the Antarctic Ice Sheet

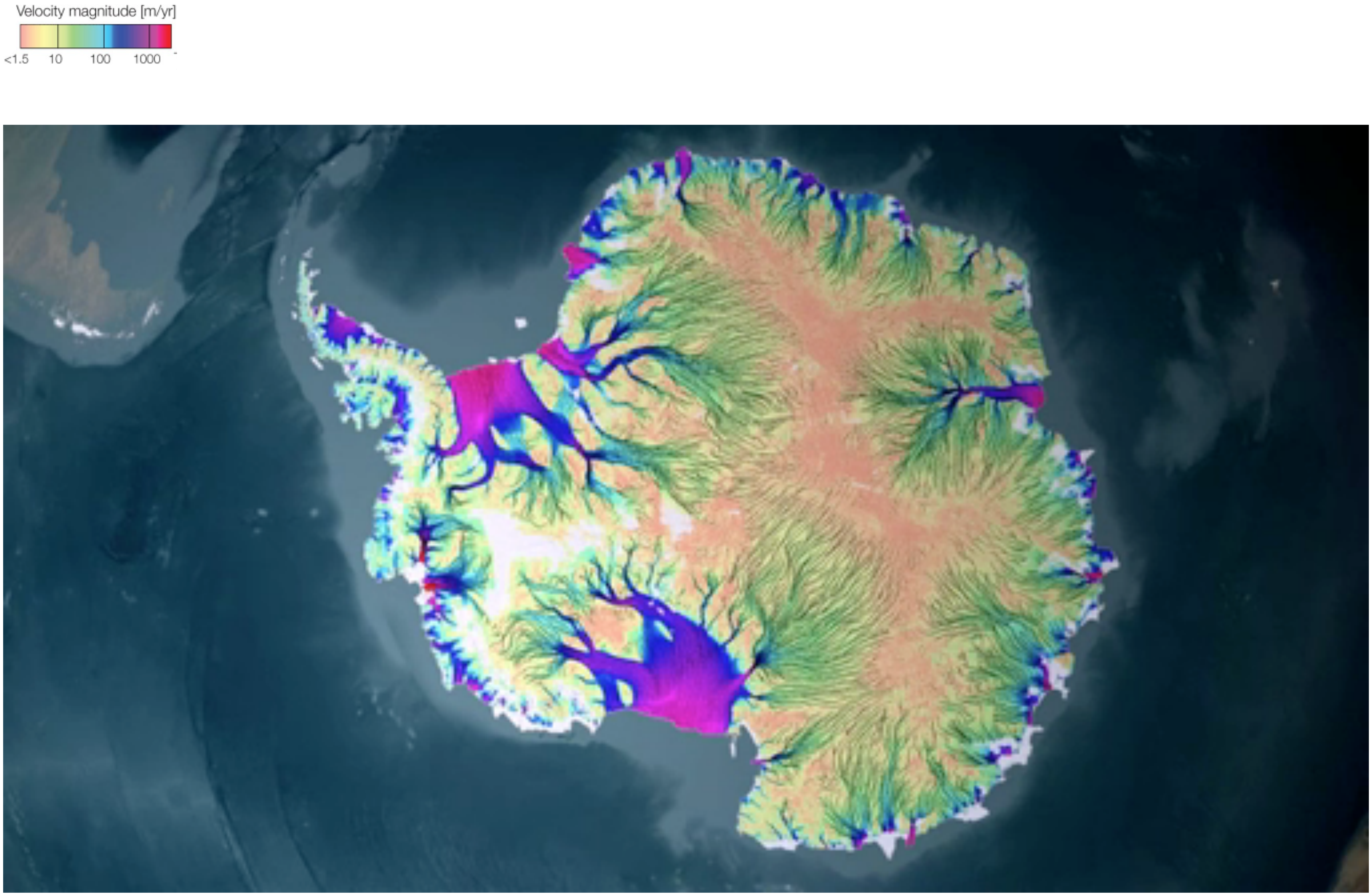

Rignot et al. 2011

Proposed Paleo-Ice Streams

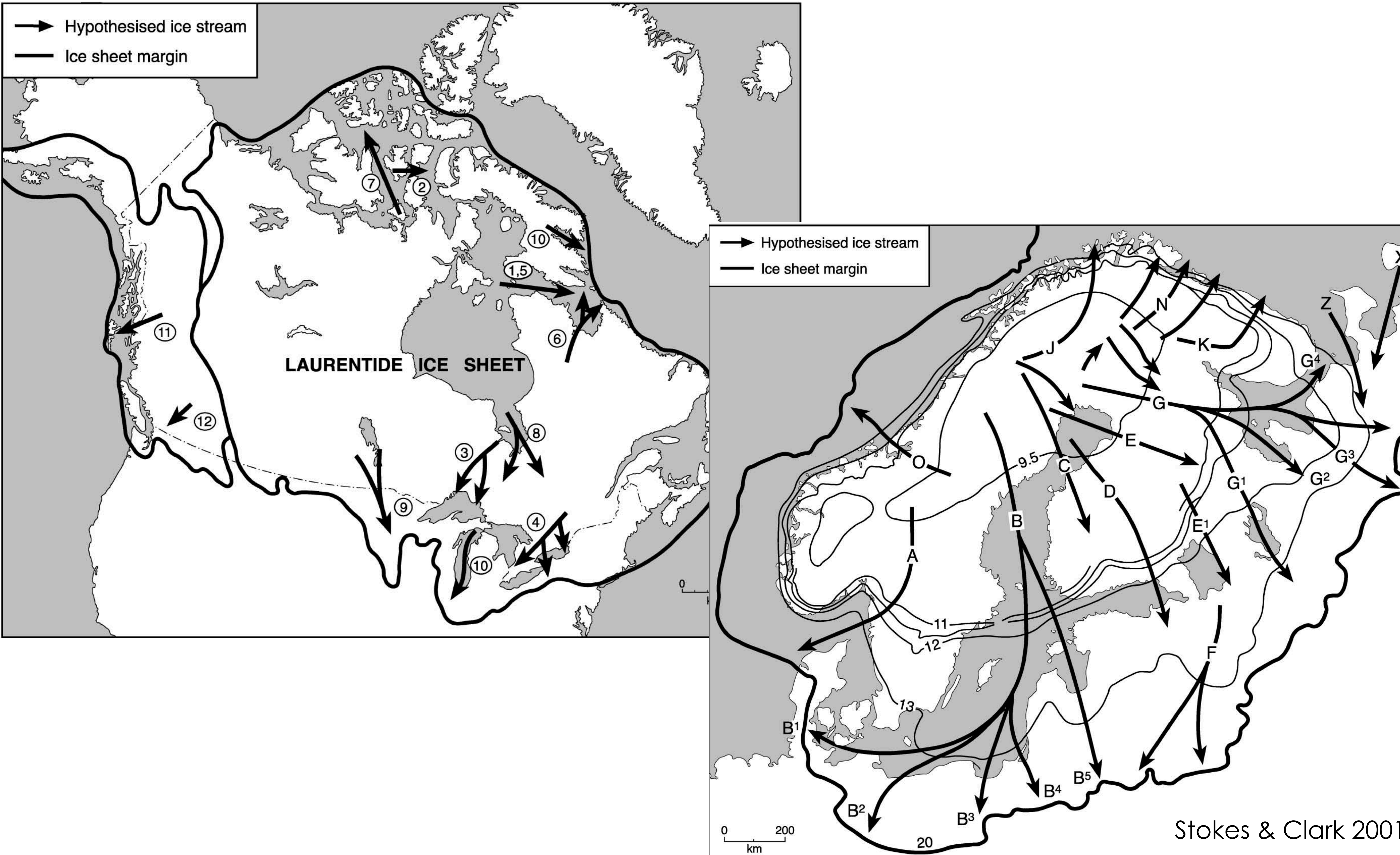

Stokes & Clark 2001

Proposed Paleo-Ice Streams

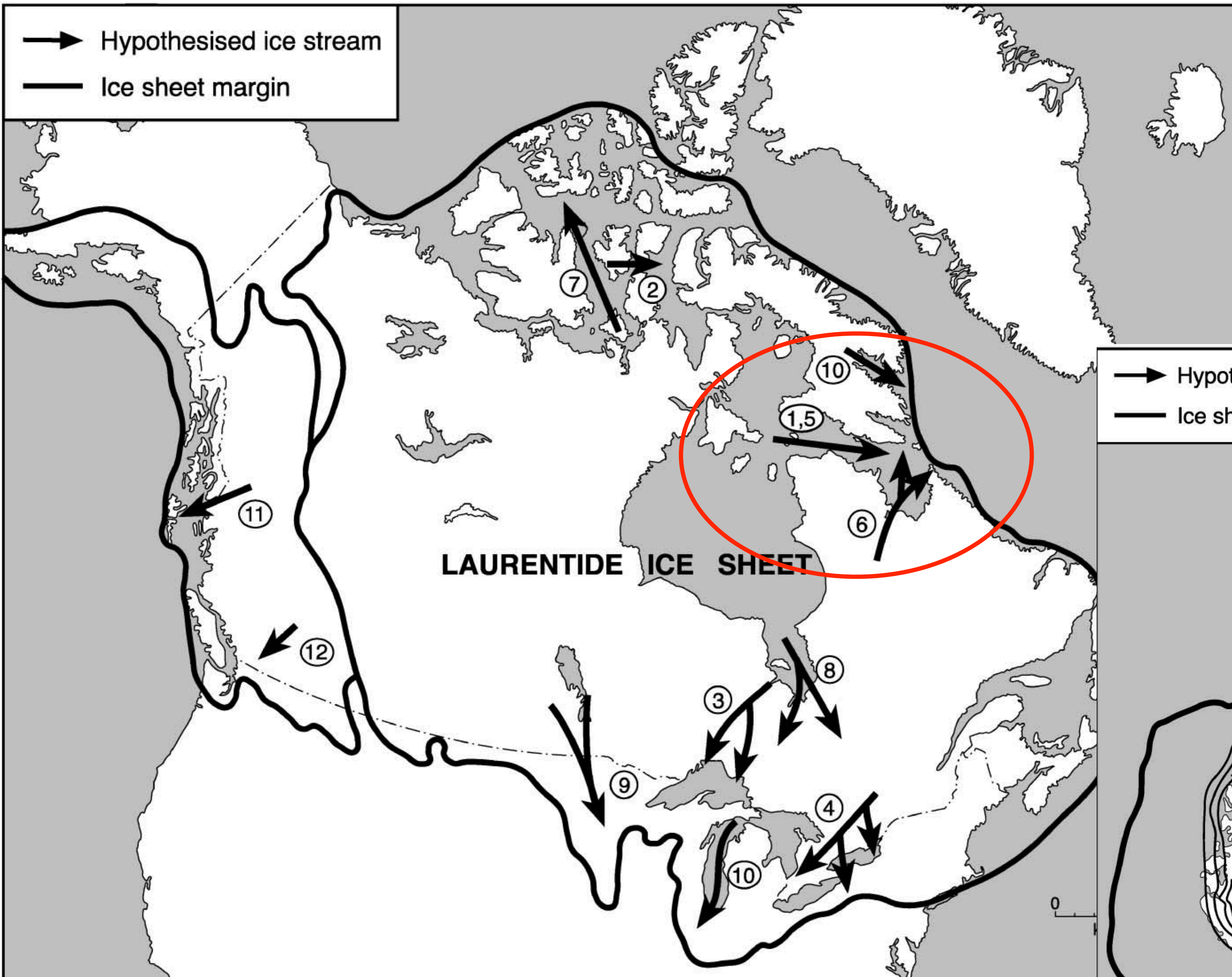

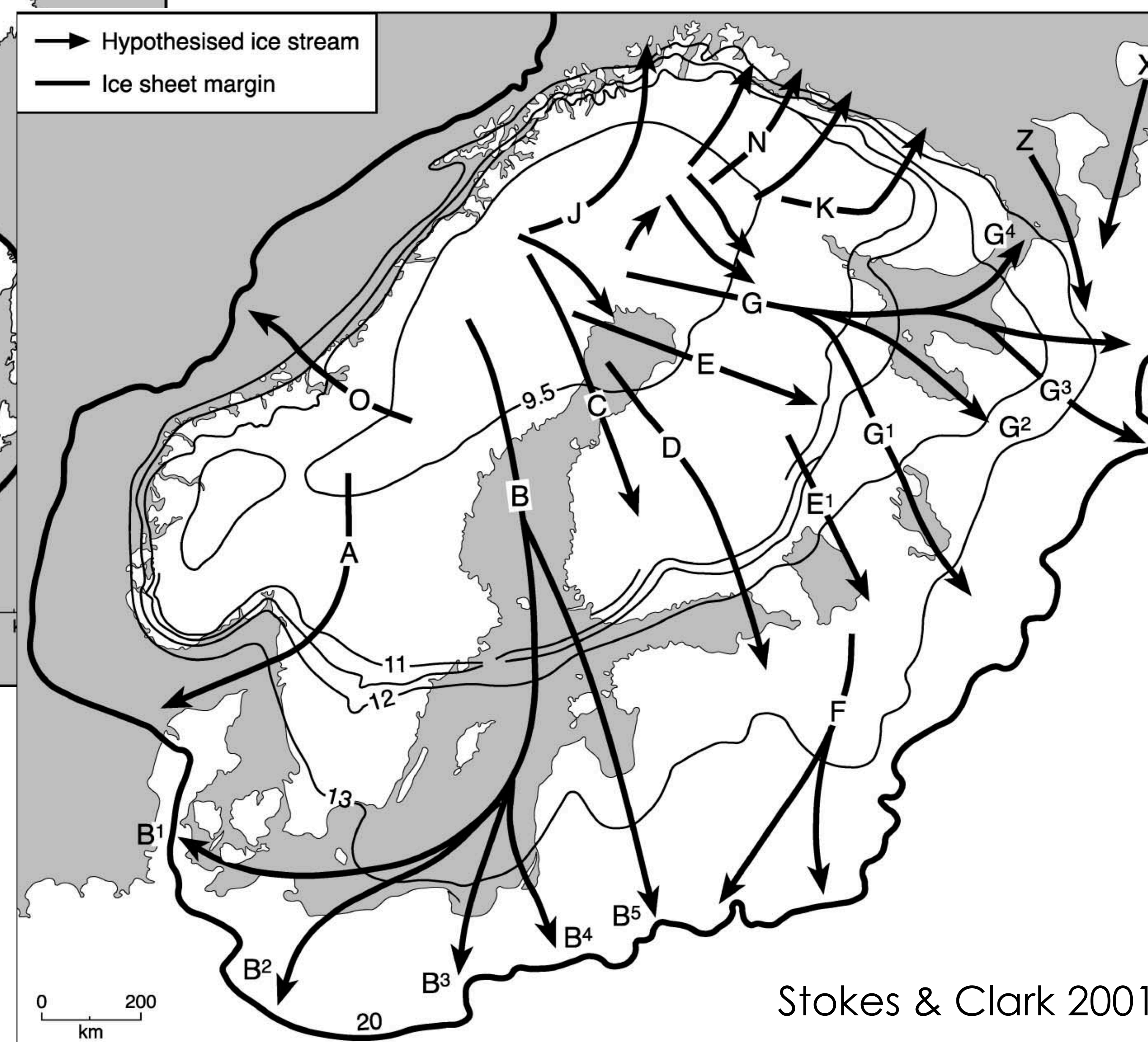

Stokes & Clark 2001

Hypothesis 1: MacAyeal's (1993) Binge-purge oscillator

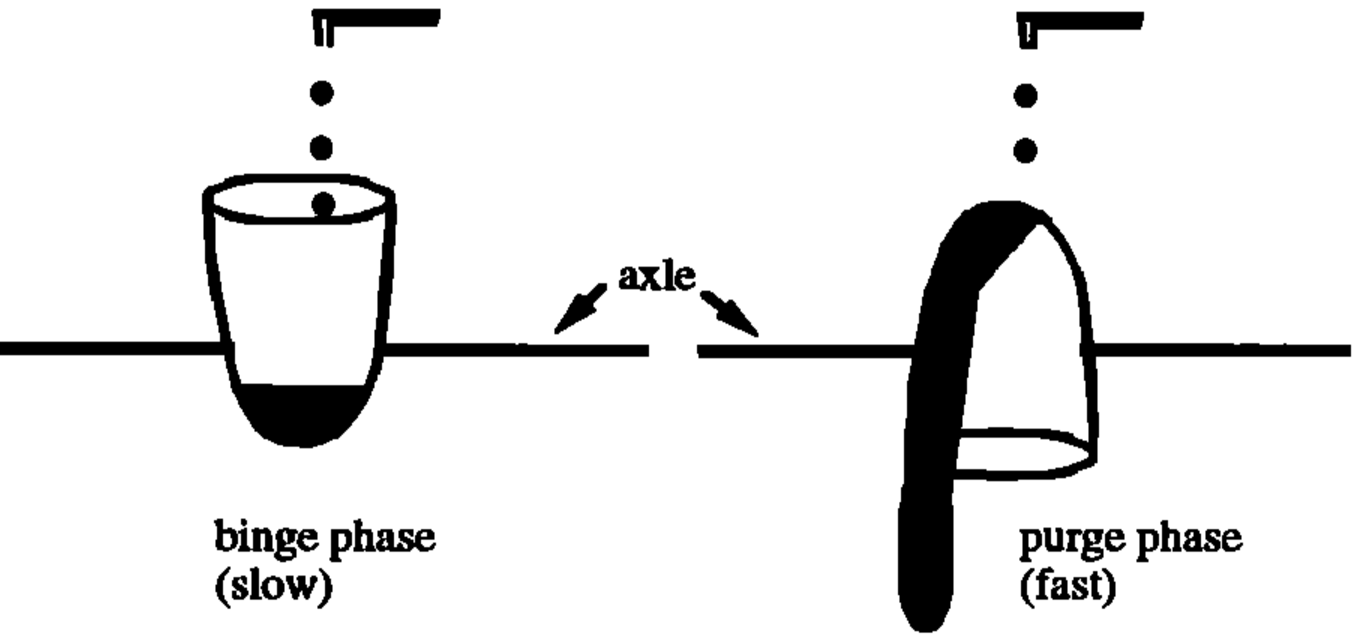

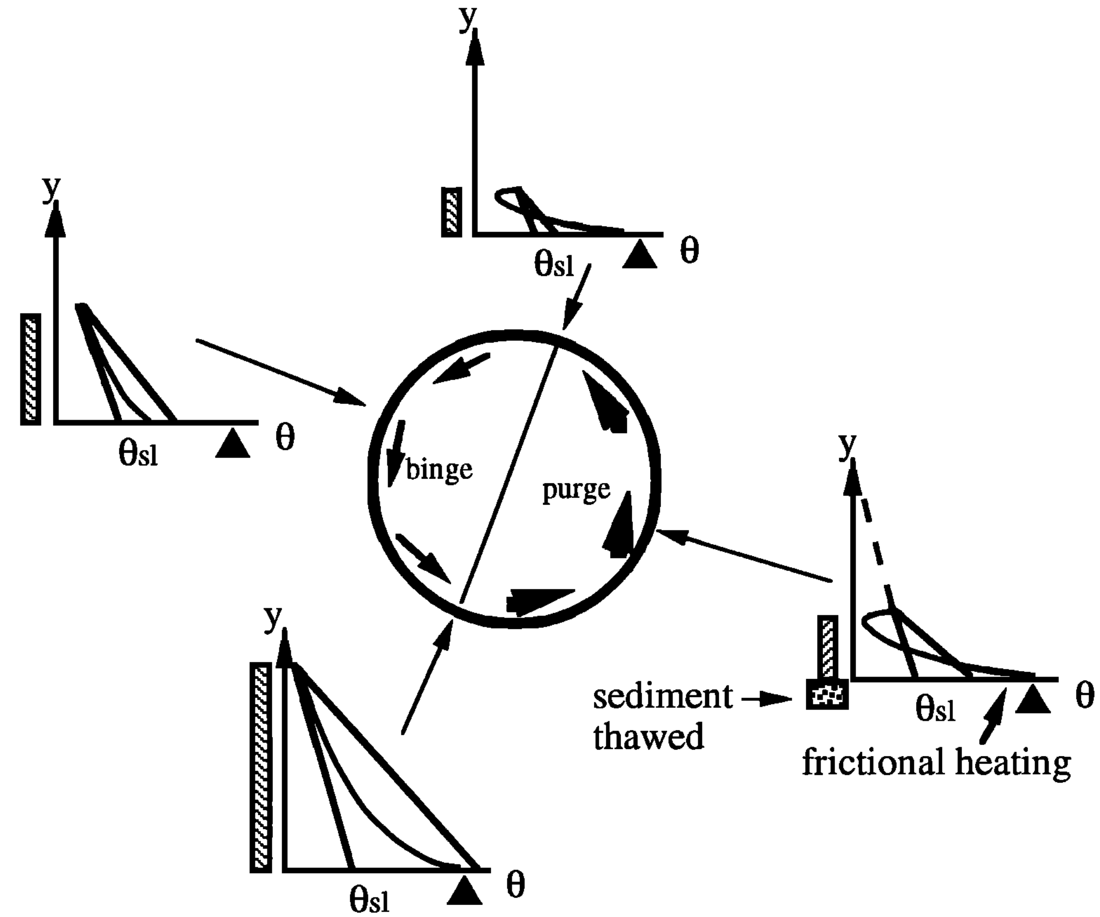

A relaxation oscillation(!)

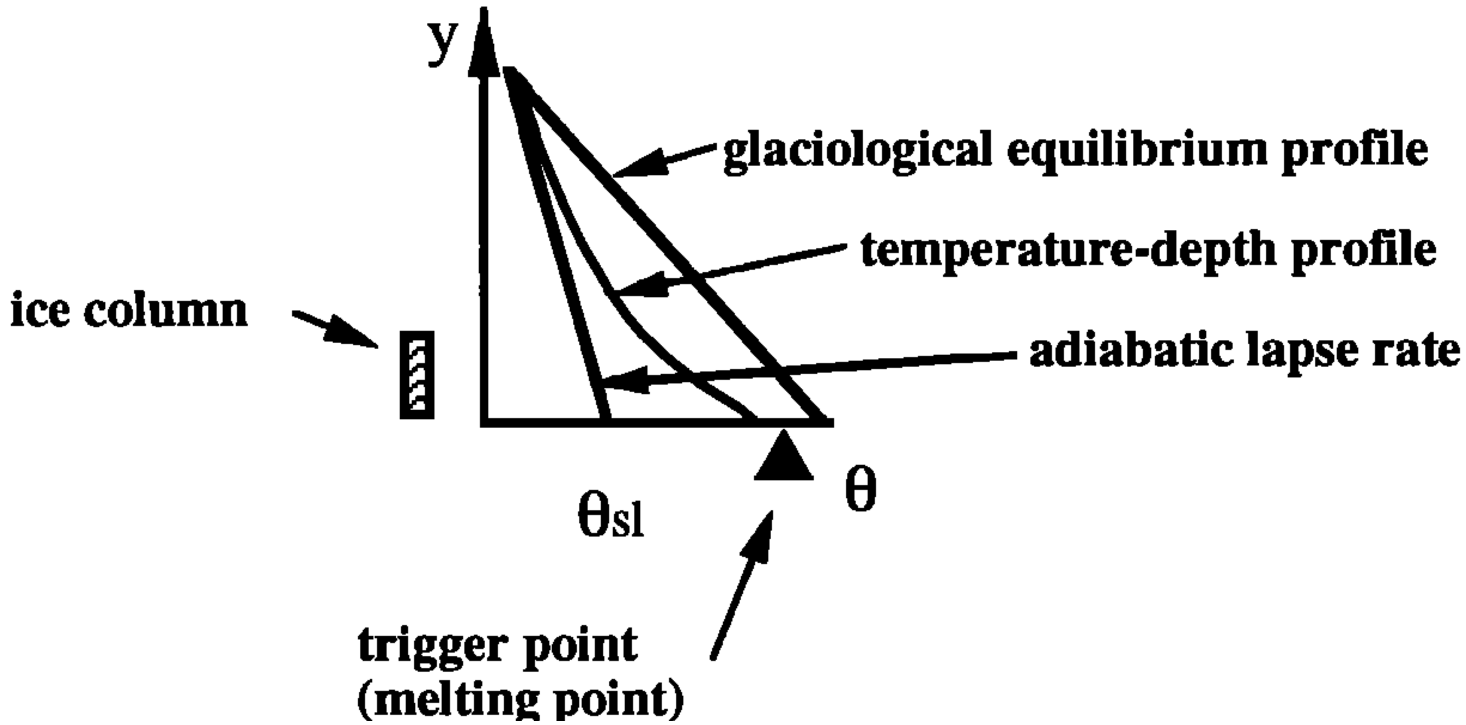

Fig. 2. A conceptual view of the temperature-depth profile $\theta(y)$ in an ice column during the binge/purge cycle of the Laurentide ice sheet. Vertical elevation from the base of the ice column is denoted by y and θ represents temperature. The annual average sea level atmospheric temperature is denoted by θ_{sl}. The melting temperature of ice is represented by the black triangles. The four graphs surrounding the central circle display the sequence of states through which the ice column evolves during a complete cycle. Time passage is represented by counterclockwise progression through the sequence of graphs.

Hypothesis 1: MacAyeal's (1993) Binge-purge oscillator

(idealized model only) MacAyeal's (1993) Binge-purge oscillator, except that: since we use a fully coupled model, the snow accumulation rate and the atmospheric temperature as function of time are calculated rather than specified. A different mechanism for the periodic collapses of the LIS could be incorporated into our mechanism with no difficulty...

Glacier height eqn (growth): $$\frac{dH(t)}{dt} = Acc(t) - Abl(t)$$

Glacier height eqn (collapse): $$\frac{dH(t)}{dt} = -H/\tau$$

Glacier heat (diffusion) eqn: $$\frac{\partial T(t,z)}{\partial t} = \frac{\kappa}{C_p^{ice}\rho^{ice}} \frac{\partial^2 T(t,z)}{\partial z^2}$$

or, in terms of $\zeta = \frac{z}{H(t)}$: $$\frac{\partial T(t,\zeta)}{\partial t} = \frac{\kappa}{C_p^{ice}\rho^{ice}H(t)^2} \frac{\partial^2 T(t,\zeta)}{\partial \zeta^2} + \frac{\partial T(t,\zeta)}{\partial \zeta(t)} \frac{\zeta(Acc(t)-Abl(t))}{H(t)}$$

T boundary conditions: $$\frac{\partial T(t,0)}{\partial \zeta(t)} = \frac{H(t)G}{\kappa}; \quad T(t,1) = \theta(t) - \Gamma H(t) \equiv T_{top}(t)$$

Accumulation rate: $$Acc(t) = \frac{Q_S^{atm-ocean}}{Area} * e^{\frac{-H(t)}{Z_0}}$$

Hypothesis 1: MacAyeal's (1993) Binge-purge oscillator

- Laurentide Ice Sheet (*LIS*) thickens due to snow accumulation (**binge stage**); geothermal heat is trapped at the base of thick & insulating *LIS*
- Geothermal heating melts glacier base, reduces bottom friction ➨ ice sheet slides into North Atlantic ocean (**purge stage**)
- Thiner glacier allows geothermal heat to diffuse out, base refreezes, cycle repeats

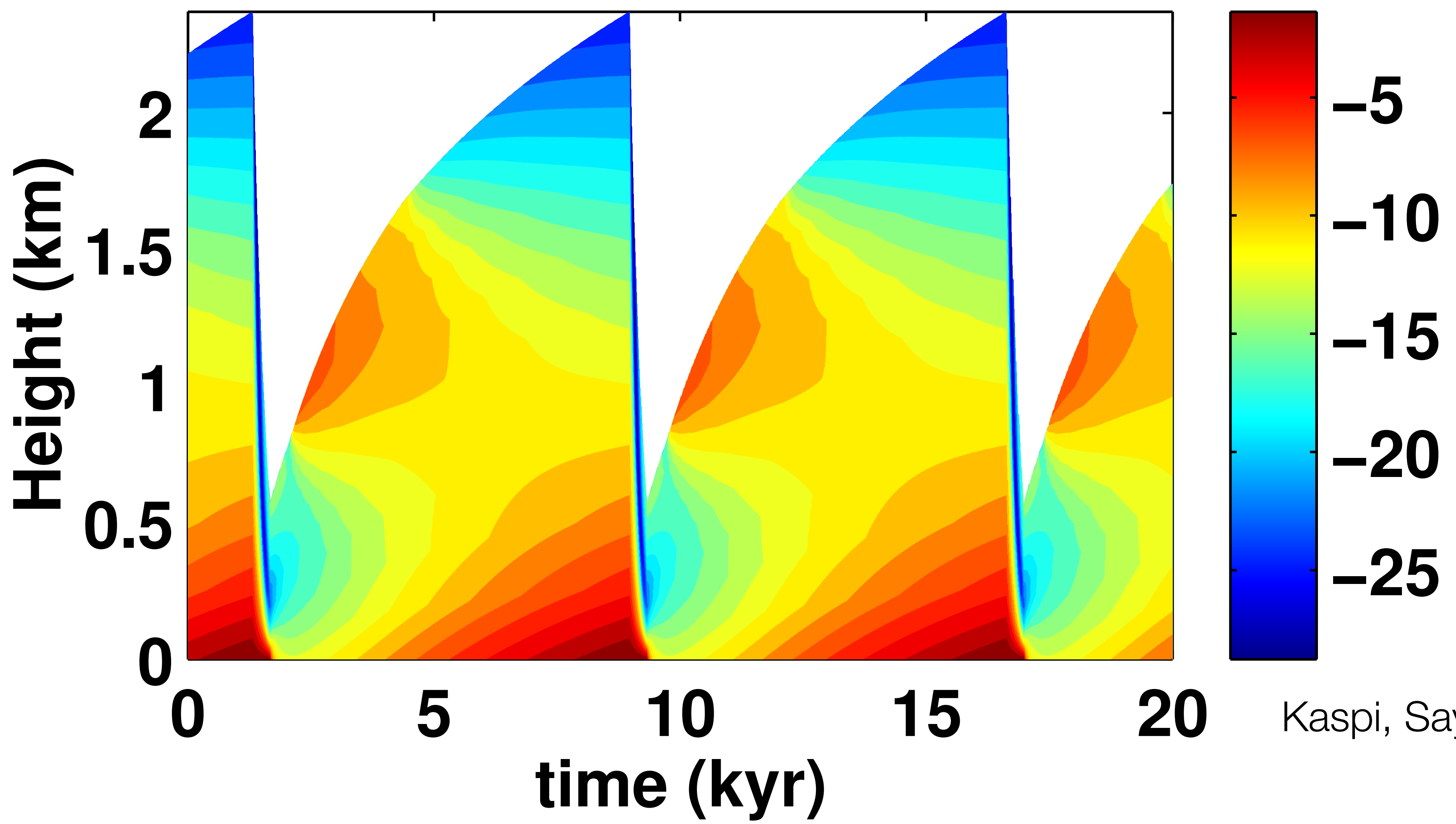

Kaspi, Sayag, Tziperman 2004

Glacier height as a function of time during a few Heinrich cycles. Colors indicate temperature within ice sheet.

Hypothesis 1: MacAyeal's (1993) Binge-purge oscillator

MacAyeal (1993a): surface/climate forcing is not likely to play a role based on temperature diffusion argument (section 2, eqns 1–5, p 777);

at surface, z=0: $\theta(0,t) = \Delta\theta\cos(\omega t)$

advection diffusion equation: $\theta_t + w\cdot\theta_z = \kappa\theta_{zz}$

for $w=0$: $\theta(z,t) = \Delta\theta\exp\left\{\frac{z\sqrt{\omega}}{\sqrt{2\kappa}}\right\}\cdot\cos\left(\omega t + \frac{z\sqrt{\omega}}{\sqrt{2\kappa}}\right)$

➨decaying oscillations in vertical, decay scale $\sqrt{2\kappa/\omega} = 314\ m$

➨ effectively no signal of surface variability at z=–2 km.

(solution for w=W=constant representing ice flow/ accumulation: same idea)

Hypothesis 1: MacAyeal's (1993) Binge-purge oscillator

MacAyeal (1993a): climate forcing not likely to play a role based on temperature diffusion argument; **However:** there are other mechanisms: Moulins, Accumulation of melt water in ice shelf cracks, collapse & elimination of buttressing/back-pressure

Hypothesis 1: MacAyeal's (1993) Binge-purge oscillator

MacAyeal (1993a): climate forcing not likely to play a role based on temperature diffusion argument; **However:** there are other mechanisms: Moulins, Accumulation of melt water in ice shelf cracks, collapse & elimination of buttressing/back-pressure

Hypothesis 1: MacAyeal's (1993) Binge-purge oscillator

MacAyeal (1993a): climate forcing not likely to play a role based on temperature diffusion argument; **However:** there are other mechanisms: Moulins, Accumulation of melt water in ice shelf cracks, collapse & elimination of buttressing/back-pressure

Hypothesis 1: MacAyeal's (1993) Binge-purge oscillator

MacAyeal (1993a): climate forcing not likely to play a role based on temperature diffusion argument; **However:** there are other mechanisms: Moulins, Accumulation of melt water in ice shelf cracks, collapse & elimination of buttressing/back-pressure

A word on Moulin mechanism and energetics

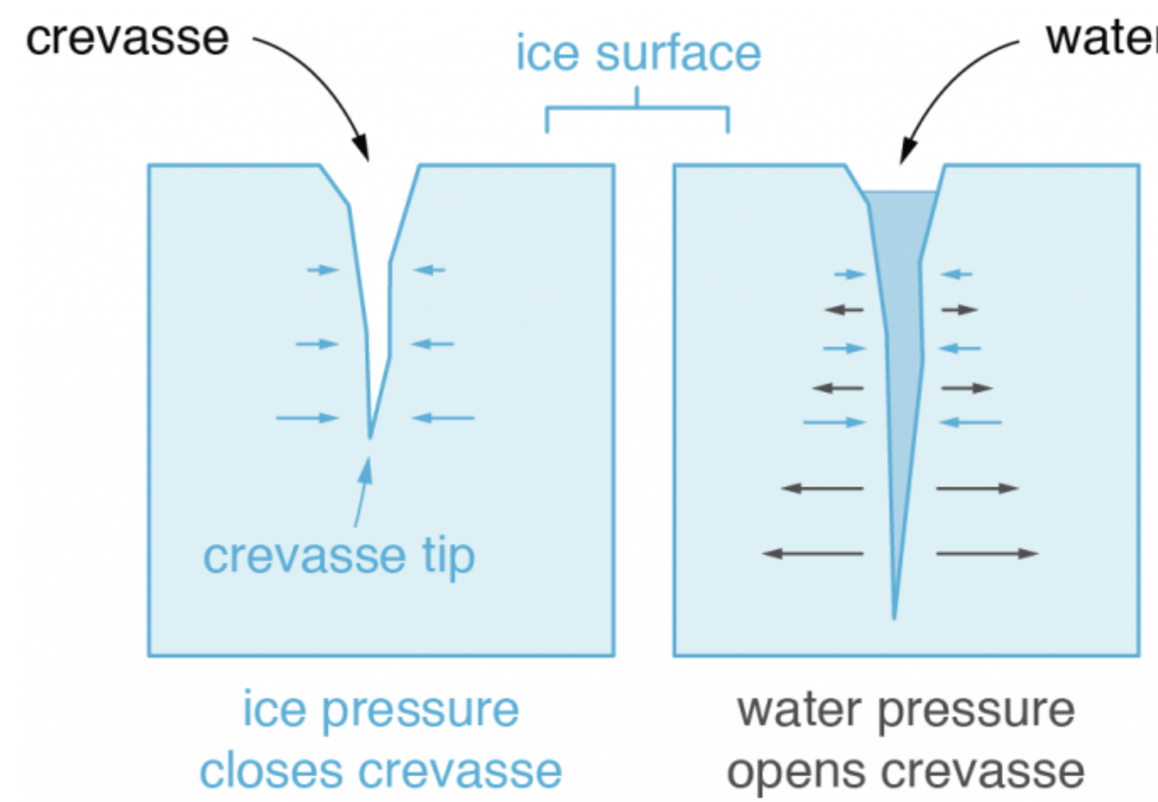

(Benn et al. 2007)

A word on Moulin mechanism and energetics

Why doesn't water flowing down a moulin freeze on its way?

The potential energy of a water parcel at the ice surface is converted to kinetic energy as it flows down, which is then converted to heat by friction with the moulin walls. To calculate the heating: energy conservation is $c_{p,water}\Delta T = g\ 1000H$, where H is the height loss in kilometers. The temperature change is therefore

$$\Delta T = \frac{g\ 1000H}{c_{p,water}} = \frac{9.8H}{4.2} = 2.33\frac{\text{K}}{\text{km}}\ H\,.$$

A drop of $H = 1$ km would warm the falling water mass by over 2K. Some of this heat is transferred to the moulin walls, causing melting and preventing their closing in.

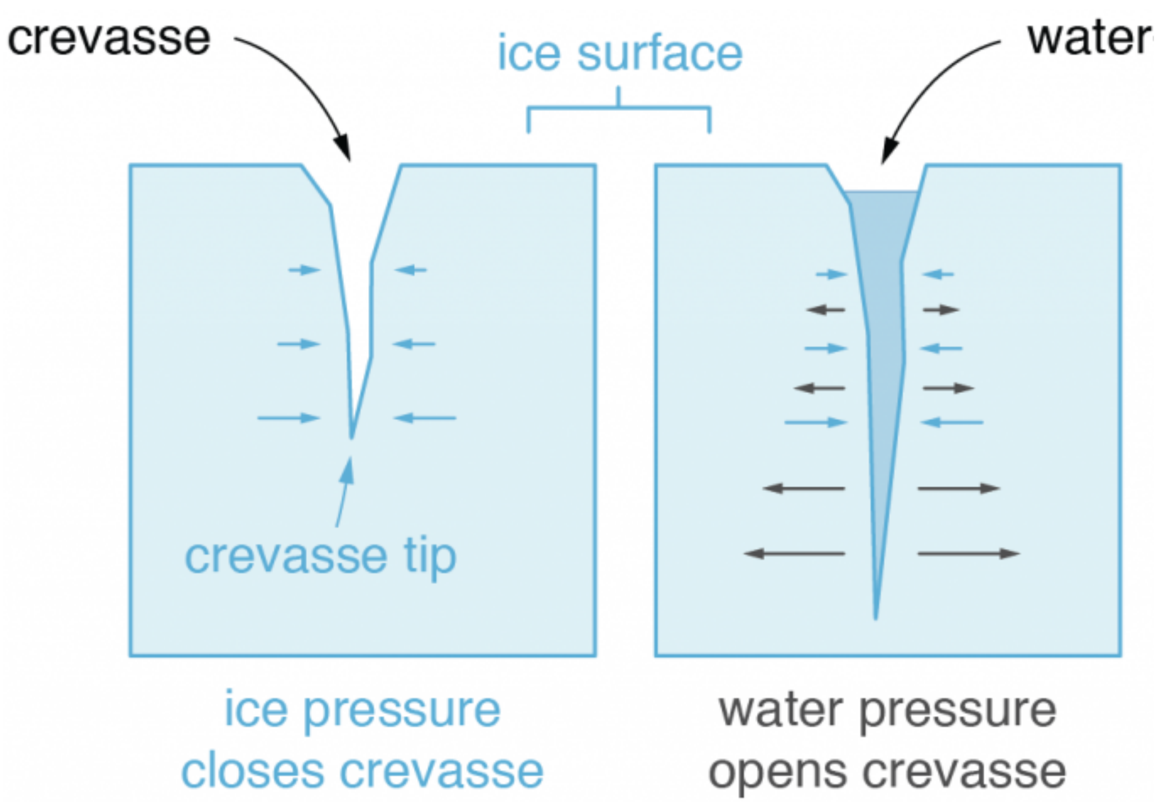

(Benn et al. 2007)

Hypothesis 1: MacAyeal's (1993) Binge-purge oscillator

MacAyeal (1993a): a heuristic argument for the time scale

(section 5, p 782, eqns 19–25, note that LHS of eqn 23, the b.c at the ground, should be $\theta_y(0,t)$)

Assume an infinitely thick ice sheet; how long would it take for geothermal heat to melt the base?

Bottom b.c.: $-\kappa\theta_y = G$; Initial conditions: $\theta_0(y, t=0) = \theta_{sl} - \Gamma y$

Separate into steady and time depend: $\theta(y,t) = S(y) + \tilde{\theta}(y,t)$

Simple diffusion eqn $\tilde{\theta}_t = \kappa\tilde{\theta}_{yy}$; initial condition: $\tilde{\theta}(y, t=0) = \theta_{sl}$

b.c: $-\kappa\tilde{\theta}_y(0,t) = G - \kappa\Gamma = \tilde{G}$

Solution: time to get to zero at y=0 is: $T_L = \frac{\pi}{\kappa}\left(\frac{-\kappa\theta_{sl}}{2\tilde{G}}\right)^2$

For $\mathrm{G} = 0.05\mathrm{W/m^2},\ \Gamma = 9^\circ/\mathrm{km},\ \theta_{\mathrm{sl}} = -10^\circ$

➡ The time to melting, hence Heinrich period: T_L=6944 years!

Connections between Heinrich and D/O events; “bond cycles”

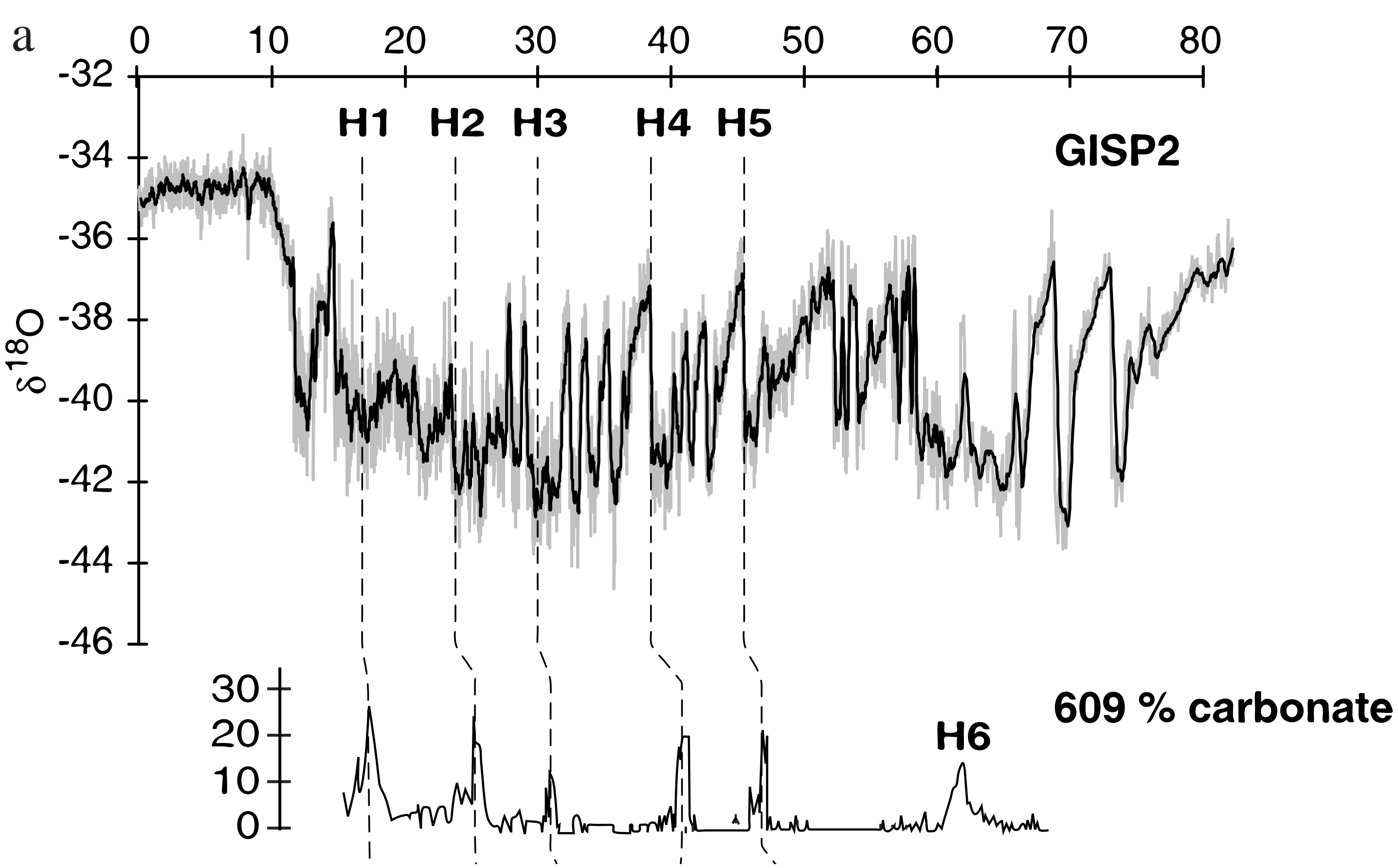

(Hemming 2004) Fig 4a

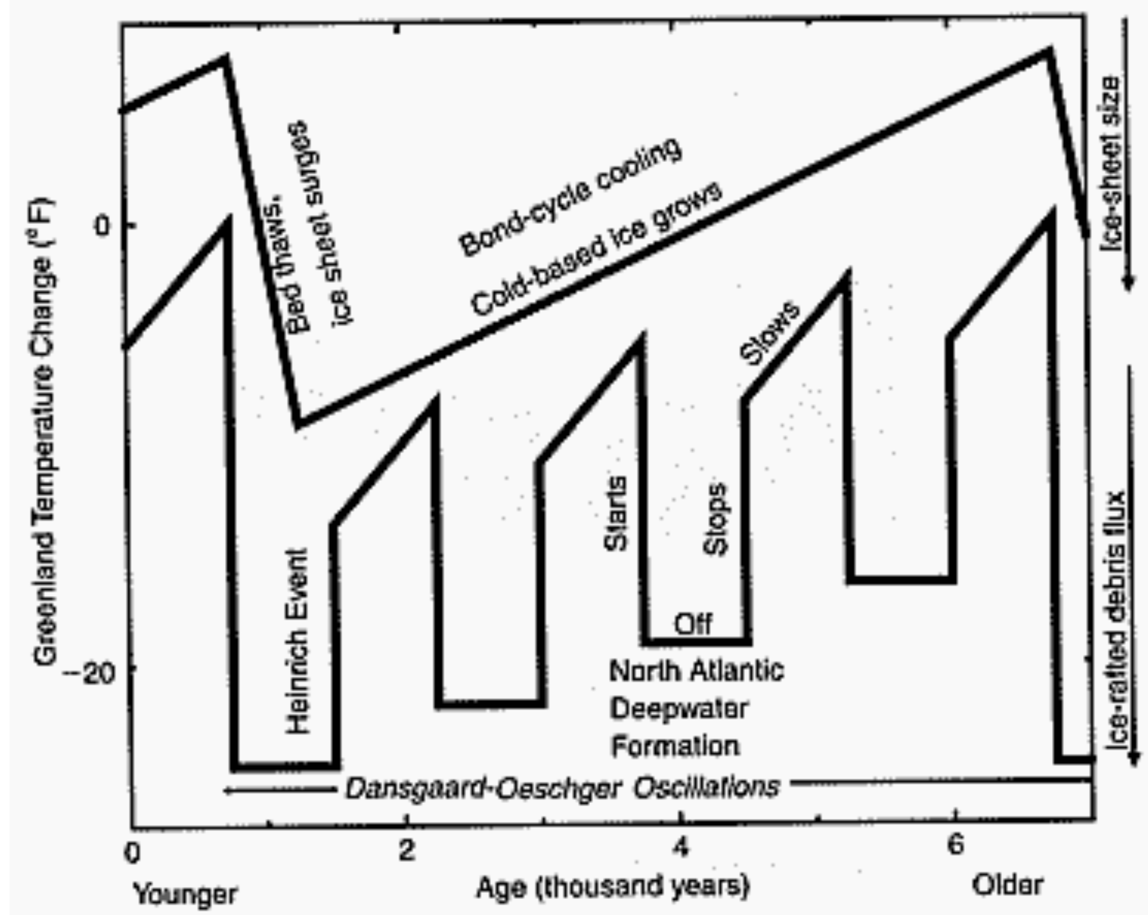

FIGURE 12.4
An idealized history of temperature and ice sheet changes in the north Atlantic region during a Bond cycle. Successive Dansgaard-Oeschger oscillations, caused by the turning on and off of the far northern sinking of waters in the north Atlantic, become progressively cooler as the cold-based ice sheet grows in Hudson Bay. Then the base of that ice thaws, and a Heinrich event surge occurs, dumping large numbers of icebergs containing rock debris into the north Atlantic. When the surge ends, the ice sheet freezes to its bed, while the ocean circulation resumes and causes an especially large warming away from the ice sheet.

Heinrich events appear to occur during cold epochs in the North Atlantic

Hypothesis 2: Catastrophic ice shelf break up

Larsen B collapse, March 2002

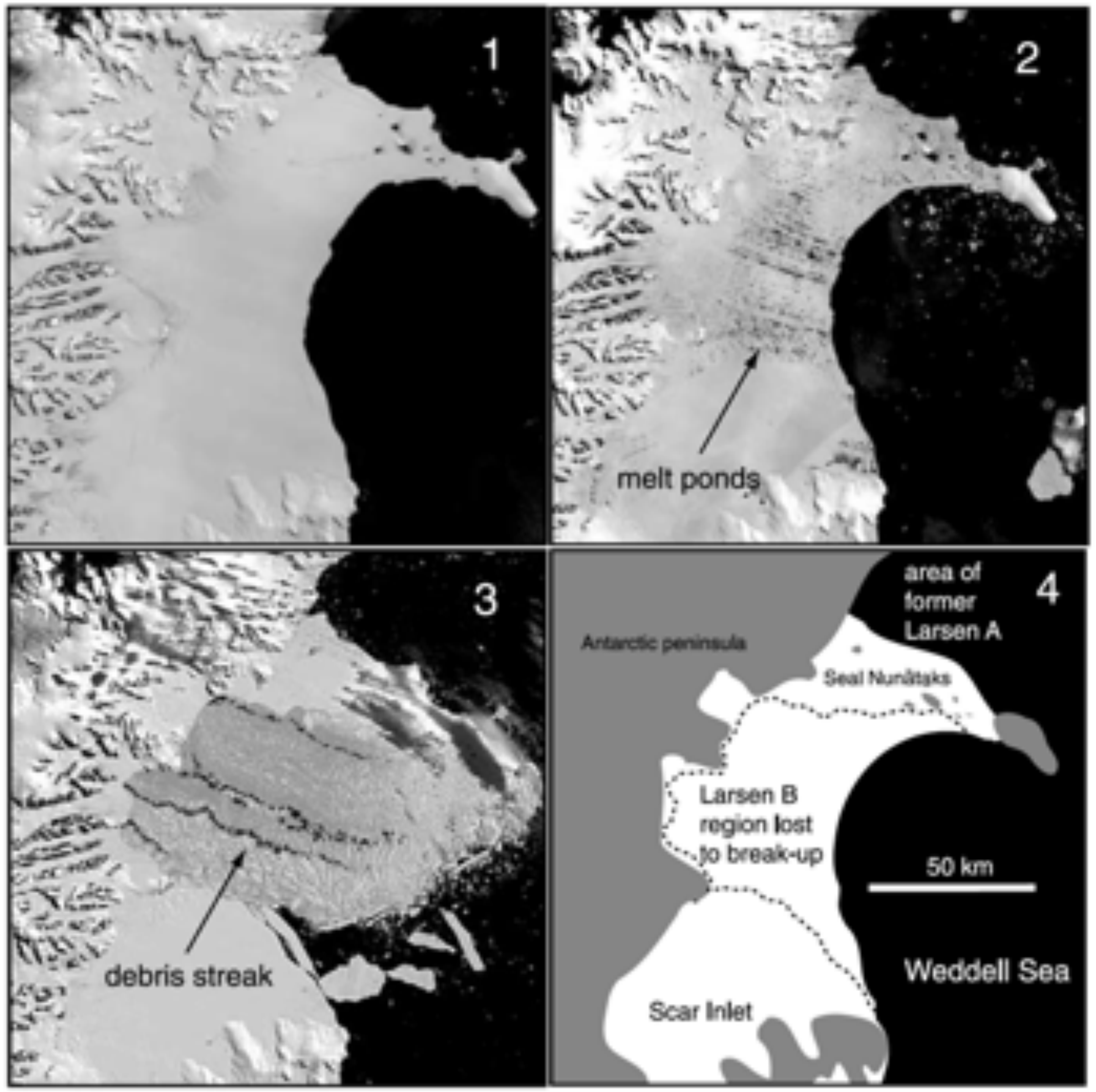

Mechanism: hydro-fracture

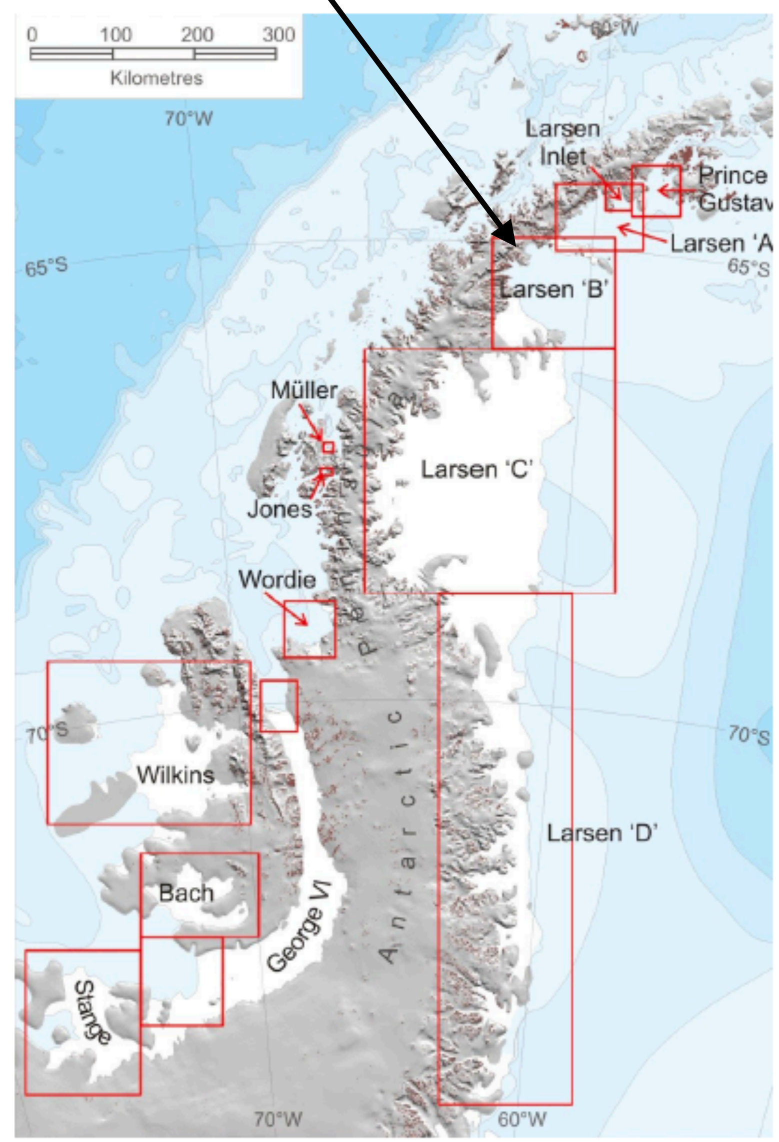

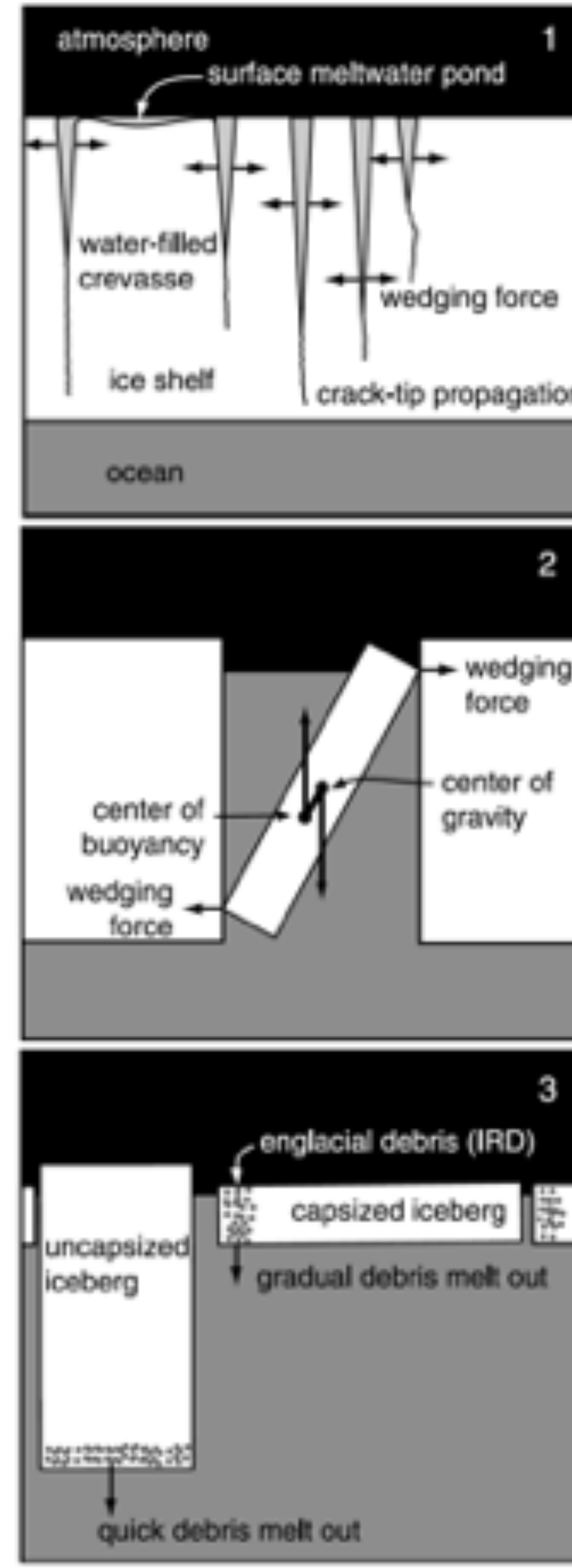

Expected signature: small sea level change except buttressing effect

(Hulbe et al, 2004)

Hypothesis 3: Abrupt retreat of grounding line across a retrograde bottom slope (Marine Ice Sheet Instability/ MISI)

(Weertman, 1974; Schoof, 2007)

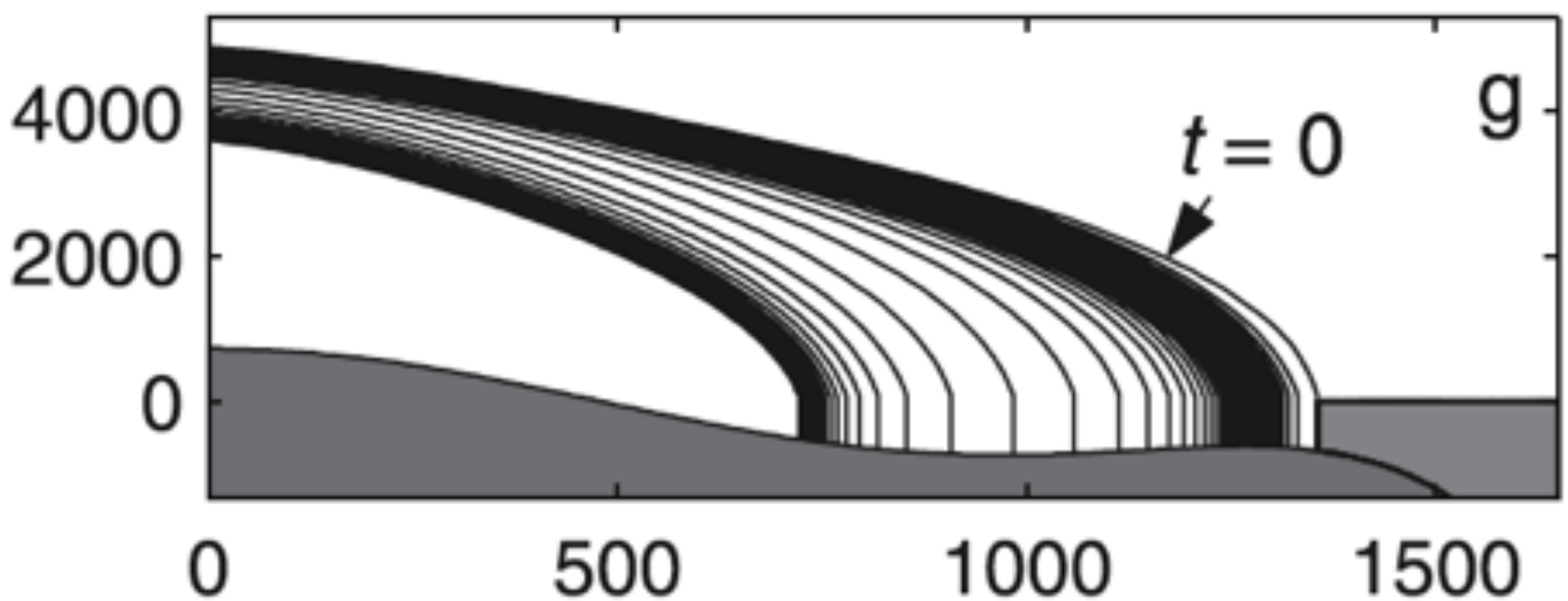

scenario 1: ocean melting at grounding line placing it upstream of unstable point

Marine Ice Sheet Instability (MISI)
scenario (1): melting by a warmer ocean

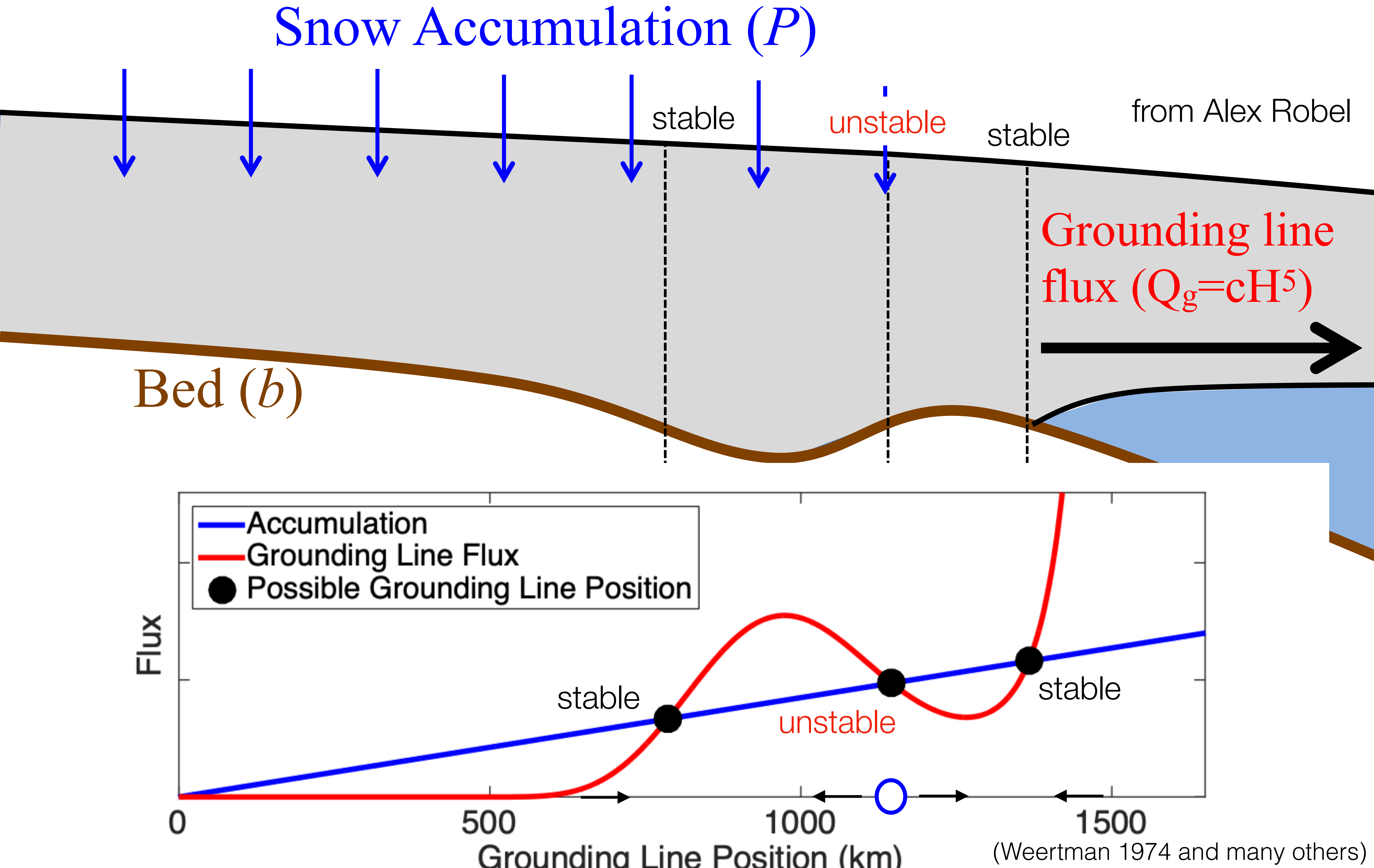

(Weertman 1974 and many others)

Marine Ice Sheet Instability (MISI)
scenario (1): melting by a warmer ocean

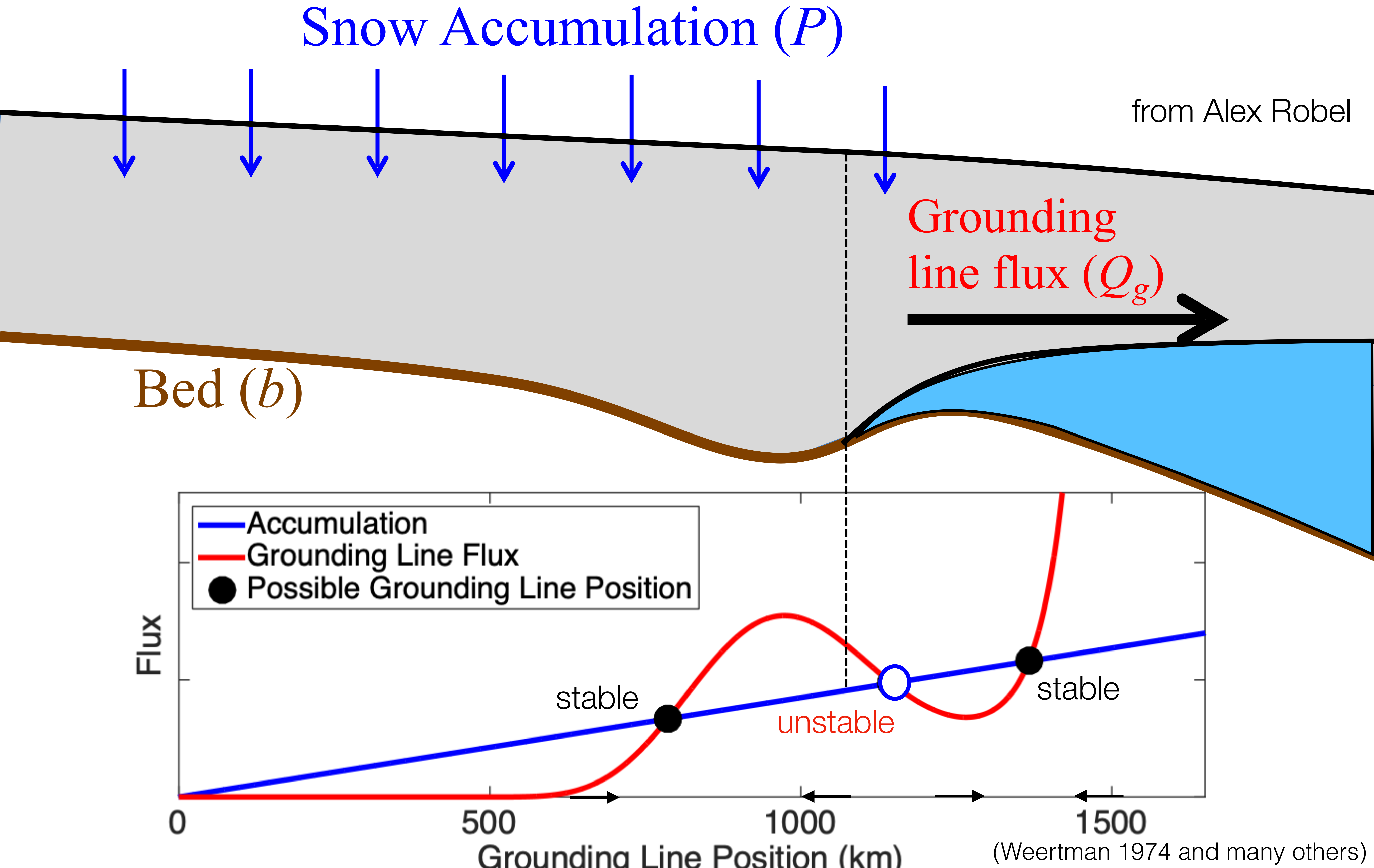

(Weertman 1974 and many others)

Marine Ice Sheet Instability (MISI)

scenario (1): melting by a warmer ocean

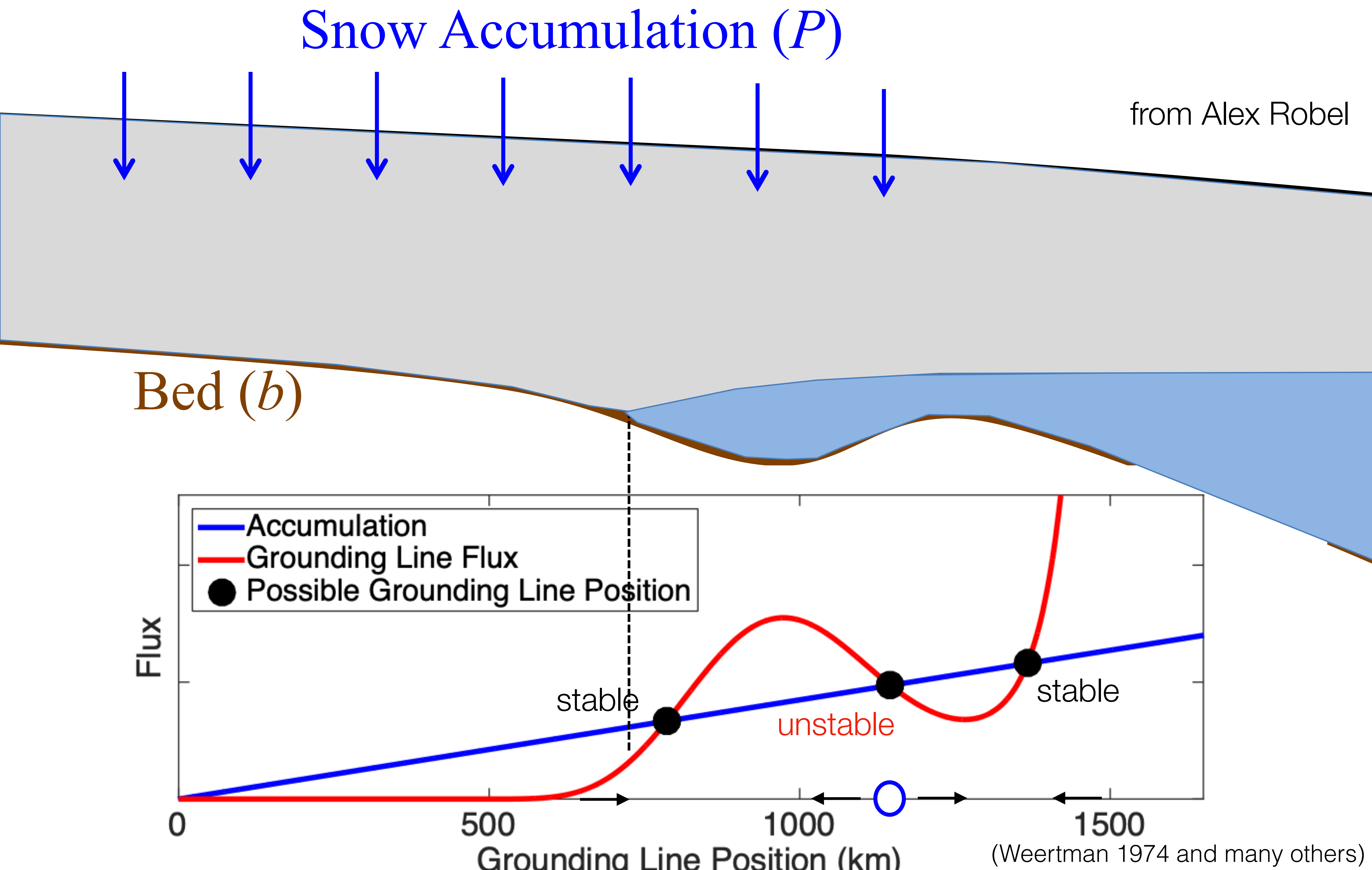

(Weertman 1974 and many others)

Marine Ice Sheet Instability (MISI) scenario 2: change in accumulation

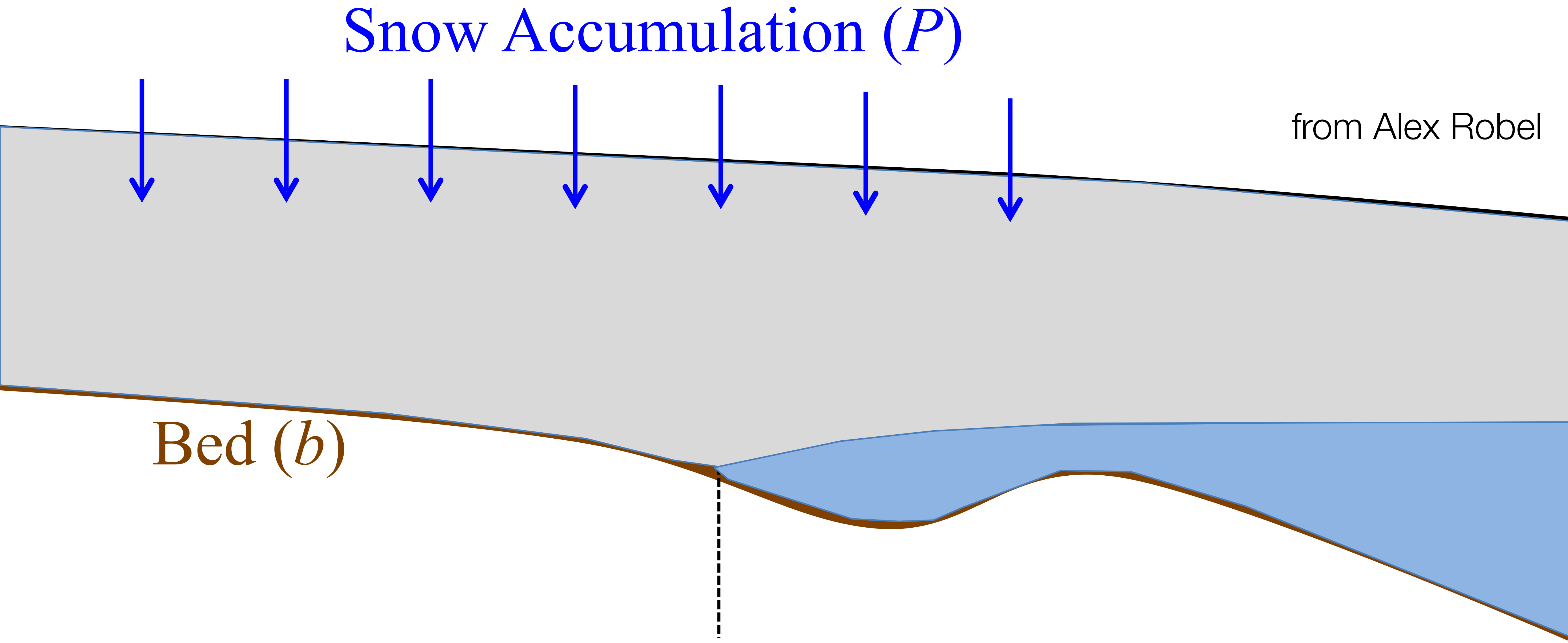

Discuss the stability of a grounding line on prograde vs retrograde slopes under a scenario of changing rate of accumulation

(Weertman 1974 and many others)

Why worry about retrograde slopes in the context of future projections? They are common in Greenland.

Results:
glacier retreat/
advance, ocean
temperature and
updated
topography

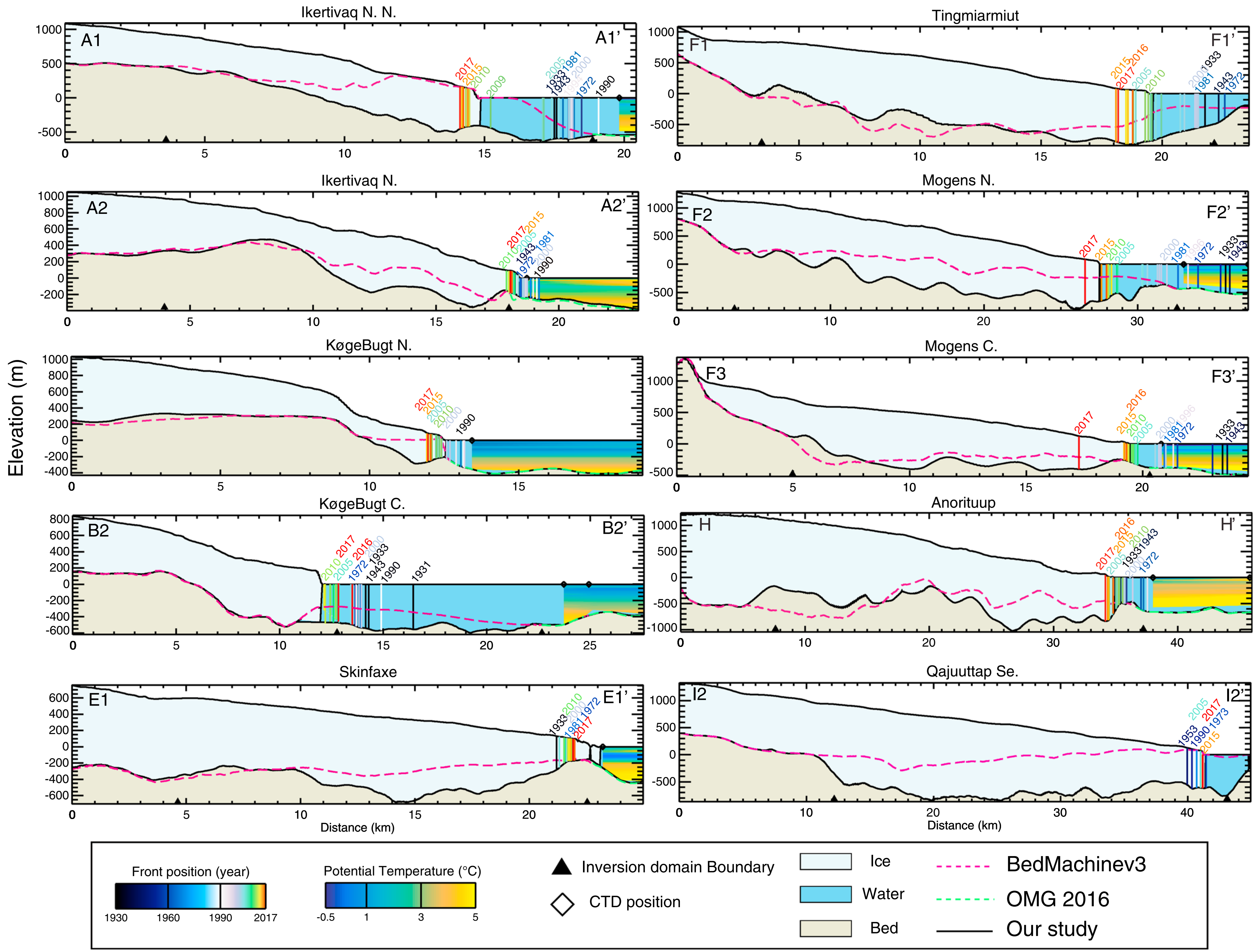

[Millan et al 2018, GRL]

Figure 3. surface elevation along profiles in Fig 2 with bed elevation from BM3 (dashed red), OMG (dashed green), and from this study (solid black). Ocean is blue, ice is light blue. Ice front positions are color coded from blue to red and labeled by year. Ocean Melting Greenland (OMG) temperature from CTDs in 2016 are color coded from blue (cold) to yellow (warm), with CTD position as a diamond. Limits of the gravity inversion are black triangles.

“Largest retreat on a retrograde slope after 1965, doubled its speed since the 1990s”

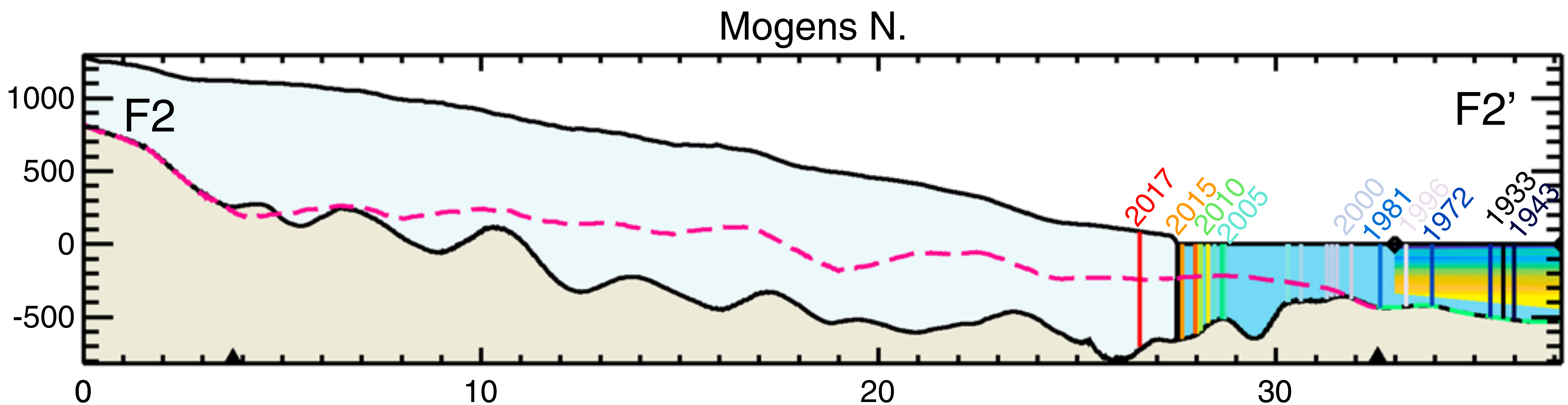

(dash red: previous estimate of topography; note large difference from previous topography)

[Millan et al 2018, GRL]

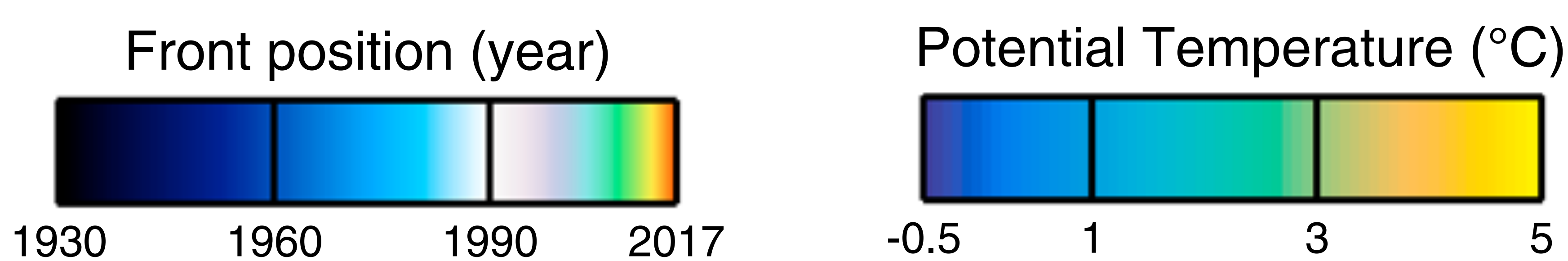

“stable due to shallow sill”

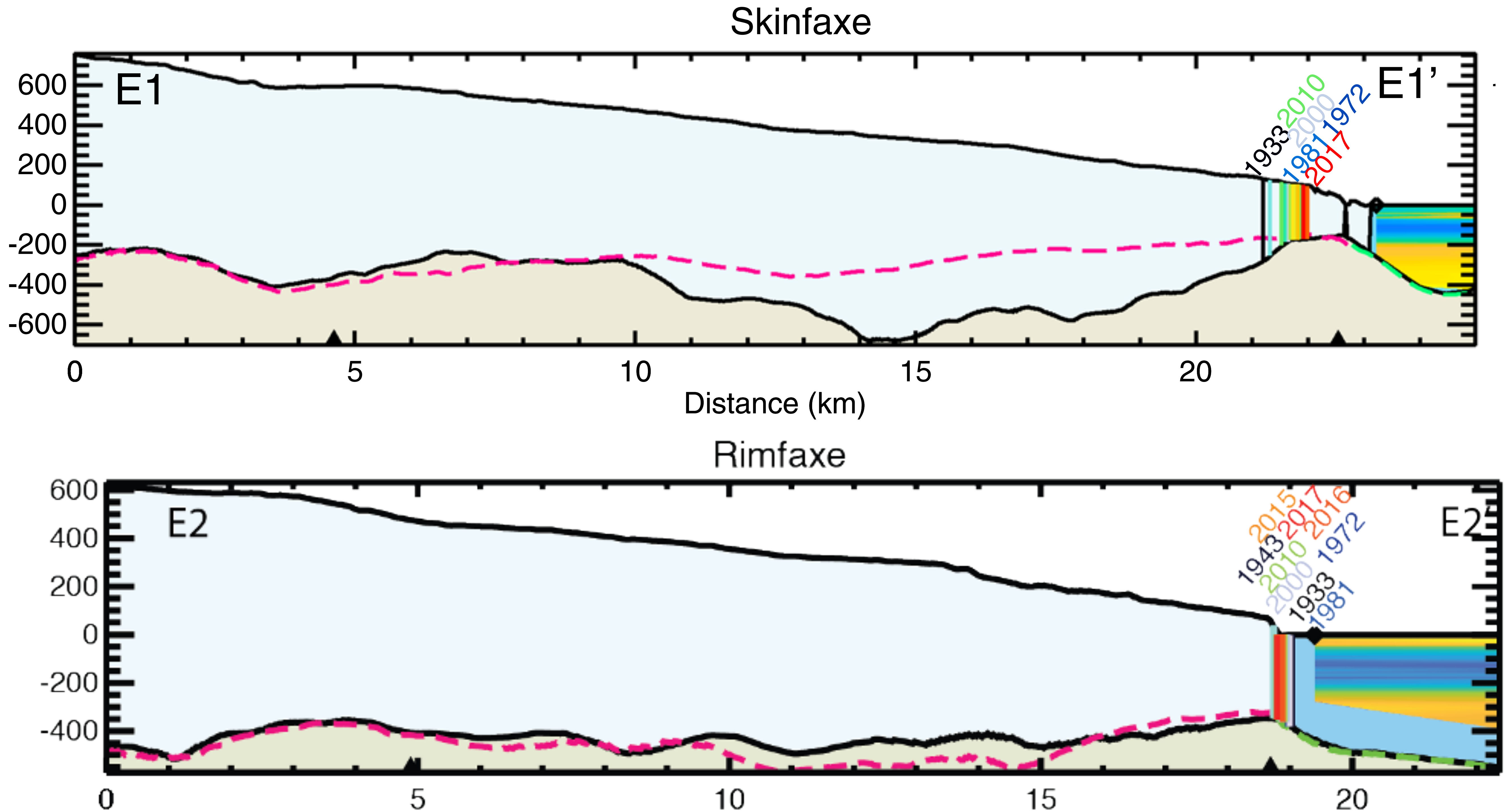

[Millan et al 2018, GRL]

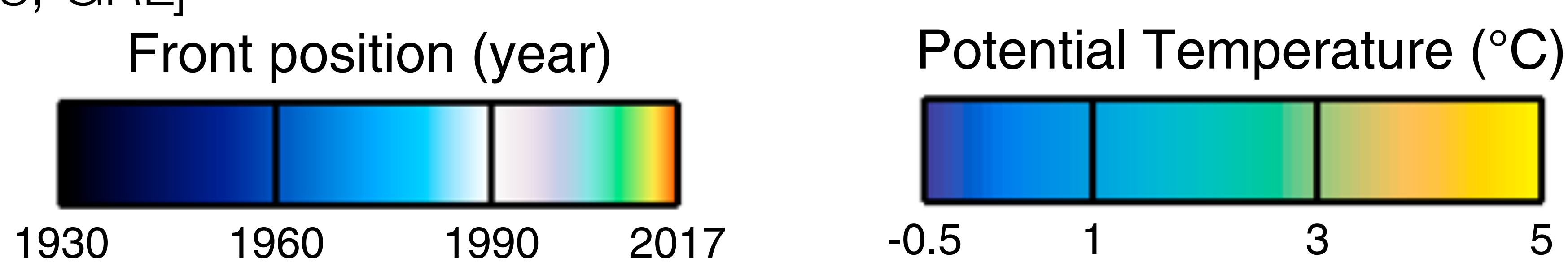

Qajuuttap Se

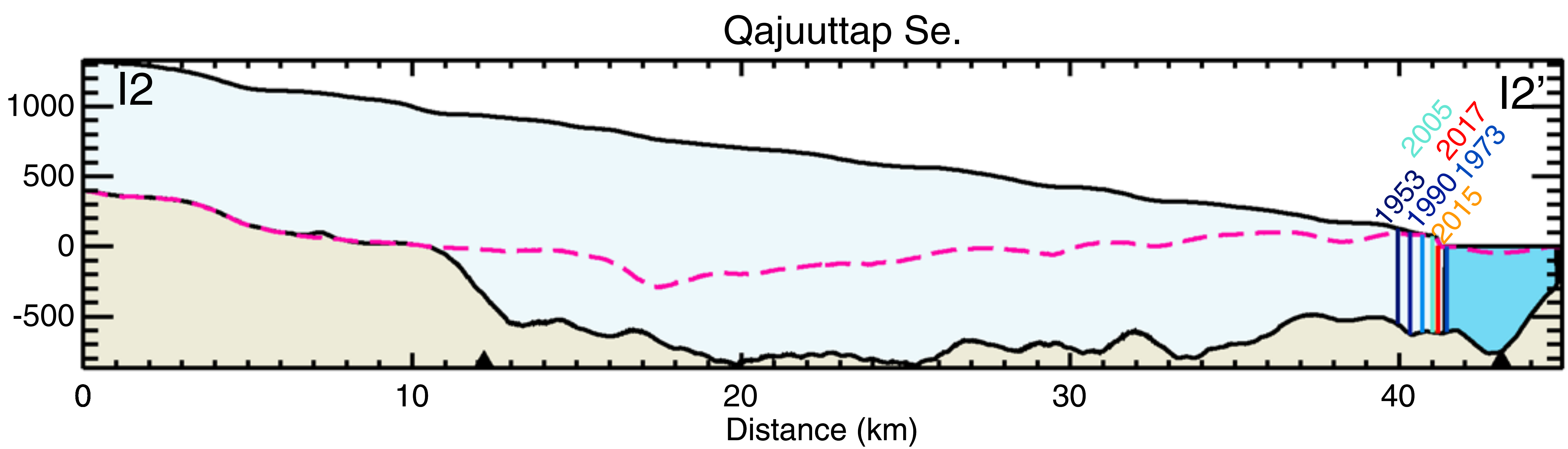

(dash red: previous estimate of topography; note large difference from previous topography)

[Millan et al 2018, GRL]

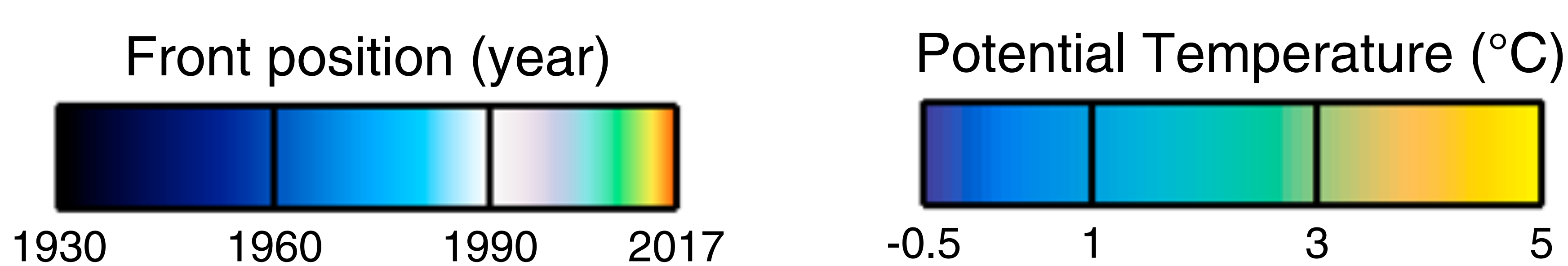

Anorituup

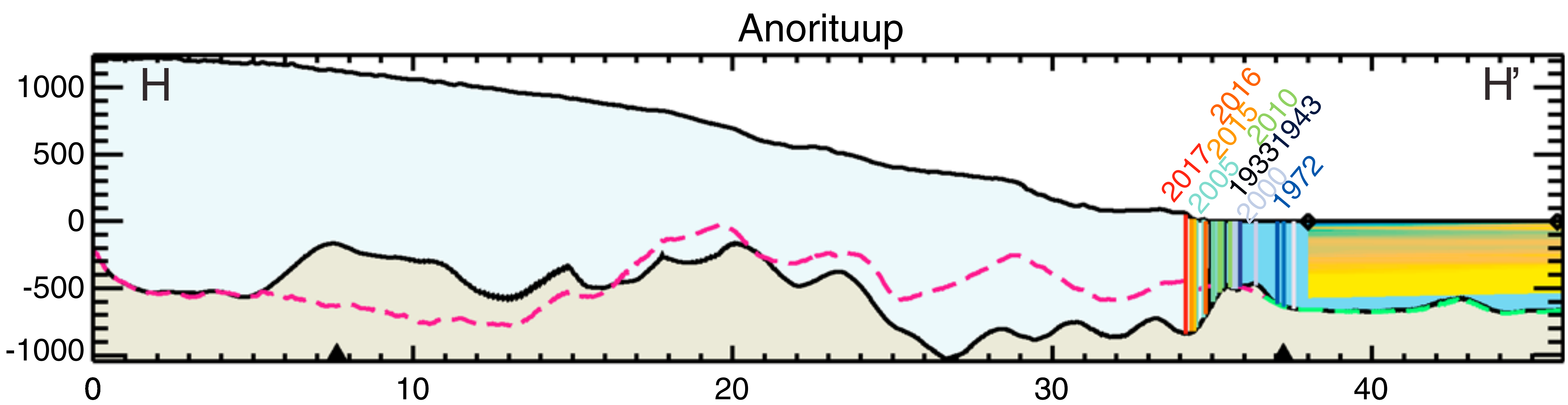

(dash red: previous estimate of topography; note large difference from previous topography)

[Millan et al 2018, GRL]

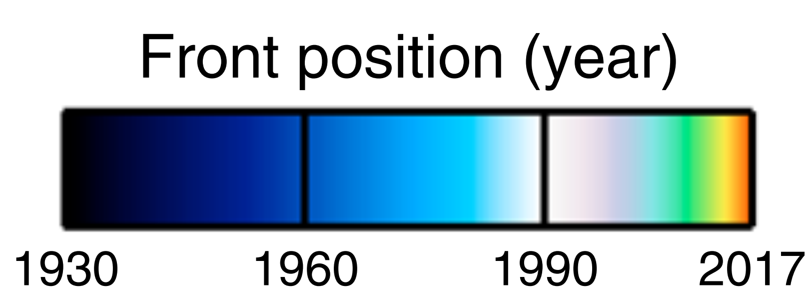

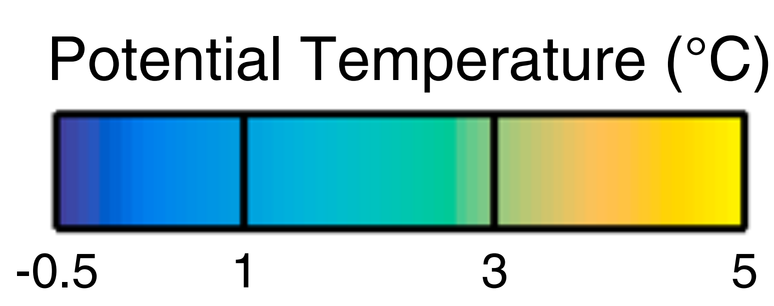

Synchronous collapses of ice sheets around North Atlantic during Heinrich events? **Precursor events**??

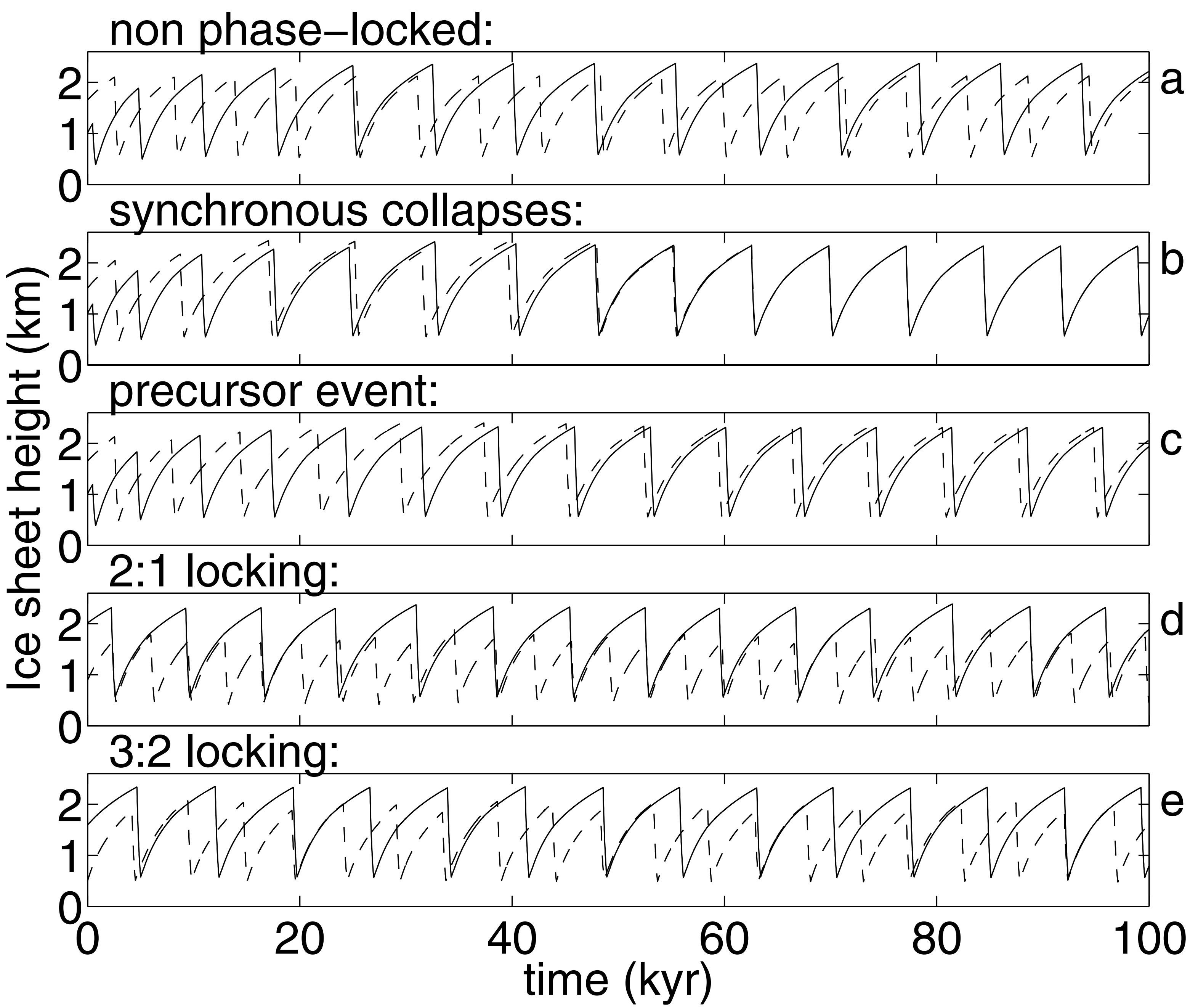

Figure 6. Nonlinear phase locking scenarios as an explanation for the observed synchronous glacier discharges. Shown are time series of the height of two glaciers, a large one (solid lines) representing the LIS and a smaller “European” ice sheet (dash).

Kaspi, Sayag, Tziperman 2004

(a) Two uncoupled glaciers oscillating at different frequencies. (b) Two coupled glaciers starting at different initial conditions, and phase locking at a 1:1 frequency ratio and with no phase lag ➨ synchronous glacier discharge, as seen for ice sheets around North Atlantic. (c) Two coupled glaciers phase locked at a 1:1 frequency ratio, such that the smaller one discharges glaciers prior to the larger one, creating a “precursor” event, as seen for Iceland ice sheet. (d & e) 2:1 (& 3:2) Phase locking in which smaller glacier oscillates twice for each cycle of larger one (and 3 times for every 2 cycles of larger one).

Heinrich events triggered by ocean forcing and modulated by isostatic adjustment

Jeremy N. Bassis, Sierra V. Petersen & L. Mac Cathles

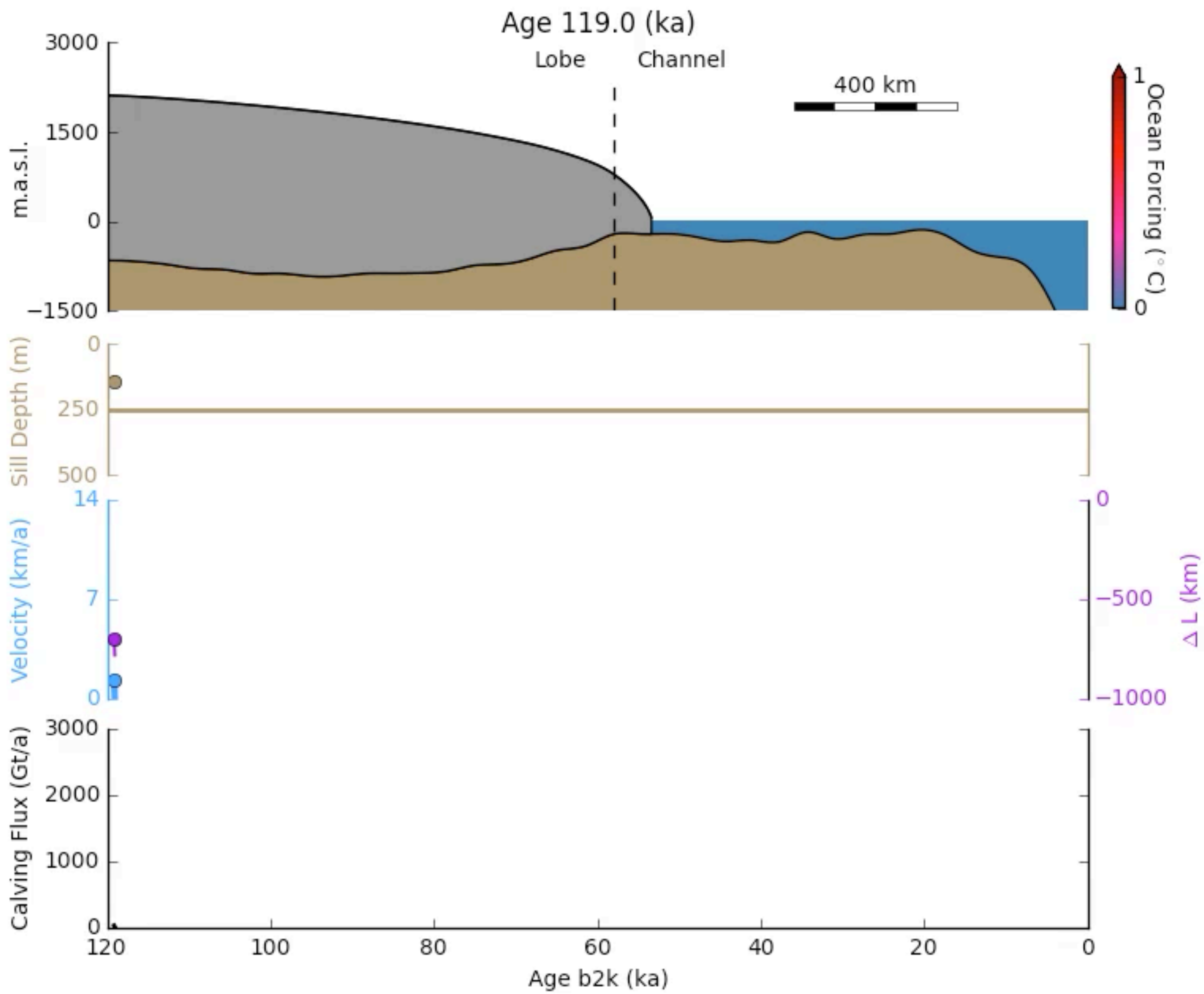

Bassis et al 2017

Heinrich events triggered by ocean forcing and modulated by isostatic adjustment

Jeremy N. Bassis, Sierra V. Petersen & L. Mac Cathles

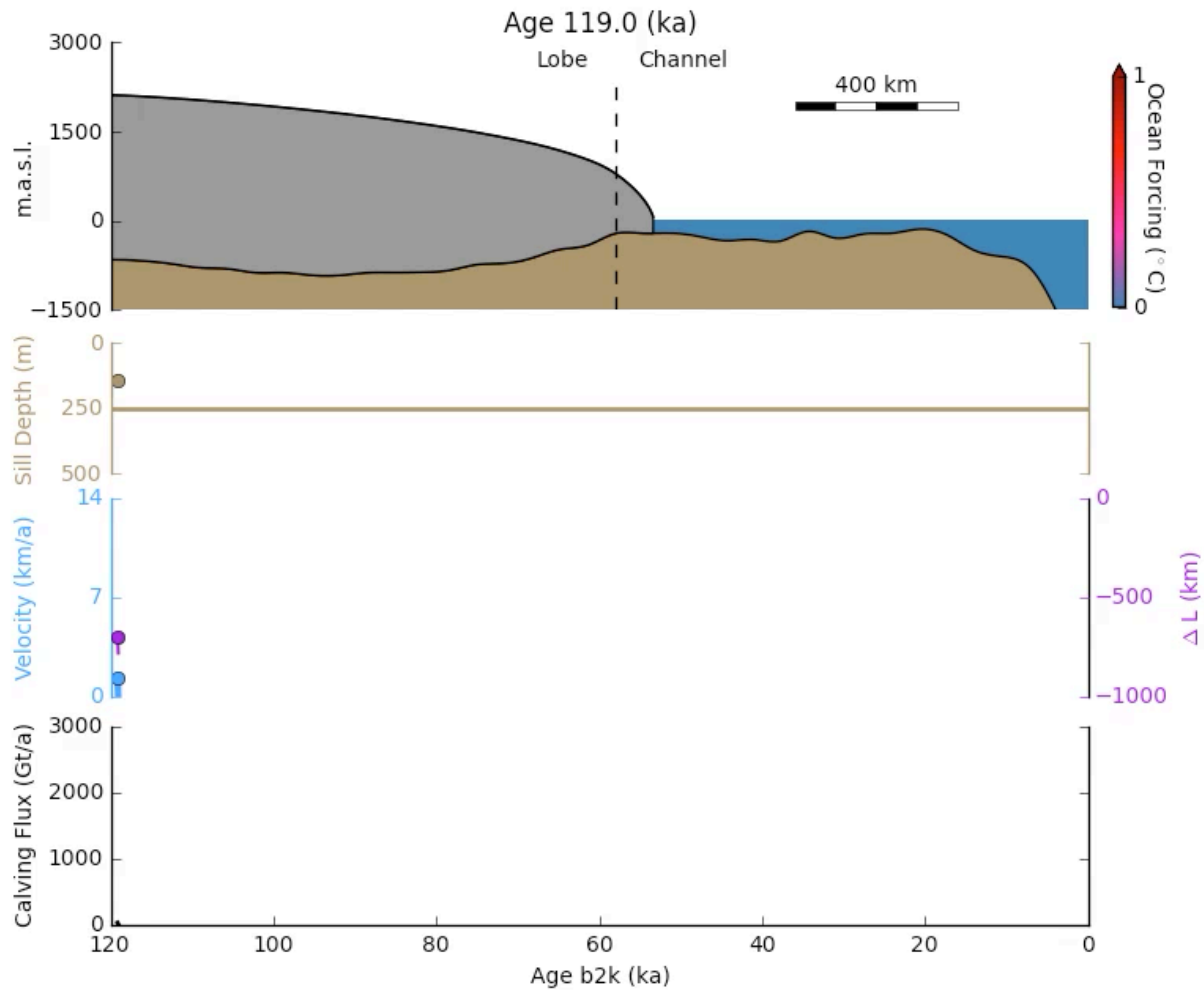

Bassis et al 2017

Conclusions: DO and Heinrich events

- During the last ice age, 20–60,000 years BP

Conclusions: DO and Heinrich events

- During the last ice age, 20–60,000 years BP
- D/O: Greenland ice cores, abrupt warming (10 °C in 20 years), sustained for ~1000 years, gradual cooling and then abrupt cooling; every ~1500 yr

Conclusions: DO and Heinrich events

- During the last ice age, 20–60,000 years BP
- D/O: Greenland ice cores, abrupt warming (10 °C in 20 years), sustained for ~1000 years, gradual cooling and then abrupt cooling; every ~1500 yr
- Possible mechanism: AMOC variability amplified by sea ice changes that lead to a strong atmospheric temperature signal

Conclusions: DO and Heinrich events

- During the last ice age, 20–60,000 years BP
- D/O: Greenland ice cores, abrupt warming (10 °C in 20 years), sustained for ~1000 years, gradual cooling and then abrupt cooling; every ~1500 yr
- Possible mechanism: AMOC variability amplified by sea ice changes that lead to a strong atmospheric temperature signal
- Suspected worldwide teleconnections: possibly via ocean waves

Conclusions: DO and Heinrich events

- During the last ice age, 20–60,000 years BP
- D/O: Greenland ice cores, abrupt warming (10 °C in 20 years), sustained for ~1000 years, gradual cooling and then abrupt cooling; every ~1500 yr
- Possible mechanism: AMOC variability amplified by sea ice changes that lead to a strong atmospheric temperature signal
- Suspected worldwide teleconnections: possibly via ocean waves
- Heinrich events: massive ice collapses seen as layers of ice-rafted sediment layers in the North Atlantic every 7,000–10,000 years

Conclusions: DO and Heinrich events

- During the last ice age, 20–60,000 years BP
- D/O: Greenland ice cores, abrupt warming (10 °C in 20 years), sustained for ~1000 years, gradual cooling and then abrupt cooling; every ~1500 yr
- Possible mechanism: AMOC variability amplified by sea ice changes that lead to a strong atmospheric temperature signal
- Suspected worldwide teleconnections: possibly via ocean waves
- Heinrich events: massive ice collapses seen as layers of ice-rafted sediment layers in the North Atlantic every 7,000–10,000 years
- Possible mechanism(s):

Conclusions: DO and Heinrich events

- During the last ice age, 20–60,000 years BP
- D/O: Greenland ice cores, abrupt warming (10 °C in 20 years), sustained for ~1000 years, gradual cooling and then abrupt cooling; every ~1500 yr
- Possible mechanism: AMOC variability amplified by sea ice changes that lead to a strong atmospheric temperature signal
- Suspected worldwide teleconnections: possibly via ocean waves
- Heinrich events: massive ice collapses seen as layers of ice-rafted sediment layers in the North Atlantic every 7,000–10,000 years
- Possible mechanism(s):
    - Binge-purge collapses of Laurentide Ice Sheet

Conclusions: DO and Heinrich events

- During the last ice age, 20–60,000 years BP
- D/O: Greenland ice cores, abrupt warming (10 °C in 20 years), sustained for ~1000 years, gradual cooling and then abrupt cooling; every ~1500 yr
- Possible mechanism: AMOC variability amplified by sea ice changes that lead to a strong atmospheric temperature signal
- Suspected worldwide teleconnections: possibly via ocean waves
- Heinrich events: massive ice collapses seen as layers of ice-rafted sediment layers in the North Atlantic every 7,000–10,000 years
- Possible mechanism(s):
  - Binge-purge collapses of Laurentide Ice Sheet
  - Hydrofracturing of ice shelves Mechanism

Conclusions: DO and Heinrich events

- During the last ice age, 20–60,000 years BP
- D/O: Greenland ice cores, abrupt warming (10 °C in 20 years), sustained for ~1000 years, gradual cooling and then abrupt cooling; every ~1500 yr
- Possible mechanism: AMOC variability amplified by sea ice changes that lead to a strong atmospheric temperature signal
- Suspected worldwide teleconnections: possibly via ocean waves
- Heinrich events: massive ice collapses seen as layers of ice-rafted sediment layers in the North Atlantic every 7,000–10,000 years
- Possible mechanism(s):
  - Binge-purge collapses of Laurentide Ice Sheet
  - Hydrofracturing of ice shelves Mechanism
  - MISI

Conclusions: DO and Heinrich events

- During the last ice age, 20–60,000 years BP
- D/O: Greenland ice cores, abrupt warming (10 °C in 20 years), sustained for ~1000 years, gradual cooling and then abrupt cooling; every ~1500 yr
- Possible mechanism: AMOC variability amplified by sea ice changes that lead to a strong atmospheric temperature signal
- Suspected worldwide teleconnections: possibly via ocean waves
- Heinrich events: massive ice collapses seen as layers of ice-rafted sediment layers in the North Atlantic every 7,000–10,000 years
- Possible mechanism(s):
  - Binge-purge collapses of Laurentide Ice Sheet
  - Hydrofracturing of ice shelves Mechanism
  - MISI
- Synchronous collapses of different ice sheets: perhaps nonlinear phase locking; coupling provided by the ocean's MOC and temperature response

Conclusions: DO and Heinrich events

- During the last ice age, 20–60,000 years BP
- D/O: Greenland ice cores, abrupt warming (10 °C in 20 years), sustained for ~1000 years, gradual cooling and then abrupt cooling; every ~1500 yr
- Possible mechanism: AMOC variability amplified by sea ice changes that lead to a strong atmospheric temperature signal
- Suspected worldwide teleconnections: possibly via ocean waves
- Heinrich events: massive ice collapses seen as layers of ice-rafted sediment layers in the North Atlantic every 7,000–10,000 years
- Possible mechanism(s):
    - Binge-purge collapses of Laurentide Ice Sheet
    - Hydrofracturing of ice shelves Mechanism
    - MISI
- Synchronous collapses of different ice sheets: perhaps nonlinear phase locking; coupling provided by the ocean’s MOC and temperature response
- “Precursor events,” a large collapse seemingly triggered by earlier collapse of a smaller ice sheet: may be part of nonlinear phase locking instead.

The End